DEVELOPMENT OF

NOVEL SYNTHETIC TURF INFILL MATERIALS

A Dissertation
Presented to
The Academic Faculty

By

Richard Eugene Harper, Jr.

In Partial Fulfillment
Of the Requirements for the Degree
Doctor of Philosophy in Polymer, Textile and Fiber Engineering in the
School of Materials Science and Engineering

Georgia Institute of Technology

December, 2015

DEVELOPMENT OF

NOVEL SYNTHETIC TURF INFILL MATERIALS

Committee:

Dr. Fred L. Cook, Co-advisor
School of Materials Science and Engineering
Georgia Institute of Technology

Dr. John D. Muzzy, Co-advisor
School of Chemical and Biomolecular Engineering
Georgia Institute of Technology

Dr. Wallace W. Carr
School of Materials Science and Engineering
Georgia Institute of Technology

Dr. Youjiang Wang
School of Materials Science and Engineering
Georgia Institute of Technology

Dr. Matthew J. Realff
School of Chemical and Biomolecular Engineering
Georgia Institute of Technology

Date: July 1, 2015

Dedicated to my supportive wife Leslie at home

And my Granny Jean in Heaven

ACKNOWLEDGEMENTS

First, I wish to thank my co-advisors, Prof. Fred L. Cook and Prof. John D. Muzzy, for their help and patience over the years. Both professors put their faith in me to manage this study while helping me surmount problems that inevitably arose. They were my best mentors at the Georgia Institute of Technology. Equally important, I thank Drs. Wallace W. Carr, Matthew J. Realff, and Youjiang Wang for serving on my thesis advisory committee and providing valuable input and direction of my thesis research.

Next, I wish to credit my entrance and completion of courses at Georgia Tech to Prof. Anselm C. Griffin who gave me much needed encouragement. I also appreciate the Georgia Tech students and faculty for their contributed knowledge and facilities, specifically Prof. Satish Kumar, Yaodong Liu, Ryan Kincer, Prof. Meisha Shofner, Prof. Haskell Beckham, Prof. Jonathan S. Colton, and Prof. Radhakrishnaiah Parachuru.

Finally, I want to convey gratitude to the materials suppliers and consultants in the private industry including: Jim Lindsey and Jim Williams of Mohawk Industries; Russell DeLozier of Shaw Industries; Jerry Couey of Synthetic Turf Resources; Mike Chavez of Resilux; Larry Cook of Beaulieu Group; Matthew van der Sluys of Lehigh Technologies Inc.; and C-H Zah and James Hobbs of Interface, Inc. Then towards the completion of this dissertation, I give thanks to the people of American Trim in Lima, OH for their confidence and support.

TABLE OF CONTENTS

LIST OF TABLES

LIST OF FIGURES

LIST OF EQUATIONS

LIST OF SYMBOLS, ABBREVIATIONS AND TERMS

3G	Third generation synthetic turf
4G	Fourth generation synthetic turf
ACL	Anterior cruciate ligament of the knee
ASTM	American Society for Testing and Materials
ATR	Attenuated total reflectance
BD	Bulk density (grams per cubic centimeter)
BR	Butadiene rubber
$CaCO_3$	Calcium carbonate
CARE™	Carpet American Recovery Effort
CC	Cubic centimeters
COPC	Chemical of potential concern
CRI	Carpet and Rug Institute
CTE	Chronic traumatic encephalopathy
df	Degrees of freedom
DSC	Differential scanning calorimeter
DTA	Differential thermal analyzer
F	F-statistic or F-observed value
FIFA	Fédération Internationale de Football Association
FTIR	Fourier transform infrared spectroscopy
HR-TGA	High-resolution thermogravimetric analysis
g	Deceleration to gravity ratio, i.e., one “g” equals 9.81 m/s^2
GA	State of Georgia, USA
GCRI	Granulated crumb rubber infill

Gmax	Maximum deceleration during impact converted to “g”
HIC	Head injury criterion
Infill	Filler inserted between synthetic tufts or grass
ISO	International Organization for Standardization
IR	Isoprene rubber
LN	Natural logarithm
lb(s)	Pound(s)
Max/Min	Maximum/minimum
MCL	Medial cruciate ligament of the knee
MOU	Memorandum of Understanding for Carpet Stewardship
MRSA	Methicillin-resistant *Staphylococcus aureus* bacteria
MRSA-CA	MRSA spread by community assistance
MRSA-HA	MRSA spread by hospital assistance
MTBI	Mild traumatic brain injury
MSDS	Material Safety Data Sheet
MTP	First metatarsophalangeal joint of the big toe
NR	Natural rubber
NFL	National Football League
OZ	Ounce
PA	Pennsylvania
PAH	Polycyclic aromatic hydrocarbon
PCC	Post-consumer carpet
PCCB	Post-consumer carpet from broadloom
PCCT	Post-consumer carpet from tile
PE	Polyethylene

PET	Polyethylene terephthalate
PETMH	PET from Mohawk Industries
PETRE	PET from Resilux
PP	Polypropylene
PVC	Polyvinyl chloride
R^2	Coefficient of Determination
RI	State of Rhode Island, USA
RMA	Rubber Manufacturing Association
RPS	Reverse production system
SBR	Styrene-butadiene rubber
SD	Standard Deviation
SE	Standard Error
SI	Severity index
STC	Synthetic Turf Council
STF	Synthetic turf field
STMC	Scrap Tire Management Council
STR	Synthetic Turf Resources
SVOC	Semi-volatile organic compound
Tg	Glass transition
TGA	Thermogravimetric analysis
TX	State of Texas, USA
UFSTR	Ultra-fine scrap tire rubber
USA or U.S.	United States of America
v1, v2	F-statistic degrees of freedom
VOC	Volatile organic compound

WAXD	Wide angle X-ray Diffraction
WTSC	Wayne State University Cerebral Concussion Tolerance Curve
YD	Yard

SUMMARY

When introduced as AstroTurf® in the 1960's, the first simulated grass surface built on nylon blades was designed for sports activities, but became more novelty than a standard in college and professional sports due to its lack of performance properties and safety concerns. The synthetic turf field (STF) required decades of further development to rise above niche status with introduction of a third generation (3G) version in the late 1990's. The 3G STF included tire ground crumb rubber "infill" (GCRI) filling the spaces between the tuft bundles plus longer and softer materials composing the tuft blades such as polyethylene (PE) and polypropylene (PP) that mimicked the cushioning properties of natural turf. After the 1990's, health-related controversies surrounding the use of tire rubber-based infill created impetus to find safe and effective polymeric alternatives. To find a suitable replacement for rubber infill, the overarching objectives of this study first required understanding the synergistic interactions between GCRI infill and STF during the energy absorption from high value impact events, and then utilizing that knowledge base to develop viable replacement infills for GCRI originating from three polymeric waste streams: post-consumer broadloom carpet (PCCB), carpet tile (PCCT) and polyethylene terephthalate (PET) plastic drink bottles.

A variety of test methods covered GCRI source material compositions, physical structures, and mechanical reactions to impact. GCRI batches were obtained from a variety of commercial sources to determine which relevant properties related directly and synergistically with the turf to shock absorption. Test methods ASTM F355 and F1936 measured the degree of impact absorption of infill by analyzing the acceleration-versus-

time curve from an impact test and yielded multiple data such as the Gmax and Head Injury Criterion (HIC) values. Despite differences in underlying turf hardness, the majority of tested GCRI lots achieved the same level of shock absorption: an average of 115 Gmax and 333 HIC values, both well below the defined fatal impact level values of 200 for Gmax and 1000 for HIC. When compared to each other, Gmax and HIC impact curves followed similar trends in the impact vs. infill loading into the turf curves, and HIC values always reached safe levels before Gmax values. Average particle size of the six best performing lots did not correlate directly to impact performance. Testing this variety of GCRI lots helped establish the Gmax value as the impact standard and extended the acceptable average crumb particle size range from 0.5 mm to 3.0 mm.

After a GCRI performance baseline was developed, a fundamental study of filled 3G STF focused on the statistical significance of two parameters on impact performance: height of the turf pile and the amount of infill incorporated into the turf. According to statistical analyses by either linear or exponential regression, both variables were non-random and relevant to STF impact absorption. While both were essential, the loading level of infill proved to be more significant than turf pile height on impact performance. Further testing with fourth generation turf revealed other important factors such as pile density and blade cross-section. Further studies were deemed necessary to test the interactions between infill and turf, but the significance of infill loading had importance for identifying a viable alternative infill source.

The alternate infill sources originated from available polymeric waste streams including post-consumer carpet broadloom carcass with the face fibers shaved off (PCCB), carpet tile carcass with the face fibers shaved off (PCCT) and chopped

polyethylene terephthalate (PET) flake from drink bottles and their preforms. None of the received PCCB samples reached Gmax values below 180 in the 3G STF, compared to 110 achieved with one of the GCRI infills in the same turf. Physical modification of lot PCCB-1 separated the particles above 0.5 mm from those below 0.5 mm. With the former as infill in the turf, the increase in average particle size and loss of loose fibers reduced the Gmax value for PCCB infill from 208 to 177, a 15% improvement.

The alternate infill candidate from PCCT contained a thermoplastic PVC binder in contrast to the cured $CaCO_3$-filled SBR latex of PCCB, and the relatively large particles of the prepared infill penetrated the 3G STF effectively, attributed to the lack of loose fiber found previously in the PCCB material. During impact testing, every PCCT lot achieved Gmax values below 160 in turf, and lot PCCT-3 exhibited impact values close to the GCRI standard, reaching a Gmax value of 130 despite lower average particle size and lower bulk density than GCRI. Physical modification of a PCCT lot yielded a particle size distribution closer to 0.5 – 3.0 mm, but the resulting impact absorption showed no significant change from the supplied material. When repeated in 4th generation STF (4G-STF), the modified PCCT infill achieved a Gmax value of 118 in turf, a 15% improvement over 3G STF. Future PCCT infill development will have to address the economics of producing the material, since the combined cost of reclamation and preparation at the current low-volume production rate was quoted by the supplier to be ~$0.75 per pound, whereas the standard GCRI commercial-volume cost was quoted to be ~$0.22 per pound.

The final alternate infill candidate was PET plastic originating from two distinct streams: a green colored PET stream of moderate crystallinity (22 – 32%) reclaimed

from recycled drink bottles, and transparent, virgin PET bottle performs exhibiting low crystallinity (4.2%). Both streams required physical modification of the as-received thermoplastic materials to be able to efficiently fill the turf to the standard GCRI level. The resulting PET crumbs consisted of pure polymer without volatiles or filler, thus providing a stark contrast to the GCRI, PCCB and PCCT reclaimed materials. The lowest attained PET-based Gmax value was 169, achieved with semi-crystalline PET particles produced from green chopped flakes that were larger than GCRI-4 particles (average particle size of 1.53 mm for the former versus 1.38 mm for the latter) with the latter's comparable Gmax value of 110. When PET crumb was obtained with significantly reduced crystallinity (4.3%) via cryogenic grinding of clear amorphous PET bottle preforms, impact absorption in turf actually decreased, i.e., the material in turf yielded higher Gmax values. The results were contrary to the initial rationale that high amorphous content PET would be softer and more elastic than more crystalline PET, leading to lower Gmax values in turf. However, none of the PET physical properties such as bulk density, average particle size or crystallinity correlated consistently to impact absorption, although the material itself shifted the Gmax-versus-infill loading curves to more linear trends than those exhibited by the GCRI, PCCB and PCCT materials. The conclusion was that the homogenous structure of the PET reclaim created a linear volume/mass based interaction with the turf that may involve other factors such as surface structure and/or particle shape.

CHAPTER 1

INTRODUCTION

In December of 2007, New York City held a hearing concerning the use of synthetic turf in city parks [1]. The New York municipality is the largest turf buyer of any U.S. city with 28,700 acres in need of green cover to provide safe, open space to the public. Promoting urban public activity was the original purpose of synthetic turf because such locations could not sustain healthy growth of natural grass. Synthetic turf thus seemed a logical choice to replace natural grass in city parks, yet controversy arose about the wide-spread public use of synthetic turf fields (STF). In decades past, the first version of STF made a promising start in 1966 as Astroturf®, which survived conditions in domed structures adverse to growth of natural grass. Instead, STF received wide condemnation from the utilizing athletes as unsafe compared to natural turf. This negative perception persisted for decades, especially from professional football players who attributed an increase of injuries to synthetic fields dating up to a 1995 survey [1]. For the next ten years, several innovations changed the mechanical dynamics of the turf enough to reduce the risk of play-related injury as a major issue by 2007. In the pursuit of mitigating physical hazards, STF became a contender with natural turf, but other problems arose due to an improvement of third generation (3G) STF: the introduction of granulated tire rubber crumb as an energy-absorbing infill between the blade yarn tufts of the turf.

Modern STF utilizes rubber crumb to support the tufts and cushion physical impact by incorporating a product based on reclamation of post-consumer tires:

granulated crumb rubber infill (GCRI). This new 3G STF artificial grass called FieldTurf goes far beyond first-generation green nylon carpet to a more technically advanced soft composite of grass-like blade tufts made from polyolefins, a more durable backing and post-consumer, tire-derived GCRI serving as the infill [1]. An integrated layer of GCRI in the turf at a standard loading of ~2.3 lbs. / sq. ft. enhances impact safety without sacrificing athletic performance. Consequently, FieldTurf has experienced a rapid growth in professional, varsity and high school venues since its introduction in the 1990's, eventually exceeding the volume of first generation AstroTurf® introduced in the 1960's [2].

While GCRI contributes to the STF by alleviating physical and societal tire disposal issues, it also creates new challenges. For instance, rubber crumb particles are reclaimed through an extensive deconstruction process of the steel-belted post-consumer tire, which adds cost and time to production. Automotive tires are made for harsh terrain without prolonged human contact, thus they contain toxic ingredients such as heavy metals and volatile chemicals. Furthermore, reported scientific research is lacking on how GCRI interacts with turf on a fundamental level or how it affects human health after repeated exposure, including direct ingestion into the body through the mouth, e.g., by soccer goalies diving across the turf to block shots. Even injury comparisons between third-generation (3G) STF and natural turf are confined to small studies [3]. This reported research incorporates three objectives:

1. Develop a fundamental understanding of how standard GCRI infill and STF operate synergistically to meet safety performance goals.

2. Identify and evaluate polymer waste streams that lack GCRI-related environmental and health issues to serve as potential infill replacements in STF.
3. Compare the economics between GCRI and the alternative polymeric material(s) that are shown to be technically feasible as STF infills.

The completed research will contribute to the knowledge base of 3G STF performance parameters and characteristics while evaluating and projecting available polymeric waste streams as viable alternatives to GCRI.

CHAPTER 2

LITERATURE REVIEW

2.1 Synthetic Sports Turf

Synthetic turf was an American invention designed as outdoor carpet to promote athletic activity of youth in urban settings where natural turf was not feasible for durable use. STF then branched into other sports and more sophisticated constructions.

2.1.1 History of STF

In the 1950's, the Ford Foundation determined that children in urban cities were not as fit as rural children due to the lack of playground areas [1, 2]. Thus the Cord Foundation collaborated with the Chemstrand Division of Monsanto Industries to create a synthetic surface for promoting physical activity of city children [1, 2]. The first product developed was a green nylon carpet called Chemgrass™, which came out in 1964 in limited production for its first installation at the Moses Brown School field house in Providence, RI. Concurrently, the city of Houston, Texas touted the construction of the world's first domed stadium - the Astrodome - as the Eighth Wonder of the World, providing comfortable conditions for spectators and athletes year-round for various sports and activities. However, the Astrodome's transparent dome panels created indoor sun glare that distracted the players and audience. Painting the panels black solved the glare problem, but the natural light level was lowered too much for the original natural grass turf to survive. The Chemgrass™ design, of course, did not require sunlight, water or trimming. Thus, the Astrodome natural grass turf was subsequently replaced with the synthetic grass in 1966, which led to its new brand name, AstroTurf®.

The popularity of STF quickly grew to other sports arenas and outdoor fields, and numerous companies produced different brands. Although the new synthetic field owners liked the novel invention, athletes remained unimpressed and complained about injuries and distorted playing conditions due to the hardness of the original artificial surfaces [3]. Consequently, wide spread use of STF over natural turf was hindered for decades by safety complaints coupled with the high initial costs of artificial construction.

To accommodate customer demands, several versions of STF attempted to improve surface feel and performance, leading to second-generation STF by the 1970's. The most notable changes came in 1976 with elongated tufts and different polymeric materials. Frederick T. Hass, Jr. added a layer of sand to fill the space between the artificial tufts and hold the turf blade yarns in place [2]. Despite improvements, STF playability was still a problem for running traction, ball bounce, etc. [4]. Playability did not improve through the 1980s, and athletes pushed strongly for outright bans of STF, e.g., by the English Football (soccer) Association in 1988. The backlash continued in the USA into 1995, when a survey found that a resounding 93% of National Football League (NFL) athletes attributed higher injuries to STF over natural turf. Consequently, stadiums reverted back to natural grass, even the replacement facility of the Astrodome in Houston [1].

Despite the long-term backlash, companies introduced new varieties of turf products, including a third-generation (3G) STF during the 1990's. The design changes in 3G turf included longer, softer tufts that replaced nylon with polyolefins like polyethylene or polypropylene with rubber particles (GCRI) placed in between the tufts as a sand replacement for cushioning [1]. After these 3G enhancements, the STF

industry experienced a boom with the number of new fields jumping from only seven new generation fields constructed in 1998 to 3,500 new fields by 2008 in the United States alone, according to the Synthetic Turf Council (STC) of Atlanta, GA [1]. In a full circle, the new fields included indoor stadiums because the owners wanted to convert back from natural turf to the new 3G STF, exemplified by the brand name FieldTurf marketed by the Tarkett Sports Company.

After decades spent disparaging synthetic fields, the improved safety and playability of 3G STF swayed athletes' views. As late as 1994, The NFL Players Playing Surfaces Opinion Survey showed many American football players complained about the original AstroTurf® field as an unsafe working surface [5]. Then a decade later, athletes saw huge safety and play improvements with 3G STF that elevated the safety level of STF to be equal to grass turf. Safety was still the top demand in the 2006 NFL-based survey, but 3G STF joined the survey list of player's responses to important safety needs:

1. Make all fields grass to prevent injuries.
2. Keep all grass fields well maintained.
3. Do not allow baseball fields or multiple use fields.
4. Put artificial infilled surfaces in inclement weather cities.
5. Set standards for quality and texture of all fields based on safety, performance and comfort. [5]

Apparently, safety qualities of improved STF finally achieved wide acceptance by NFL players for practice and actual play.

In addition to personal welfare, the artificial constructs of 3G STF had other advantages for sport facilities. For example, the underlying foundation and turf overlay had high initial installation costs, but long term maintenance was half the cost of natural fields [6]. The maintenance costs were more economical because the turf required no insecticides or watering. Furthermore, the soft blade yarn tufts endured greater abrasion than organic grass before breaking and could be used at any time, day or night. Without waiting for grass to recover, STF endured 8-12 times more use than natural fields [6]. After long term use, the artificial field retained a more level surface than a natural field for at least 10 years. Overall, the improved safety of 3G STF coupled with the original performance advantages associated with synthetic turf have contributed to a rapidly-growing market across all types of recreational sports fields since the late 1990's.

2.1.2 Construction of STF

In the 1960's, the first generation of synthetic turf was a simple green carpet with nylon tufts projecting out of a flexible backing over a shock-absorbing under-pad. The basic structure came from the tufted carpet industry: "…artificial turf companies that have been more successful and have the greatest tenure in artificial turf are those that have been closely aligned with the carpet manufacturing industry" [2]. Like indoor carpet, the turf's nylon-based pile yarns were tufted or knitted through a flexible backing, but the major difference was that the normal carpet face yarn was replaced with wide monofilament fibers, or blades, that physically and visually simulated natural grass. Second-generation STF of the 1970's exhibited longer blade yarn tufts made from softer polyolefins, and sand filled the space in between the tufts, hence becoming the first infill. During short-term use, sand infill improved impact cushioning by keeping the long tufts

upright. Plus, the sand also became weight ballast that kept the turf in place, thus negating the need for adhesives underneath the backing. However, repeated use caused sand compaction and hardened the surface below the tufts. Sand infill thus reduced cost and maintenance of STF, but did not improve playability and safety sufficiently for athletes to abandon the preferred natural grass turf [4, 7].

To surpass natural turf in play performance and safety, third-generation STF improvements mimicked the construction of natural turf. The blade yarn tufts became longer, fibrillated and wider like natural grass with spaced rows. Also, the force absorbing pads underneath the backing were reduced or eliminated. As replacement for impact force abatement, post-consumer, tire-derived granulated crumb rubber of small particle size between 0.5 – 3.0 mm was added as infill between the tufts, hence creating GCRI (Figure 2.1).

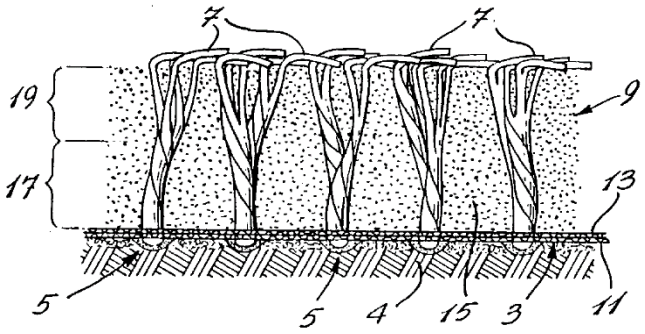

Figure 2.1. *Synthetic Turf,* USP 6,723,412 B2 [7]

The GCRI partially or completely replaced the sand infill in the third-generation turf. Interaction between infill and turf enhanced overall shock absorption, attributed to a combination of compressive infill particles and reinforcement of tuft flexibility. The small vulcanized rubber particles mimicked non-compacting aerated soil that absorbed

the impact of a foot, head or falling body without becoming hardened after repeated use [7]. GCRI also improved STF playability because athletic cleated shoes could penetrate the crumb, and then the crumb released the cleats without resistance. Athletes occasionally moved on previous versions of STF with the tufts locking on the shoe cleats, increasing stress on joints of the leg and resulting in a unique STF injury called turf lock [2]. Among the variations of 3G STF's, GCRI became a common feature, and the FieldTurf design rapidly replaced AstroTurf® [1].

STF placed indoors or outdoors always required an artificial foundation underneath the turf instead of the soil used by natural turf. Indoor settings like the Houston Astrodome already had the substructure, and the lack of rainfall negated a drainage system. In contrast, outdoor surfaces required a level foundation to provide an even playing field while controlling water drainage (Fig. 2.2).

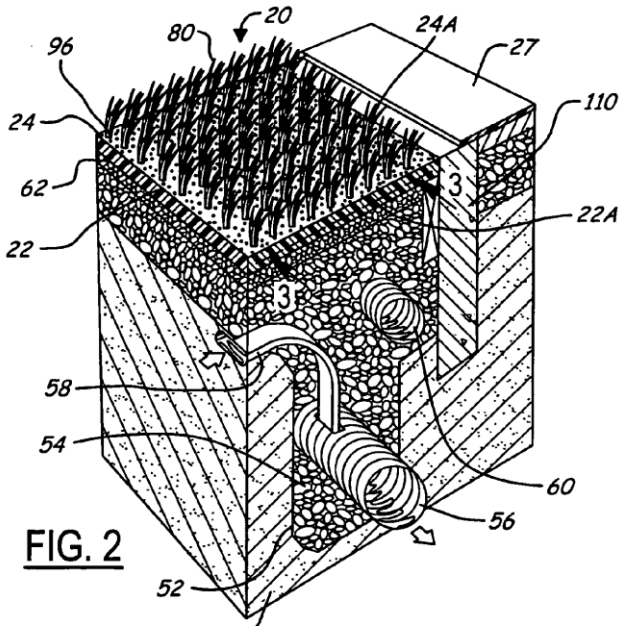

Figure 2.2. *Synthetic Sports Turf Having Improved Playability And Wearability*, USP 7,189,445 B2 [8]

The backing of modern turf was made from flexible fabric that held the upright tuft pattern. Also, the turf backing allowed water drainage due to punctured holes punctured through fabric and coating [7, 8]. The size of the punctured holes became an infill performance factor because small particles could block water drainage if small enough to flow through the backing. Beneath the turf, the underlying layers of fine and coarse gravel also needed clear pathways to direct water towards drainage pipes and prevent flooding above the surface. The gravel also provided physical support for the level surface. Furthermore, the foundation prevented compaction of the turf and enhanced impact absorption. Overall, these turf designs and construction of the gravel substructure required a capital investment typically larger than natural turf, which made them significant factors in field selection.

2.1.3 Selecting STF

Before the invention of STF, outdoor sports required manicured natural grass fields to provide safety and playability. These fields had level, loose soil for living grass growth and grooming. Year-round use of fields necessitated maintenance so professional athletes could train and perform on the optimum grass surfaces. However, urban growth replaced rural fields with environments non-conducive to growing healthy grass, thus leading to the development of artificial sports surfaces. The original intent behind STF was not to replace natural turf nor provide a better surface for athletes, but to be a substitute in cities for youth activities [2]. Nonetheless, selection between natural and artificial turf provided options for all amateur, school/university-level and professional sports.

Selection of the appropriate turf involved multiple criteria based on factors such as cost, utility, safety, and playability. Initially, high investment cost and professional athletic disfavor impeded STF utilization. Advent of 3G STF improved athletes' views of the turf's safety and playability, but capital costs remained high. Selecting natural versus STF field was governed by numerous advantages and disadvantages (Table 2.1).

Table 2.1. Comparison of Factors Dictating Turf Selection [2]

	Type of surface	
Factor	Natural grass	Artificial turf
Initial construction costs	Lower initial cost	Higher cost of installation
Replacement	Less cost	Higher cost
Maintenance costs	Higher cost of adequate maintenance	Lower maintenance costs
Field life	Indefinitely given proper maintenance. May require resodding	Limited to 10 to 15 yr of heavy usage
Repairs	Relatively continuous depending on weather conditions	Sporadic repairs depending on use
Usage	Limited number of games	Number of games limited only by schedule
Weather conditions	Limited use under adverse weather conditions	May be used under all but most adverse weather conditions
Consistency	Playing surface may be quite variable	Very consistent playing surface
Versatility	Limited activities (e.g., football, soccer, and other field sports)	Multipurpose use (e.g., band practice, concerts). Can be used in covered stadiums
Playability	Preferred by soccer and football players when field conditions and weather are good	Preferred by field hockey because of consistency
Injuries	Fewer minor injuries. Incidence of serious injury controversial	Greater incidence of burns and abrasions. Incidence of serious injury controversial

Cost was the universal factor for both surfaces, and the list of criteria in Table 2.1 reflected its high priority. STF had a high initial investment and limited field life, which restricted application to urban centers or environments hostile to grass. However, lower costs and elimination of chemicals like fertilizers and pesticides from STF maintenance were long-term benefits, both economic and environmental. The other STF variables covered turf performance and safety issues that were dependent on the chosen sport and

the activity's inherent hazards. Out of the remaining selection criteria, synthetic turf advantages included wider versatility of activities, longer playing schedules and a consistent level surface under adverse weather conditions. Studies calculated the additional playing time and variety of activities on STF to equal 8-12 times greater use than natural turf under most environmental stresses [2, 3, 5]. Finally, the remaining selection criterion, safety, had comparisons between natural and artificial turf that tended to favor natural fields until third-generation turf addressed most of the safety concerns. However, safety remained a controversial issue since some injuries were mitigated by STF but other hazards arose [1, 3]. In the final analysis, cost of the land and facilities became paramount while the other criteria played smaller roles [2].

For the purposes of this study, the important criteria were not related to cost or facilities, but the last one in Table 2.1, safety. When turf selection involved non-cost factors such as safety or performance, the type of sport became important due to the athletes' physical interaction with the turf [2]. Player-surface interaction dictated many mechanical properties of synthetic turf such as hardness, traction and coefficient of friction, but the exact mechanism and interdependency of these properties were not well understood [9]. For example, traction was a complex interaction between turf material, horizontal forces and vertical forces that reacted to athletes walking and running on the surface [10]. In contrast, hardness came from responses to only vertical compaction within the tufts and backing. When crumb rubber became a part of STF, many turf properties depended on the interaction between GCRI and tuft fiber:

> The infill layer provides: support for the fibre layer, resilience for ball bounce, fall cushioning and together with fibre condition forms the basis for traction and grip

potentials. The depth of infill material as well as its orientation or distribution is the most important point of concern. [4]

Traction was important for playability of STF, but its related safety issues were not detrimental beyond skin abrasions due to a too-high coefficient of friction of the polymer blade material. Hardness could affect playability, but its relationship to vertical material compression also contributed to hazardous injuries such as joint damage and concussions. Although these properties were related to safety and performance, the specifications of STF were consumer-driven and required a "compromise between safety and function" [1, 2]. With little available research to help selection of safety and performance properties, the customer decided turf specifications through arbitrary experience and anecdotal evidence.

Since playability and safety of STF depended on the specific sport, American-style tackle football (henceforth referred to a "football") became the focal point of this research. Originally, urban physical fitness was the initial purpose of synthetic turf, but it rapidly expanded into football. Modern football has an elevated status due to a high incidence of injury that requires a functional, reactive artificial surface [2]. Eventually, STF branched into other sports such as soccer, baseball, tennis, field hockey and today, horse racing; yet professional athletes held back large-scale use due to poor opinions and conceptions of synthetic turf originating from the AstroTurf® introduction. The introduction of GCRI and 3G STF sparked renewed interest in artificial surfaces for football and other sports. Due to the sport's long association with STF, concentrating on football-related safety issues was thus the logical choice for this study.

2.2 Crumb Rubber Infill

The first STF infill was sand, introduced in the 1970's as ballast. By 2000, infill function switched from dead weight to impact cushioning. Sand was an impact material for non-turf or low-concussion sports like volleyball, baseball and golf. However, sand and turf interaction was ineffective for high-impact cushioning because sand was non-elastic and the narrow rows of tufts blocked sand from lateral movement [7]. Subsequent heavy use and rainfall compressed the sand into a hardened layer that made the STF less resilient to impact energy absorption and impeded water drainage. When the markets developed infill from reclaimed tire rubber, the more elastic particles in GCRI partially or completely replaced the harder sand in third-generation turf. Crumb rubber thus prevented compaction and hardening of the turf due to its elastomeric composition that allowed movement within the tufts in multiple directions and its ability to return to its original particle shape.

2.2.1 Tire Recycling

Before crumb rubber markets existed, various agencies in industry and government made a coordinated effort to find alternate uses of rubber obtained from post-consumer tires. The modern automotive tire was the result of extensive development to make an economical product blending safety, performance, comfort and durability for the open road [11]. Automotive transportation demanded a durable product, leading to development of a unique soft composite of fibers, polymers and steel with elastomeric rubber as the most critical component. The rubber composition of the entire modern tire mass (the popular steel-belted radial passenger tire) is 41% by weight, pervading every section of the construction (Table 2.2).

Table 2.2. Rubber in Steel-Belted Passenger Tire by Weight [11]

TREAD	32.6%
BASE	1.7%
SIDEWALL	21.9%
BEAD APEX	5.0%
BEAD INSULATION	1.2%
FABRIC INSULATION	11.8%
INSULATION OF STEEL CORD	9.5%
INNERLINER	12.4%
UNDERCUSHION	3.9%
Total:	**100.0%**

After long term use, the tire wears down especially along the treads on the outer trim that touches the road. Although treads can be rebuffed a limited number of times to increase the useful life of the tire, the remaining tire carcass and its contained rubber material becomes scrap designated for disposal, an important issue in the U. S. with ~223 million post-consumer tires generated each year [12] .

The irony of the tire's strong durability was expensive disposal and environmental dangers due to its composition that would not decay when placed into landfills after overloading the local stock piles. In 1990 alone, the 223 million scrap tires added to the existing stockpile of one billion tires, which was estimated to contain 2.5 million tons of total municipal solid waste (MSW) according to the Rubber Manufacturing Association (RMA) [12]. Although the scrap tire mass constituted only 1.2% of the total generated municipal solid waste estimated by the United States Environmental Protection Agency (EPA), the tires became sites for vermin infestation, water-borne diseases and uncontrolled fires that released hazardous particles and air pollutants [13]. By 1985, such problems prompted states to pass laws to reduce tire scrap from landfills reaching 49

states with such laws by 1999, and only eight states had no landfill restrictions governing tires [1, 14].

Further regulatory pressure for finding affordable alternate uses of scrap tires pushed the RMA to establish in 1989 the Scrap Tire Management Council (STMC). The STMC worked with government agencies to create scrap tire-based markets based on social and economic incentives to recycle commercial waste materials. The development found new uses for scrap tires as tire-derived fuel, civil engineering components and rubber crumb. Consequently, scrap tire markets created trends within two decades that consumed millions of scrap tire units per year (Figure 2.3). Within four years, demand for scrapped tires even reduced U.S. tire stockpiles outside of landfills (Figure 2.4).

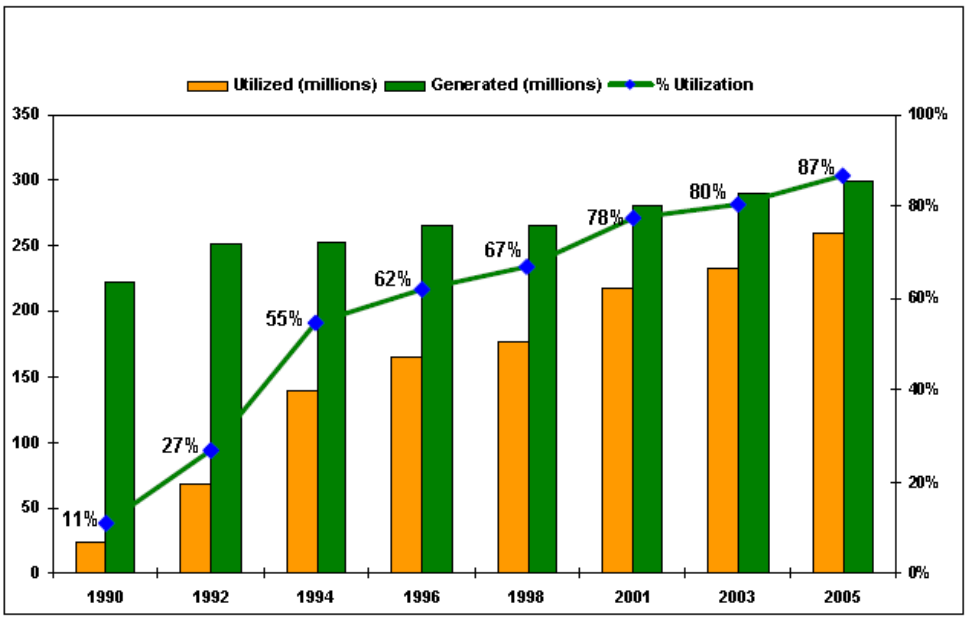

Figure 2.3. Tire Units Diverted From U.S. Landfills [12]

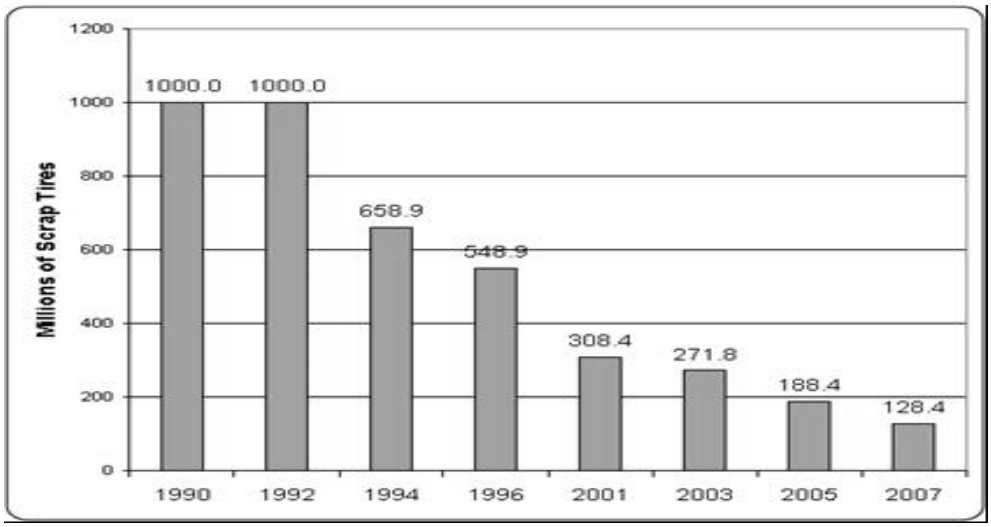

Figure 2.4. Tire Stockpile Reductions [12]

On an annual basis, scrap tire markets consumed waste otherwise designated for stockpiles and landfills while reducing the amount of units already in local storage. As demand grew, huge volumes of tire scrap went into beneficial waste consumption by commercial enterprise, and thus created a process with "a more enlightened objective contrasted with simply processing materials within the narrower definition of recycling" [15]. Overall, the reduction of scrap tires reflected an efficient reclamation method that could apply to other polymeric waste streams.

2.2.2 Ground Rubber

Ground rubber is a type of the scrap tire product relevant to STF because of its ability to penetrate turf and absorb physical shock [12]. Since the 1960's, acceptable impact absorption properties of STF required rubber pads or mats to be installed underneath the turf since the fibrous tufts provided little physical impact energy dampening. Although mats alleviated impact injuries, the extra vertical movement that

reduced hardness also increased muscle fatigue of the lower extremities, which took energy away from athletic performance, such as running or walking [2]. Nonetheless, rubber mats remained the standard shock absorber with no suitable replacement until the 1990's. When GCRI was applied to STF, players experienced reduced overall hardness during free fall against the turf surface plus reduction of leg fatigue that correlated to infill distribution [4].

For turf application, evolved processing techniques created granulated GCRI particles small enough to penetrate the space between the tufts. The GCRI was prepared by either ambient (unregulated temperature) or cryogenic grinding of the whole tire. Cryogenic grinding had high costs due to liquid nitrogen used in the milling step, but the resulting crumb was almost completely free of polymer and steel fibers [16]. Conversely, ambient grinding produced lower-cost, less-immaculate crumb. After either process, the crumb went through metal sieves to filter out particles too small or too large to meet contractor requirements, hence producing GCRI. While short-term use showed similar impact benefits from both types of GCRI, the long-term effects of human exposure to all tire rubber crumb received little research attention when third-generation turf became popular.

In addition to recoverable elasticity, another essential crumb property was its particle size: small enough to fit between the fibers, yet too large to obstruct drainage of water through the perforated backing. Description of GCRI lacked fundamental research on particle size or impact energy absorption properties in turf, while the private industry created methods based on internal testing and consumer feedback. Product specifications originated from private vendors who constructed the turf or tested STF performance in

labs and outdoor fields. One such company was Synthetic Turf Resources (STR) of Dalton, GA, which produced synthetic turf for Astroturf®. For optimum safety and performance, STR recommended GCRI particle diameters between 0.5 to 1.5 mm. The RMA formally classified rubber particles between 0.18-2.0 mm (mesh 80 to 10, respectively) as ground rubber [11]. Another industry standard, ASTM D5603-2001, categorized coarse rubber as between mesh 40 to 10 (0.425-2.0 mm, respectively). No peer-reviewed study defined which specific range was desirable, so commercially available infill had few guidelines. For example, one environmental study found GCRI particle size reached 3 mm [1]. The minimum infill particle size was dictated for preventing drainage issues in the turf substructure, since fine particulates block water flow in gravel [4, 7, 8]. Overall, no studies found an optimized particle size range for GCRI.

According to articles about turf maintenance, the ideal amount of infill loading penetrated the turf with enough material to reach two-thirds of tuft height for maximum impact effect while leaving enough tuft exposed for surface playability [5, 7]. While infill loading levels were not specified in the literature, STR recommended a loading of 2.3 to 3 pounds GCRI per square foot of field to influence impact without overwhelming the tufts. However, no sources provided empirical data that correlated crumb size or loading of GCRI infill for impact reduction in STF applications, i.e., objective GCRI standards were not available for these two critical parameters.

Another unaccounted quality was crumb particle shape, although there was mention about cryogenic and ambient grinding effects on it. Generally, ambient grinding produced irregular shaped particles with rough surfaces and large surface areas, while

cryogenic grinding created smooth, fractured particles with smaller surface areas [7, 11, 16]. Even though shape was not mentioned as relevant to impact attenuation, bulk density was listed in crumb rubber-based ASTM D5603. If particle shape directly affected packing and hence bulk density, then shape was overlooked. Consequently, infill research presented many potential areas of study such as the optimum shape, size and/or loading of GCRI particles into 3G STF.

2.2.3 GCRI Issues

Before media coverage of the long-term brain damage due to repeated high-energy impacts (both with other players and with turfs) suffered by football players, investigators attributed other types of athletic injuries to STF. Most safety studies examined joint and muscle-based problems when comparing natural to synthetic turfs. While STF introduction eliminated problems with excessive field wear and pesticide/herbicide usage, it created new, unique issues like “heat island”, the infill acting as a black body heat absorber with peak field temperatures reaching 160° F as opposed to only 100°F on a grass field [1]. Other distinctive STF hazards included turf toe and turf burn. In the years prior to its dissemination to the consumer, no research was found that compared the older generation STF to 3G turf to gauge the effect of the turf changes on the known issues listed in Table 2.3.

Table 2.3. STF Associated Injuries

Term	Source	Ref #
Turf Burn	Burning of bare skin caused by friction against an abrasive, hard surface	17
Turf Toe	Tearing of the cap above the first metatarsophalangeal joint (MTP) by hyperextension (bending backwards) of the big toe	18
Lead	Exposure to toxic metals due to tuft and/or rubber incorporation	1, 17, 19
ACL, MCL	Tearing of knee ligaments due to turf locking of the foot and rotation of the leg	17, 20
Muscle Fatigue	Extreme exhaustion caused by running on an elastic surface.	2, 21
Heat exposure	Increased air and surface temperatures compared to natural turf.	1, 2, 17
COPC	Exposure to potential irritants and carcinogens especially in elevated temperatures	1, 17
MRSA	Pathogenic infection of skin abrasion or cuts caused by tufts	1, 17

Most of the issues in Table 2.3 were due to the whole synthetic turf system rather than rubber crumb itself. The infill addressed mainly one problem – cushioning of high-energy impacts. However, the addition of rubber infill contributed to other problems inherent to synthetic surfaces while creating its own.

Prior to turf application, GCRI was reclaimed from tire rubber, which was not a 100% efficient process. The heterogeneous tire mix of steel and thermoplastic fiber belts in a vulcanized rubber matrix hindered simple salvage and economical processing to separate the components. Consequently, a high-volume of scrap tire consumers such as cement kiln operators burned the entire scrap tire as waste fuel with the rubber component representing the bulk of the heat value, i.e., as waste fuel [12]. Table 2.2 lists the outer two treads as composing only 33% of the total rubber in the tire mass [11].

Consequently, viable use of tire rubber for GCRI production required separating the remaining carcass or utilizing the whole tire. Due to the ease of separating fibers under extremely low temperatures, cryogenic grinding produced cleanest crumb after grinding the whole tire, but the use of liquid nitrogen entailed additional costs and energy requirements to the material separation [11, 16]. As the cheaper option, ambient grinding of the entire tire still required separation of metal and thermoplastic fibers from the rubber, but it was inefficient at removing the fibers completely. So the process produced a more-contaminated GCRI than processes that utilized cryogenic temperature grinding. The choice between a cleaner crumb versus cheaper crumb led to selecting the ambient method for 60% of tire grinding in North America by 2002 [16]. Consequently, the majority of rubber infill contained remnants of fiber and steel that increased chemical exposure and may create unknown consequences for the environment.

After the introduction of rubber crumb, chemical contamination received higher attention from turf users. Concerns arose in 2007 when California released a report on testing the chemical content of recycled tires, noting exposure to high levels of volatile organic compounds. Soon other studies added to a list of possible chemical hazards [1, 17]. Aside from known allergens like natural rubber, the chemicals of potential concern (COPC) included carcinogenic polycyclic aromatic hydrocarbons (PAHs), phthalates, volatile organic compounds (VOCs), semi-volatile organic compounds (SVOCs), and hazardous metals such as lead. Lead contamination became controversial when a 2008 New Jersey study found high levels of lead in STF fields installed next to a scrap metal processing facility [19]. However, both studies made no definitive conclusions about the hazards of GCRI or STF. Subsequent tests of recycled rubber found very low levels of

lead, but exposure was negligible due to encapsulation by the durable rubber. Nonetheless, the potential hazard sparked new studies into COPC of infill because crumb rubber lacked long-term research to negate or substantiate the concerns. The chemical hazard was potentially worse due to the small size of crumb, which made transport easy from the field to almost any location including homes of athletes [1]. The small crumb had multiple routes of invasion such as attachment to clothes, inhalation by players through the mouth during heavy breathing and accidental digestion. With possible contamination and exposure, some venues such as New York City, Los Angeles and several European countries did not wait for the science to address these concerns, with legislatures pushing for bans on GCRI in STF. Whether such bans were a prudent course or over-reaction, finding a solution was a challenge since modern tire construction was highly variable between producers while chemical characterization was under-utilized [1, 11, 16].

Another problem that was well documented and shared by all STF vendors and installers was intensified by the introduction of GCRI in warm climate athletic fields: heat elevation of the surrounding environment. GCRI addition to 3G STF introduced an added effective black body heat absorber in sunlight, accentuating previous studies that demonstrated a re-radiating effect of earlier-generation synthetic turfs dating from the 1970's [1, 2, 17]. The air above early STF's reached 3.4° to 4.5° C higher temperatures than grass turf, and the tuft surface itself reached 19.5° to 27.8° C higher temperatures. The hot atmosphere exposed active players to heat exhaustion, and the extremely hot turf surface created skin burns and blistering. After GCRI application, the black color and heat capacity of the carbon black-filled rubber absorbed thermal energy from sunlight

even more effectively than the unfilled turf, thus contributing to a "heat island" effect [1, 17]. When 3G STF was tested as a heat island in a 2007 New York City study, the surface was 16° C (60° F) hotter than grass turf and reached 71° C (160° F) on clear sunny days [1]. In addition to heat exhaustion, direct skin contact to a surface at 122° F for more than ten minutes causes skin injuries. In a 2007 Missouri study, STF heated to 78° C (173° F) while nearby natural grass was 41° C (105° F) [17]. The problem could be moderated by installed shade and water irrigation systems, but at added cost and limited duration. In its current form, GCRI intensified 3G STF heat-related problems without a viable remediation.

The prior listed issues with infill raised public concern about safety of the latest turf development, but one 3G STF issue created brief public alarm due to the specter of pathogenic illness caused by methicillin-resistant *Staphylococcus aureus* (MRSA) bacteria. Unlike problems inherent to infill such as heat and chemical exposure, this new type of infection was created away from the field and the rubber vendors. In the 1950's, antibiotics almost eliminated bacterial infections inherent to bodily injuries and surgeries. Then the underlying pathogens evolved into antibiotic-resistant strains such as MRSA. Staphylococcus (staph) is a type of naturally occurring bacteria normally found living on the outer skin of humans that normally does not cause harm. Staph only poses danger when it is introduced into the bloodstream via cuts or abrasions of the skin [22]. The first case of MRSA infection came in 1968 after nine years of antibiotic use in hospitals, and it only attacked unhealthy patients via surface-to-skin transmission [23]. The hospital-assisted (MRSA-HA) strain was restricted to medical facilities for decades. Containment was broken when an outbreak of a second MRSA strain sent people to the emergency

rooms in the 1990's. However, this second strain did not originate from the hospital but from the outside community filled with healthy people. The second generation of MRSA resulted from the over-use of antibiotics in commercial products, but this new strain showed lower resistance to antibiotics than MRSA-HA. The community-sourced MRSA spread like its predecessor by person-to-person and person-to-surface contact, so simple hygiene practices like hand washing and showering inhibited the second strain. In time, the second strain merged with MRSA-HA to form a third deadlier strain spread by community assistance, MRSA-CA. The new virulent MRSA-CA transmitted by multiple routes, caused various types of tissue damage, and possessed higher antibiotic resistance than the previous strains. MRSA-CA became prevalent among athletes exposed to person-to-person contact, shared facilities, and skin abrasions caused by STF turf burns attributed to the tufts' durable polymer and thin**,** sharp edges. As a facilitator of germ transmission, synthetic turf could turn skin abrasions into infection sites, although the tuft surface of the turf itself could not harbor MRSA-CA [1, 17]. Instead, without adequate cleaning, the shared facilities carried the pathogen that could infect many athletes. To prevent MRSA infection, maintenance of STF and associated facilities required cleaning agents for molds and bodily fluids. However, skin cuts could still acquire the MRSA-CA infection and transmit via contact by player-to-player and unguarded surfaces.

With no previous pathogenic study, GCRI was a feared contributor to MRSA transmission because athletes could carry small infill particles outside the field via clinging to uniforms, incidental inhalation or even ingestion. However, pathogen studies showed MRSA growth was not possible on GCRI:

> These infilled systems are not a hospitable environment for microbial activity. They tend to be dry and exposed to outdoor temperatures, which fluctuate rapidly. Plus, the infill media itself (ground-up tires) contains zinc and sulfur, both of which are known to inhibit microbial growth. Considering the temperature range for growth of S. aureus is 7-48°C (44.6-118.4°F), we didn't expect to find this bacterium in fields exposed to sunlight, since the temperatures on these fields far exceed 48°C frequently. [17]

Thus, the chemistry of GCRI, which might cause potential harm for humans with its zinc/sulfur composition, had effective antibiotic properties. In fact, possible substitution of GCRI rubber with less hostile components increased bacterial activity in the infill. For example, a mixture of sand and rubber could harbor bacterial levels 50,000 times higher than GCRI alone [1]. Consequently, scientific research thus revealed that rubber crumb made 3G STF resistant to the survival and growth of pathogens such as MRSA, and any future infill substitute thus has to perform in a similar antimicrobial fashion.

2.3 Alternative Polymer Waste Streams

To paraphrase Dr. Liesemer, an enlightened objective was using recovered material for other commercial purposes in addition to the material's original application [15]. The creation of scrap tire markets provided avenues for automobile rubber other than hazardous storage or expensive disposal. One of these markets was ground rubber, which became GCRI infill and improved impact safety and performance of synthetic turf. Other markets existed such as tire-derived fuel, civil engineering projects, and other ground rubber applications such as tire retreading, rubber-modified asphalt, and many

play surfaces besides fields [12]. The combination of reclamation markets consumed tire stockpiles while demand continued to rise yearly. The increased demand for tire rubber plus safety issues with GCRI created incentives to find an alternate infill that keeps cost down while promoting safety in STF. Since discarded tires constituted only 1.2% of municipal solid waste, the landfills had other potential streams for infill. Regardless of source, the new material had to possess the same safety enhancements and environmental benefits of rubber infill without the GCRI issues.

2.3.1 Post-Consumer Carpet

Similar to automotive tires, tufted carpet became a major consumer staple during the latter half of the 20th century. However, tires were designed for traveling comfortably on dirt and harsh road surfaces, while tufted carpet provided comfort and aesthetics for the indoors. Many kinds of carpet were developed in numerous cultures over thousands of years, and the modern tufted pile carpet was created with synthetic yarns by the American carpet industry in the 1950's [24]. After an initial period of U. S. domination, tufted carpet manufacturing shifted to other countries and left the U.S. with only ~45% of the world market by 1999. By the start of the 21st century, American carpet manufacturing had consolidated to a few regions such as Dalton, GA, which supplied ~70% of U.S. demand.

2.3.1.1 Tufted Carpet Construction

Since its modern re-invention during the 1950's, carpet became a flexible composite made of yarn facing upwards (tufts comprising the pile) that was locked in place (tufted) by a woven base fabric (the primary backing), a bonding compound, and often a woven secondary backing [24]. By 1990, carpet came in two basic constructions:

broadloom and tile. The common feature between these two carpet types was the tufted face pile, with ~90% of mass-produced carpet being tufted rather than woven by 1999 [24]. The tufted face yarns occurred as either loop pile, cut pile or a combination of both (Figs. 2.5 and 2.6).

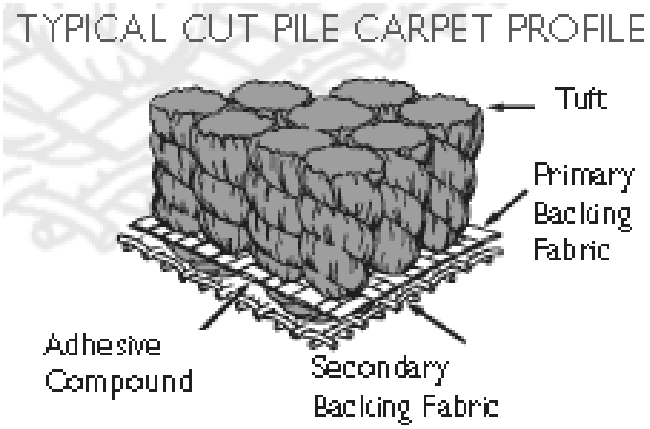

Figure 2.5. Cut-Pile Broadloom Carpet Construction [24]

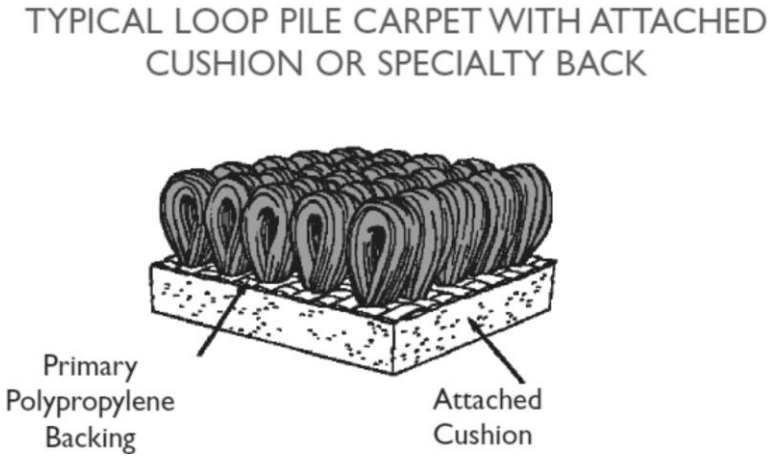

Figure 2.6. Loop Pile with Specialty Backing [24]

The materials beneath the pile and primary backing defined the type of carpet as tile or broadloom. Broadloom carpet used a flexible, cured styrene-butadiene rubber (SBR)

latex filled with ~60% by weight powdered CaCO3 bonding formulation that allowed rolling up the finished carpet for transport, storage and eventually floor installation. Broadloom carpet became the preferred floor covering material for homes and schools because the flexible backing and soft pile felt comfortable for walking or resting. Consequently, soft tufted broadloom carpet became the most voluminous floor covering material in the U. S. comprising 74% of the carpet market that produced 1.9 billion square yards in 1999 [24].

In contrast to residential property, the heavy, voluminous foot traffic in commercial facilities such as airport terminals, office buildings, etc., demanded a carpet floor covering that was more durable and designed to be functional. Tile or modular tufted carpet was designed with "hard backs" made of thermoplastic polymeric layers coupled with a single nonwoven fiberglass layer that were stiffer and withstood heavier foot traffic stress than residential broadloom tufted carpet (Fig. 2.7) [24, 25].

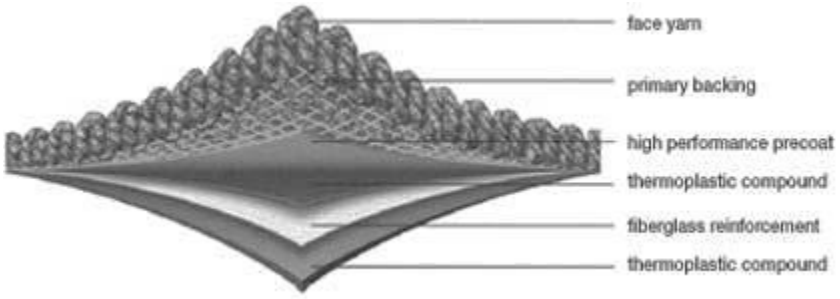

Figure 2.7. Tile or Modular Carpet Construction [25]

Compared to broadloom carpet, tile backing incorporated more numerous and varied materials that determined its specific function. The enhanced durability of the backing was too inflexible to roll up, so dimensions were reduced to manageable and stackable portions for transport and storage (the standard carpet tile size today is a 2 ft. by 2 ft.

square). Another benefit of the tile dimensions and stiffness was easier replacement of selected areas due to wear, stain damage or changing aesthetics, instead of replacing an entire floor area of carpet. Regardless, the characteristics of the backing made carpet tiles feel harder to the touch or to lay upon than broadloom carpet, thus confining the product mainly to commercial locations.

For tufted yarn, the fibers came from a variety of polymeric materials such as nylons, polyolefins, polyesters, acrylics, wool or cotton, but the vast majority of fibers (99%) came from synthetic sources, and in particular, the first three materials listed [24]. With improved production technology and high demand, pile yarn production increased each passing year since the 1950's. By 1999, the largest tufted carpet manufacturer alone consumed two million pounds of fiber per day [24]. The primary and secondary backing supported the pile, although the type of material changed according to residential and commercial carpet type. Residential carpet backing normally used polypropylene woven tape fabric of different constructions for both the primary and secondary backings bonded with styrene-butadiene latex filled with powdered calcium carbonate (~60% by weight filler). For carpet tile, the tufted backing contained more varied compositions such as plasticized polyvinyl chloride (PVC), amorphous resins, polyurethane and fiber glass. Overall, both broadloom and tile tufted carpets have evolved as highly-complex, soft composite constructions in both form and chemistry in order to meet high performance consumer demands with little degradation from extensive use. In that sense, the products mimic modern passenger tires.

2.3.1.2 Carpet Reclamation

When carpet was discarded to landfills, the scraps reached huge volumes that proved difficult to contain. Carpet manufacturers asked CRI to study possibilities for making production sustainable and for recycling used carpet. In 2002, CRI recommended to manufacturers a Memorandum of Understanding for Carpet Stewardship (MOU) leading to work with government at various levels seeking alternate uses of post-consumer carpet (PCC). The MOU set goals over a ten-year timeline to divert all PCC away from landfills [26]. The Carpet American Recovery Effort (CARE™) of CRI monitored progress of PCC diversion and its specific uses over the decade (Table 2.4 and Figure 2.8).

Table 2.4. PCC Diversion from Landfills, 2002-2012 (CARE™) [24]

	Actual (million pounds)											
Year	2002	2003	2004	2005	2006	2007	2008	2009	2010	2011	2012	2013
Total Discards[1]	4,409	4,396	4,588	4,916	4,687	4,560	4,228	3,718	3,373	3,816	3,540	3,703
Diversion												
Reuse	9	0	0.3	0	0	0	4	12	2	1	5	12
Recycled	46	87	98	194	239	275	243	246	271	250	294	172
Int'l Recycle (43.6%)												13
TOTAL RECYCLE	55	87	98.3	194	239	275	247	258	273	251	299	197
Waste-to-Energy	1.9	7	9	27	21	19	41	47	38	46	42	58
CAAF or Cement Kiln	0	0	1	3	0	2	2	12	26	36	11	23
Landfill[2]												254
TOTAL Landfill Diversion	57	94	108	224	260	296	290	317	337	333	352	534
Recycling Rate	1%	2%	2%	4%	5%	6%	6%	7%	8%	7%	8%	5%
Diversion Rate	1%	2%	2%	5%	6%	6%	7%	9%	10%	9%	10%	14%

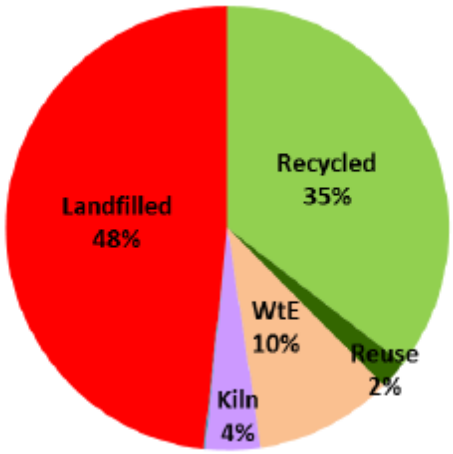

Figure 2.8. Carpet Reclaim Destination [26]

From 2002 to 2011, the recovery effort fell short of yearly goals due to cheap virgin material and limited results from developing new markets. Most of the research focused on recycling the carpet face pile composed of synthetic fibers, a uniform material stream [27]. During production, the carpet pile constituted 50% of carpet mass but contributed 85% to the cost [24, 27]. Recycling efforts naturally focused on the most expensive part of the carpet, i.e., the component with the highest added value. The remaining materials from PCC broadloom included unrecovered face fibers (from the "back loop" of yarn located back side of the primary backing and locked in the cured SBR adhesive layer); the woven primary and secondary backings; and the fine calcium mineral filler particles surrounded by SBR latex binder, all together creating a mixed polymeric thermoplastic/thermoset waste with added abrasive $CaCO_3$ that required costly disposal without a viable market. For PCC tile, the back-tuft fiber and primary backing contributions to the waste were the same, but the plasticized PVC and nonwoven fiberglass backing layers added a separate level of recycling complexity.

For the duration of this study, the material remaining after removal of the carpet face fibers from PCC was placed under the umbrella term "carpet carcass", specifically the thermoplastic PVC/fiberglass backs from tile carpet and the primary PP backing glued with $CaCO_3$-filled SBR latex to the secondary PP backing from broadloom carpet. As a collection of benign discard materials, ground and prepared carpet carcass crumbs became alternate infill candidates for STF because they were cheap, available and environmentally benign to human contact. The discarded carcasses were analogous to tire rubber since both had an elastomeric polymeric matrix with incorporated filler. Unlike tire rubber, tufted carpet was intentionally designed and constructed to be safe for extensive, direct human exposure, e.g., it did not contain lead, COPC or any substance with known adverse health effects. The available sources of post-consumer broadloom and tile carpets also provided a wide variety of material streams such as styrene-butadiene rubber (SBR) latex, calcium carbonate ($CaCO_3$), PVC, polyurethane, synthetic back-tuft and primary/secondary backing fibers, and fiberglass. The different materials held potential differences in STF infill impact energy absorbance while creating a spectrum of properties to fit individual fields. However, material suitability depended on other variables for synergistic STF interaction with the carpet-based crumb infill in order to perform similar to standard GCRI.

2.3.2 PET

Polyethylene terephthalate (PET) bottle flake was another possible thermoplastic polymeric waste stream for STF infill crumb since it was non-hazardous chemically and could be ground into particle sizes similar to GCRI. Carpet suppliers already utilized PET from discarded drink bottles (soda, juice, water, etc.) after they were chopped into

flakes and extruded it in other products like carpet fiber, especially colorless PET fiber that was dye-able to any desired post-extrusion shade [26, 28]. However, a portion of the recycled PET drink bottles were tinted green with pigment concentrate added into the initial melt molding formulations of the bottle preforms, which limited the subsequent dyed-over carpet face fiber to only six acceptable commercial shades [28]. The remainder of the green PET stream was directed toward low value-added products such as extruded box/bale strapping, or simply diverted to the landfill. However, as a potential STF infill candidate, the green tint of the PET bottle flake stream presented a benefit rather than a detriment, as it would color-blend as crumb with the green STF blades to eliminate the "black cloud" formation when players impact the turf, and by being green instead of black in color, it would simultaneously lessen the black body heat island effect that GCRI entails. In addition, PET drink bottles were designed to contain fluids for human consumption, and therefore derived infill crumb would be safe for human contact.

Despite availability of material and an established record of recyclability, PET could pose unique issues not shared by carpet backing. This type of PET was a non-plasticized and non-filled system with no chemical or structural similarity to crumb rubber. In addition, the glass transition of bulk semi-crystalline PET was determined to be 70° – 76° C (158° – 169° F), dictating that the material is in its hard/brittle state at ambient temperatures. However according to industrial sources, moderately crystalline (60%) PET fibers exhibited 95-100% recovery after being subjected to a 2% strain force and an ultimate strain-to-break of ~30%, indicating that the material possessed mild elastomeric properties at room temperature. In summary, the green PET recycled

bottle flake stream provided a marked contrast in material purity and elastomeric properties to the GCRI and carpet-derived infill candidates.

2.4 Competitive Products

When GCRI became popular in 3G STF, demand for infill created an economic incentive to develop original competitive products made from cheap virgin materials. The public and government entities then expressed concern about health hazards of GCRI, and producers of substitute infill materials derived from virgin polymers claimed them to be safer (albeit much more expensive) alternatives. For example, the company TargaPro, Inc. (www.targapro.com) advertised Organite™ in 2008 as "Greener than Grass" with none of the problems of GCRI:

> Organite™ is an all-natural proprietary composite of organic and inorganic materials, which provides an environmentally-friendly, biologically safe alternative to recycled tire rubber and/or sand, as an infill in artificial turf. The product granules contain NO synthetic chemicals and, therefore, contain no polycyclic aromatic hydrocarbons (PAHs); butylated hydroxyanisole (known carcinogens found in both ambient ground and cryogenically ground recycled-tire-rubber); silica-sand or any other particulate known to cause respiratory irritation. Sand is not permitted as a component of any infill matrix or formulation, incorporating Organite™. This infill alternative eliminates possible exposure to carcinogens; respiratory exposure to toxic or irritant particulate from rubber dust or silica-sand; ingestion of toxic chemicals by children; as well as run-off contamination of the aquifer by the infill materials. (sic) [29]

In addition to this promotion in 2008, Targapro listed several titled articles about the perils of tire-based infill such as "*NYC Crumb Rubber Fact Sheet Ignores Warnings*" and "*California Initiates Study That Questions the Use of Crumb Rubber in Synthetic Turf"* [30]. However, the released statements did not include costs or components associated with the Organite™ virgin material or the AEGIS® antimicrobial finish applied to the surface of the product. The only detail of the product's technical specifications came from the Organite™ website (Table 2.5).

Table 2.5. Reported Organite™ Physical Properties [29]

SPECIFIC GRAVITY	1.2– 1.4
pH VALUE AT 25ºC (IN WATER)	4-6
FREE MOISTURE (80ºC FOR 15HRS)	3-9%
G-MAX (ASTM F-355) [turf construction specific]	110 – 160
HARDNESS-VICKERS NO	25-30
MOHS SCALE	3-4
BULK-DENSITY (LBS PER CU. FT.)	42 +/- 2

Overall, the Organite™ website was an advertisement without extensive peer-reviewed, academic or industrial research that directly compared the infill alternative to the rubber crumb. The only point of direct comparison was a specification in Table 2.5 of the product's Gmax value in turf that was 10-15 units higher than GCRI along with a higher bulk density at 42 lbs/ft^3 (0.67 gm/cc). No reference to Organite™ was found in the

scientific literature review or any other alternate STF infill material derived from virgin sources.

Although a commercial infill was not part of this study, the alternate infill products highlighted a health issue concerning GCRI pathogen infections [1, 17]. Any viable replacement to GCRI would need resistance to pathogens like MRSA, either innately or by applied finish. The AEGIS® applied finish product utilized with the Organite™ infill product is a chemical composition made from 3-(trimethoxysilyl)-propyl-dimethyl-octadecyl ammonium chloride as the active ingredient, a quaternary ammonium compound with known bactericide properties [31]. The quaternary ammonium works by two different mechanisms to create an antimicrobial bio-barrier: adhesion and cytolytic damage [32]. First, the silane portion creates chemical bonds with the substrate's surface to remain permanently in place instead of leaching away like other biocides such as nano-sized silver particles [33]. Next, the nitrogen's positive charge attracts negatively charged microbes to the hydrophobic tail that subsequently pierces the cell membrane (the "spear" mechanism), thus destroying the microbe. This process was known for decades and successfully utilized in the textile and medical industries to create permanently sanitized surfaces. However, exposure to outdoor soil removes this protection from cotton products, and the finish is relatively expensive [31, 33]. Application of the Aegis® finish chemistry to a technically-viable alternate infill would thus require extensive testing to prove short- and long-term efficacy and justify the extra cost of application.

2.5 Impact Measurements

The straightforward explanation of impact is an object experiencing "violent acceleration" upon hitting a surface [34]. However, the human brain was not so easy to define with a complex structure unlike any solid object and may have many intricate reactions to an high-energy impact event, e.g., as a football quarterback experiences when the back of his helmet violently strikes the playing field turf upon being tackled ("sacked") by a full-speed, on-rushing linebacker. While common injuries like abrasions and sprains were treatable and temporary, brain injuries were known to change the internal cognitive structure and carried risk for fatality. The most severe forms of brain damage were the subject of study and prevention, but little attention was given to concussions, i.e. mild traumatic brain injury (MTBI), or how multiple impacts might create long-lasting cognitive impairment [34, 35].

The human brain's vulnerability to short-term and long-term damage stems from its organic assembly: a pliable mass of tissue floating in cerebrospinal fluid and encased by a hardened skull [34]. The strain from a high-energy impact event causes many forms of motion that creates a variety of tissue damages that are categorized as focal or diffuse injury. Focal injury is defined as localized tearing of brain tissue and blood vessels that produced immediate damage such as fatal hemorrhaging (bleeding outside the brain) and hematoma (bleeding inside the brain). Diffuse brain injury is less severe but more widespread due to movement of the whole brain mass inside the skull. The cerebrospinal forces shear nerve cells and interfere with metabolic activity, leading to concussion. Both focal and diffuse injuries may occur during a single impact event, and cognitive damage can become severe, long-term and/or fatal after repeated impacts if the brain is not allowed enough sufficient time to heal. While understanding short-term brain

damage was the subject of study in impact related activities such as sports and automotive crashes, the connection between sports-related concussion and long-term mental disease was not acknowledged even as a possibility until after the 20th century [35].

In the past, sports participants used to consider mild head injuries as unavoidable work hazards that had to be "toughed out" without long-term consequence [36]. By 2009, increased public awareness elevated sports-related head injury to an important safety concern for professional and young athletes in high impact sports such as rugby, soccer and football. For example, medical research discovered early signs of Alzheimer's disease in NFL football players who suffered three or more concussions [35]. Improved brain imaging of NFL athletes found the same damaged regions in 41 retired players that matched Alzheimer's patients. Closer examination of the brain tissue from deceased athletes found unhealthy brown tangles between the neurons that were signs of chronic traumatic encephalopathy (CTE) [35]. These brains came from athletes in their 30's and 40's, and yet the neural pathways resembled those of 80-year- olds with advanced dementia.

At the beginning of CTE research, the NFL denied the possible connection between concussions and mental illness despite a spate of posthumous studies about former athletes who received repeated concussions on the field and deformations inside their brains [35]. The related reports detailed possible resulting ailments such as depression, memory loss and uncontrolled rage, which drew the attention of the U.S. Congress. The growing pressure from national and state governments prompted the NFL to fund independent research of CTE and issue stricter guidelines for diagnoses and

treatment of concussions [35, 36, 37]. MTBI was already known to be a potential epidemic within sports since 1977, and a more recent study found that emergency room visits related to concussions increased from 7,000 in 1997 to 22,000 in 2007 for 14- to 19-year old athletes [34, 36]. The higher number of concussions might have been the result of increased awareness by parents, coaches and doctors. Nonetheless, concern for child safety prompted the State Legislature of Washington to pass the nation's toughest laws in 2009 that spotlighted head injuries of student athletes, and six states considered their own laws in 2010. Soon the NFL followed suit by making definitive policy changes regarding concussions, including notifying professional athletes about the possible dangers of concussions by July 2010 [38]. Because of increased research and public awareness, sports-related concussions shifted from a mere annoyance to an important safety issue thanks in part to the research that is still ongoing at the time of this thesis report.

Although public awareness of the detrimental effects from concussions helped change sports institutions, scientific research of high velocity impacts began to include sports-related concussions by the end of the 20th century. The hard, detrimental impacts experienced during football games came from a variety of sources including player-to-player and player-to-surface contact. Previous studies covered the varieties of sports injuries without focus on synthetic turf, although unsuitable surfaces might be the cause of 79 – 100% of severe cognitive damage [30]. Even when narrowed to only surface impacts, an objective measurement of impact severity lacked consensus despite availability of methods from several organizations such as ASTM, ISO (International Organization for Standardization) and the Fédération Internationale de Football

Association (FIFA), an international governing body for soccer [21]. Prior to introduction of 3G STF in the 1990's, the number of impact test methods and affected organizations made universal standards difficult to adopt. For example, the U.S. Consumer Product Safety Commission previously denied the NFL League Players Association its last petition to establish a surface standard in 1976, almost four decades before concussive head injuries became paramount [21]. In addition, the industry methods tested older synthetic turf, while 3G STF possessed new factors such as infill addition and longer tufts designed specifically to absorb high-energy impacts. Despite the lack of peer-reviewed literature about 3G STF testing, ASTM implemented methods for measuring impact properties of playing surfaces which were implemented in this research, including ASTM F355, F1551 and F1936.

Even though the correlation between a mechanical test and athletic injury was questionable, the impact test selected for this study was designed specifically for artificial sports surfaces to produce a variety of measurements, all related to shock absorption [2, 39, 40]. ASTM F355 and F1936 described the device components as a broad shaped weight called the missile, a rigid restraining ring to keep all movement vertical, and an acceleration transducer to measure the forces of deceleration during impact. When initiated, the cylindrical impact missile would fall 61 mm inside the restraint to simulate a human head falling to the turf surface without unwanted vibrations while the various sensors simultaneously measured rapid deceleration, usually with a piezoelectric accelerometer, during missile impact [2]. Subsequent computer analysis of the resulting electrical signal produced an acceleration-versus-time curve that covered milliseconds of

the impact event. According to ASTM F355, F1551 and F1936, an additional two tests produced an average curve that required further mathematical assessment.

With further analysis, the acceleration-versus-time curve was transformed into several values related to impact, namely the Gmax, Severity Index and Head Injury Criterion (Fig. 2.9).

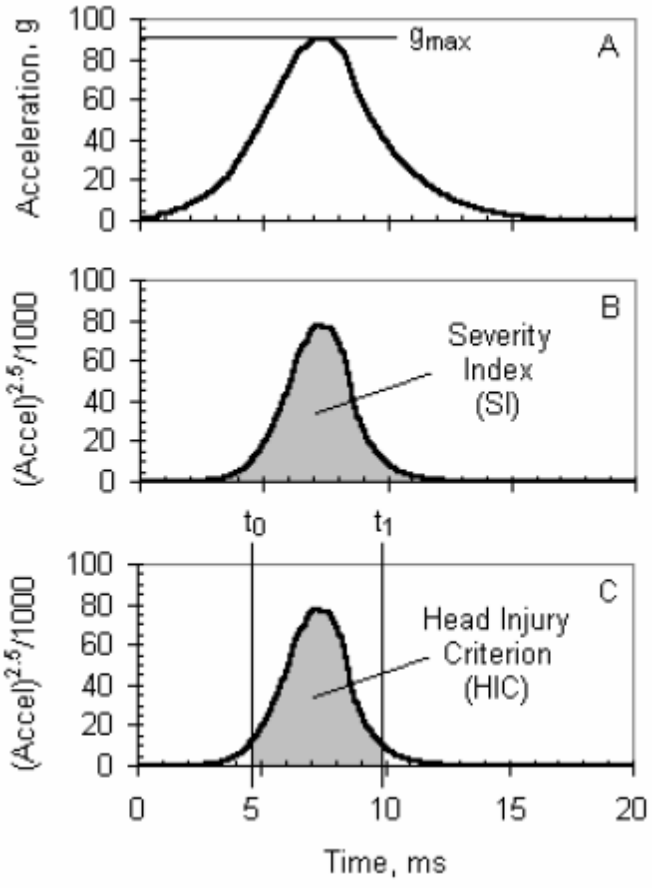

Figure 2.9. Three Different Results from Measuring Singular Impact [34]

Despite the similar curves in Fig. 2.9, each one used different approaches to gauge shock absorption capability [21, 34]. First, the acceleration (or more specifically, the deceleration) of the missile during impact was converted to units of "g" where one "g"

equaled the constant acceleration of gravity, 9.81 m/s^2. The peak of this initial curve was the point of maximum deceleration experienced during impact, thus designated as the "Gmax" value. By measuring the maximum deceleration of a falling head, the magnitude of the Gmax value could also gauge shock and shock-induced concussions [34]. Overall, the Gmax value was easy to determine and predicted immediate danger from the acceleration-time curve, making it one of the most ubiquitous measurements of shock absorption.

However, the impact tester had issues due to misunderstanding the evaluation of impact absorption. For example, two peaks on different turf fields could reach the same Gmax value, e.g., 80, but the span of the Gmax curve of one field could last eight milliseconds while the other field covered only six milliseconds [21]. The difference between the whole curves meant that a falling body would experience the force of impact two milliseconds longer on the second field, thus increasing the probability of injury. Another source of confusion was the dual use of the term "hardness". Hardness was related to the comfort of touch or to compaction of surface, both unrelated to safety [21]. Yet hardness also became associated with Gmax and impact attenuation of turf fields in numerous studies and contracts [17, 41, 42]. The Gmax value by itself would thus not be sufficient or distinct enough to gauge or describe the effects of high-energy impacts, especially for long-term cognitive injuries, which was also controversial.

Since the same Gmax value could exist for different fields with non-comparable exposure to impact forces, the impact curve was further modified to correlate the dissipation of impact energy to the probability of cognitive injury, thus creating the latter two plots in Fig. 2.9: the Severity Index (SI, Plot B) and Head Injury Criterion (HIC, Plot

C). SI and HIC differed from Gmax for two reasons, empirical data and exposure time. Starting in the 1950's, researchers at Wayne State University developed a physical model based on early experiments with animals and human cadavers [34, 40, 41]. The researchers applied known impact forces to the skulls of the subjects while they measured intracranial pressure that indicated degree of injury severity. According to the data, minor injuries with reversible brain damage could be divided from major brain damage that caused severe brain malfunction or death, thereby creating a tolerance curve from the acceleration-time impact data (Fig. 2.10).

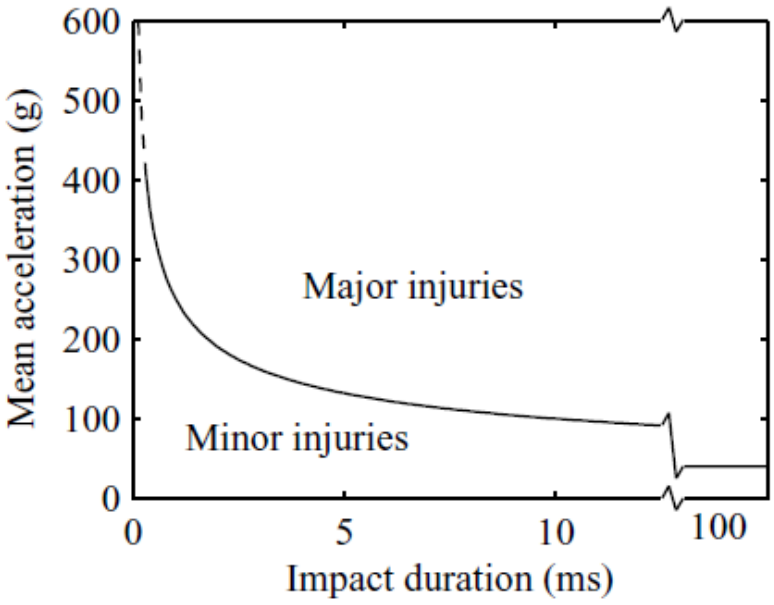

Figure 2.10. Wayne State University Cerebral Concussion Tolerance Curve [40]

The Wayne State University Cerebral Concussion Tolerance Curve (WSTC) demonstrated a non-linear relationship between impact exposure and severity of injury. In short, the human brain could endure high "g" for only short durations but could not tolerate lengthy exposure times even under low "g". As a result of the Wayne State

University research, impact analyses needed to account for time in order to accurately predict the severity of a concussion, an important cause of long-term, sports-related brain damage.

After the Wayne State curve showed a non-linear relationship between impact time and brain damage severity, C.W. Gadd proposed a Severity Index (SI) for the overall acceleration-time curve (Equation 2.1).

$$G = \int_{t_1}^{t_2} [a(t)]^{2.5} dt$$

Equation 2.1. Gadd Severity Index Integral [40]

Equation 2.1 originated from shifting the WSTC to a logarithmic scale and fitting the results to a function by least squares linear approximation, Eq. 2.2 [34, 40].

$$2.5 \log \bar{a} + \log \Delta t = 3$$

Equation 2.2. Fitting the Nonlinear Wayne State Curve [40]

With a logarithmic base of 10, the slope of the function equaled -2.5 and the intercept reached 3. With a base of ten, the intercept equaled a SI value of 1000 meters$^{2.5}$/seconds^{4}, which defined a critical limit of human tolerance to impact before reaching life-threatening trauma. Then the impact acceleration-time data from a curve such as the first one in Fig. 2.9 was shifted by exponentially increasing the acceleration

data with 2.5, which was discerned from Eq. 2.2. Next was integration of the weighted acceleration values with Eq. 2.1 to approximate the total exposure during the impact event and calculate the Severity Index. Through the SI value, any impact curve from a sports facility turf field could be related to the WSTC, which was originally designed for car crashes and helmets [2, 21, 40]. However, an equivalent Gmax value between two fields did not mean equal safety nor even an equal SI index if the impact curves covered different lengths of time because the human brain could endure low "g" values at the millisecond exposure at both ends of the acceleration-time curve. Therefore, the integral had to be restricted to times of the higher Gmax regions of the impact curve that most likely caused severe head injury, hence creating the Head Injury Criterion (HIC).

$$\mathrm{HIC} = \max_{t_1, t_2,\ t_2 - t_1 \leqslant \Delta} \left\{ \left[\frac{1}{t_2 - t_1} \int_{t_1}^{t_2} a(t)dt \right]^{2.5} (t_2 - t_1) \right\}$$

Equation 2.3. Head Injury Criterion Integral [40]

The HIC curve in Fig. 2.9 came from applying Equation 2.3 to the impact curve, which counted the high "g" portions of the curve that most likely caused brain injury. Before application to turf, the HIC was proven in other types of crash studies such as automobiles, playground, and helmets to name a few [34, 40]. The accumulated results expanded the knowledge of injury-versus-impact correlations to probability of the severity of injury (Fig. 2.11).

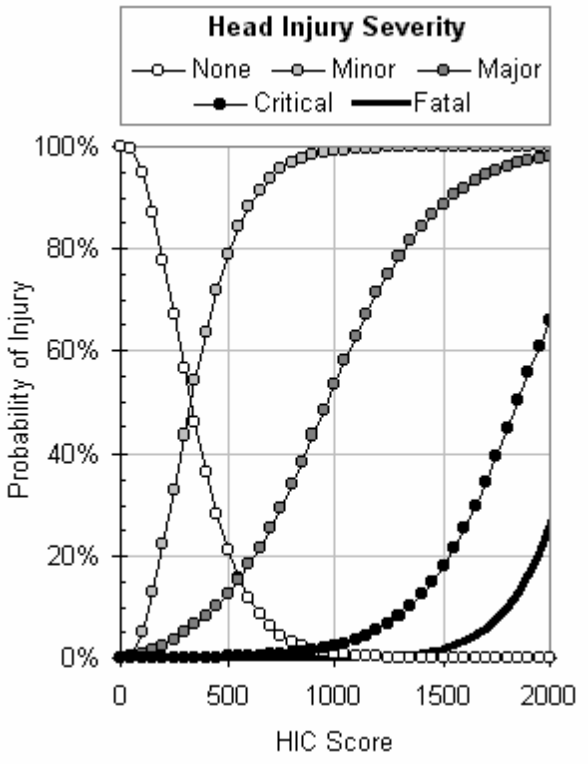

Figure 2.11. HIC Value Correlated to Injury Type [34]

According to Fig. 2.11, a person experiencing a 500 HIC value had a 79% probability of developing a minor injury like a concussion and a 13% probability of a major injury such as a skull fracture. Going above 1000 HIC guaranteed dangerous brain damage, and the risk increased exponentially with higher HIC. Eventually, the Head Injury Criterion of 1000 became a factor for selecting play surfaces, although 200 Gmax remained the preferred standard, which was easier to determine and approximate [21, 34].

For the purpose of this study, the most widely used impact limits for preventing critical injury became 200 for Gmax and 1000 for HIC, but these values did not guarantee absolute safety from any cognitive injury. Both were baselines in this study to ensure low probability of long-term cognitive damage. However, the application of third-generation turf as a sports surface and the use of HIC on synthetic turf were both

relatively new, so absolute values for risk were not available [21, 34]. Therefore, the results of this research only apply to comparisons of different infill materials, before turf application and then integrated into turf of two different turf constructions (3G and 4G STF's) since no athletes were harmed in the commission of this study.

CHAPTER 3

SCOPE OF RESEARCH

3.1 Objectives

The overall objectives of the reported research were to first investigate GCRI impact absorbance performance alone and in turf, then target polymer waste streams to identify, develop and demonstrate technically-viable, functional replacements for the GCRI currently used as standard infill in 3G and 4G STF's; and finally evaluate the economics of GCRI and the chosen alternate(s). The infill replacement or replacements not only had to mimic the impact absorption of GCRI, but also minimize the safety and environmental concerns while being projected as reasonably cost-competitive in commercial-volume production. Although granulated rubber infill was the culmination of 40 years in synthetic turf development, 3G STF and its integrated GCRI infill lacked extensive published research to verify improvement of safety or provide a basis for comparing different materials [2, 21, 39, 40, 41]. Industrial test methods also provide only impact performance specifications that aid facilitation in the field, but not future infill development. Lack of established, reported research provided an opportunity in this work to study a specific and critical infill performance characteristic: high-energy impact attenuation.

Due to the varieties of available activities, setting the priorities of performance and safety variables depended on the chosen sport. For example, a football player needed padding and protective clothing for body-to-body impact protection, while a soccer player dressed relatively lighter for enhanced speed and coordination. Regardless of the

sport, athletes depended on the field surface to be safe enough for playability without creating major health issues, so impact absorption against this surface was fundamentally important. For this study, cognitive health was considered paramount to other types of impact damage since mental cognizance could affect life beyond the sports field. The principal sport played on most artificial fields in the U.S. has historically been American football, which involves violent impacts with the players and the playing field turfs [2]. The long-term effects of such impacts were beginning to be acknowledged by 21st century medical research such as a 2012 study that found NFL players were four times more likely than the general public to develop mental degenerative disorders such as Alzheimer's or Lou Gehrig's disease (ALS) [43]. Concentrating on the cognitive effect of surface impact thus guided the research towards finding an alternate, comparatively-economic infill that achieved a significant cognitive safety factor. Finding GCRI substitutes required multiple steps with individual benchmarks:

1. Develop a test protocol for GCRI in synthetic turf under laboratory conditions
2. Study fundamental GCRI/3G STF variable(s) that affect impact absorption
3. Test the performance of alternate infill samples in 3G STF
4. Compare the economics between GCRI and viable infill alternative(s)
5. Make recommendations for future research

Each task developed improved understanding of turf/infill interactions, while identifying and developing an alternative infill(s) to GCRI from targeted polymer waste streams that would be economically competitive against virgin material.

3.2 Technical Approach

After determining individual tasks based on the overall objectives of the research, the next step was selecting available material and appropriate tests. The experimental work had specific logistical needs such as the third generation turf, crumb rubber infill, polymeric waste streams and an impact testing setup. These supplies were important to the technical work that was divided into five overlapping phases:

1. Test selected properties of GCRI and establish a GCRI baseline for impact performance.
2. Test the synthetic surface and its interaction with GCRI with two independent variables, pile height and infill loading.
3. Test infill alternates by the same test methods.
4. Select one property of each alternate to modify and retest performance.
5. Study the economic feasibility of the most viable alternate infill candidate(s) as compared to GCRI.

3.2.1 GCRI Baseline

Granulated crumb rubber came from a variety of vendors that processed automotive tires via two possible grinding processes. Whether by ambient or cryogenic processing, the whole tire was pulverized multiple times for the crumb to reach a size range that could penetrate the STF tufts, although particle form was random without extra treatment [11, 16, 39]. Standards for optimized infill properties such as shape, chemical composition or tire sources were absent from published research or industry-made specifications. Determining the relevant qualities of the granulated rubber crumb thus required a survey of the product available in the market. Multiple vendors supplied

samples as listed in Table 3.1, with designations assigned according to chronological order of shipment and processing. None of the rubber recycling facilities kept large inventories of GCRI, so processing occurred relatively close to the shipment date. The location of the processing facility, source of rubber and type of processing were confirmed by phone interviews with the company liaisons.

Table 3.1. GCRI Sources

Lot #	Date Received	Plant Location	Tire Source	Process
GCRI-1	July 10 2008	Calhoun, GA	Trailer	Ambient
GCRI-2	October 31 2008	Calhoun, GA	Trailer	Ambient
GCRI-3	August 19 2011	Houston, TX	Proprietary	Ambient
GCRI-4	August 31 2011	Calhoun, GA	Trailer	Ambient
GCRI-5	November 15 2011	Braddock, PA	Passenger Car	Ambient
GCRI-6	November 15 2011	Braddock, PA	Passenger Car	Cryogenic
GCRI-7	June 13 2012	Tucker, GA	Proprietary	Cryogenic
GCRI-8	June 25 2012	Tucker, GA	Proprietary	Cryogenic

The samples of rubber crumb provided a regional overview of the GCRI product available in the marketplace. When entering the experimental phase, the data from a laboratory setting served as a baseline for the infill alternatives.

3.2.2 Turf Evaluation

Due to the availability of multiple 3G STF's, the selection of a standard synthetic turf surface depended on determining the most popular brand sold by a national supplier. In 2008, Synthetic Turf Resources recommended the most popular brand STF was

AstroTurf® Gameday Grass™ 3D-52. By 2011, new brands of STF were on the market with enhanced shaped tuft blades and improved resilience [39]. Towards the end of research, a sample of blade shape-enhanced AstroTurf® (3D-60H), a 4G STF, was compared to the standard. Product specifications from the vender are summarized in Table 3.2.

Table 3.2. AstroTurf® GameDay Grass™ Brands

Turf Sample	**Standard**	**Enhanced**
Brand	3D-52	3D-60H
Primary Yarn Fiber	Polyethylene	Polyethylene
Yarn Blade Cross-Sectional Shape	Diamond	Horseshoe
Nominal Pile Height (mm)	57	51
Face Weight (gm/m^2 [**oz/yd^2**])	1763 [**52**]	2034 [**60**]
Total Fabric Weight (gm/m^2)	2915	3187
Total Yarn Linear Density (gm/10,000 meters)	17,490	16,500

The 3D-52 3G STF provided the body of research data and infill comparisons, while 3D-60H results demonstrated ongoing 4G STF development. Even if the infill alternates displayed sufficient impact performance with the standard turf, the enhanced turf could improve impact absorption with the same infill material and loading level, hence the comparison of the two AstroTurf® variations.

Regardless of 3G STF improvement, the literature review found little mention of the interaction between the infill and turf. After selecting the standard turf, two fundamental turf properties became test factors for quantifying the influence of turf-infill interaction on shock absorption: pile height and infill loading. At initial study, the weight (load) of rubber infill per square foot of turf was added at increments up to the maximum

amount suggested by the infill suppliers. Pile height (the distance from backing to the top surface of the tufts) was modified to gauge interaction with the infill when variable loading was retested. Consequently, analysis of the relationship between the infill and the tuft helped indicate simple (linear) or complex (non-linear) interactions.

3.2.3 Waste Stream Selection

While GRCI came from dedicated reclamation facilities, the alternate waste streams came from recovery processes attached to product manufacturing or disposal. Regardless, the primary objective was to find new use for otherwise discarded polymeric components. The concentration of carpet producers in Georgia provided a logistical opportunity for an academic study with potential application to private industry. Local carpet suppliers also confined the number of samples to a manageable volume. Finally, carpet waste carcasses became a logical choice as an infill replacement candidate since Georgia is the largest producer of tufted carpet in the U.S.

In addition to logistics, the waste carpet carcass stream shared certain characteristics with GCRI. The cured. filled SBR adhesive in the waste broadloom tufted carpet carcass was difficult to reclaim due to its composite structure, along with its occluded PP and back-tuft fibers, so the majority of the mass generated from the post-consumer carpet deconstruction processes went to the landfill. In contrast, waste carpet tile carcasses had thermoplastic polymers adhered to primary PP backing and a nonwoven fiberglass layer. The common thread between broadloom and carpet adhesive was filler solid particles (powdered calcium carbonate) encased by a polymeric matrix, usually SBR rubber for broadloom and PVC for tile. This construction was akin to tire's

carbon black surrounded by polymeric rubber, which was also usually discarded until feasible markets were developed.

As for the PET waste stream, other carpet centers collected discarded plastic PET drink bottles to produce carpet fiber. The reclaimed PET stood in stark contrast to both broadloom/tile carpet and tires since its unfilled polymer matrix created a solid homogeneous structure. The selected green PET flake stream had limited application compared to clear flake in tufted carpet production, as the former was restricted to only six over-dyed shades for the tufted carpet market. In conclusion, the carpet industry provided three polymer waste streams that served as possible infill alternatives to GCRI in 3G STF without significant cost or difficulty of acquisition.

3.2.4 Waste Stream Modifications

After initial testing, the waste streams' comparisons to GCRI prompted questions about relevance of certain properties and possible improvement. The general assumption remained that any change that affected performance also increased cost of the final product, but cost might be justified by exceeding desired impact performance and/or negating GCRI-based problems. In addition, changing a fundamental property of the alternate material could help quantify its relation to impact absorption. The possible modifications had three categories: physical, thermal and chemical. Physical change involved mechanical action such as particle separation or grinding to achieve a desired composition or particle size akin to rubber infill. Next, thermal treatment changed the structure of infill by melting plastic fibers, boiling away plasticizer or reducing crystallinity. Chemical alteration was another option, but it was not feasible for this study due to additional material costs and unknown health hazards. The modifications

occurred under laboratory settings since the suppliers could not adjust their processes to generate relatively small quantities for research. Overall, the goals of infill modification were to understand the influence of a material property if not improve impact absorption, keep cost of the alternate infill to a minimum, and prevent additional hazards.

3.2.5 Economic Feasibility

Towards the end of the project, the best-performing alternate infill material(s) required an analysis of economic feasibility in comparison to standard GCRI. The total projected cost per pound of the infill included collection, transport and processing of the stream. Regardless of chosen stream or company, the cost was preliminary since each facet was subject to variations such as material and collector availability; energy and time costs for collection; volume of production to leverage economy-of-scale; and the overall economics of physically processing the material(s) to GCRI specifications. Towards that end, the estimate was compared to the cost of crumb rubber in order to project economic viability in the market and future research paths.

CHAPTER 4

EXPERIMENTAL

4.1 Materials

4.1.1 Synthetic Turf Setup

The first phase of this study developed an infill test protocol that required a standard synthetic turf platform. The initial task was to select the standard turf surface that was the most popular selling brand: GameDay Grass™ 3D brand manufactured by Astroturf®, Dalton, GA. The turf provider, Synthetic Turf Resources (STR), supplied two brands of GameDay Grass™ (GameDay for short): 3D-52 and 3D-60H. Both brands had similar zones filled with different kinds of blades (Fig. 4.1).

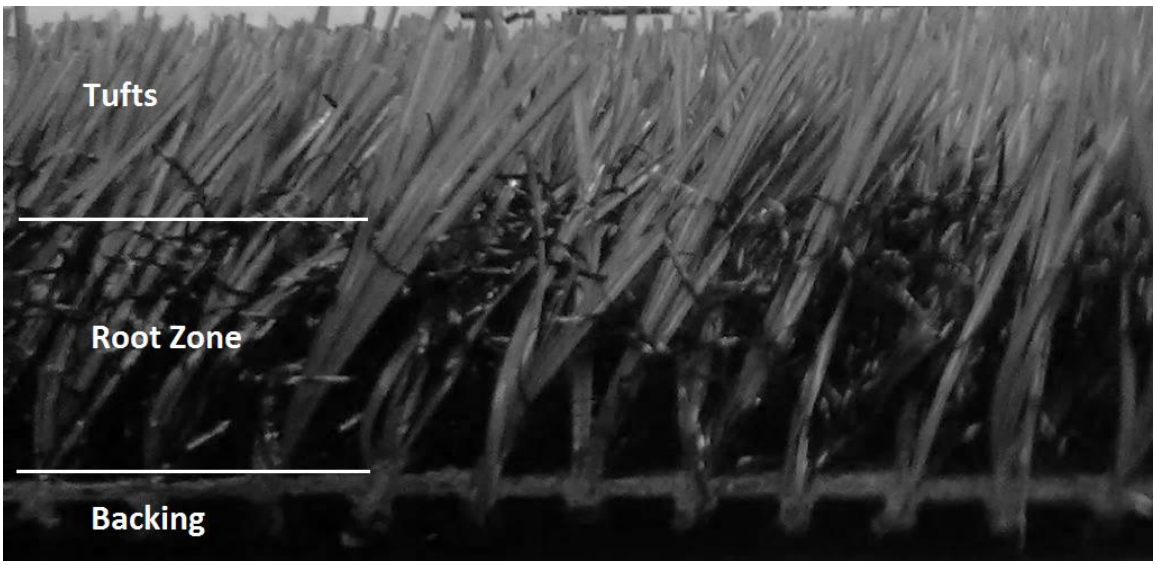

Figure 4.1. Synthetic Turf Zones

The bottom level backing was a flexible mat that supported the vertical blades that projected into both upper levels [7]. According to literature and the turf vender, the root zone contained curly nylon fibers that supported the taller tufts made from multiple polyethylene blades twisted together and helped prevent compaction of infill [7, 20]. The differences between the two brands of turf are summarized in Table 3.2 and highlighted in Figures 4.2 and 4.3.

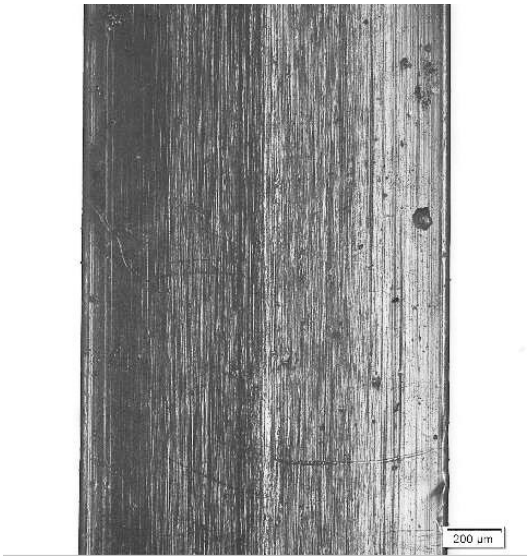

Figure 4.2. Longitudinal View of 3D-52 Turf Diamond Cross-Sectional Blade

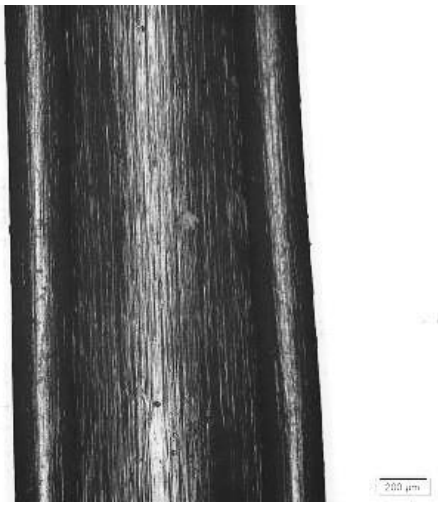

Figure 4.3. Longitudinal View of 3D-60H Turf Horseshoe Cross-Sectional Blade

The Diamond Tuft of the 3D-52 turf, which was the standard surface for this study, exhibited a thickened mid-section with straight edges (Fig. 4.2). The Horseshoe tuft was introduced in 2010 in the 3D-60H turf with two end columns and a thicker diameter than previous yarns to improve stiffness and mechanical memory, an improvement attributed to fourth generation turf (Fig. 4.3) [39]. The newer 3D-60H version of GameDay Grass™ was compared to 3D-52 to gauge the effect of tuft cross-section shape, although the 3D-52 remained the standard for all infill testing.

For testing in a laboratory setting, the preferred setup was a wooden box or frame that accommodated test instruments [9]. For this study, the wood was the pressure treated variety that came from local retailers. The wood height was 1.5 inches to encompass the infill after filling the turf, and width was 5/8 inches to provide a sturdy foundation to attach the turf backing after shaving off tufts off the affected edges. The length of the wood was cut to create 12-inch sides inside a square test frame with the joints attached by metal screws. During standard impact tests, the turf provided the bottom of the test frame by cutting 13.25-in by 13.25-in plots of turf, shaving off the tufts at 5/8-inches along the edges, and stapling the remaining backing to the frame. However, evaluation of the turf fundamental properties utilized a thin aluminum sheet as the bottom for containment. Then the turf was reduced to 12 by 12 sq. in. to fit inside of the wood frame and removed after testing. Although both types of frames provided a stable test surface, the purpose of each setup depended on whether the infill was stored permanently or temporarily.

4.1.2 Granulated Crumb Rubber Infill

The next step for creating the standard platform was finding suitable rubber infill. To create a survey of available GCRI product, the rubber crumb came from a variety of vendors (Tables 3.1 and 4.1).

Table 4.1. GCRI Samples and Supplier Companies

Lot #	Date Received	Plant Location	Company
GCRI-1	July 10, 2008	Calhoun, GA	Liberty Tire Recycling
GCRI-2	October 31, 2008	Calhoun, GA	Liberty Tire Recycling
GCRI-3	August 19, 2011	Houston, TX	Genan Inc.
GCRI-4	August 31, 2011	Calhoun, GA	Liberty Tire Recycling
GCRI-5	November 15, 2011	Braddock, PA	Liberty Tire Recycling
GCRI-6	November 15, 2011	Braddock, PA	Liberty Tire Recycling
GCRI-7	June 13, 2012	Tucker, GA	Lehigh Technologies
GCRI-8	June 25, 2012	Tucker, GA	Lehigh Technologies

The granulated crumb rubber infill samples in Table 4.1 were assigned lot numbers based on chronology of receipt. The inventory of GCRI was integrated with the preselected turf, one at a time, to create a lab platform and produce a baseline of performance for impact testing, later utilized for comparing alternate infill. In addition, the GCRI baseline aided the investigation of variables affecting turf-infill interaction.

4.1.3 Alternative Infills

Several companies supplied the polymeric waste streams for infill comparisons with GCRI. The first waste streams came from the carcass of post-consumer carpet from

broadloom (PCCB) that was pulverized during collection of the carpet face fibers. The PCCB mixture contained hard particles of elastomeric SBR latex encapsulating $CaCO_3$ filler and surrounded by short fibers, likely polyamide and polypropylene according to visual microscopic inspections and the Material Safety Data Sheet (MSDS) (Figure 4.4 and Table 4.2).

Figure 4.4. PCCB Crumb and Fiber from Broadloom Carcass

Table 4.2. PCCB Composition by Weight According to Mohawk

Component	**Min %**	**Max %**
Calcium carbonate	60	80
Latex SBR	10	20
Nylon 6,6	0	10
Nylon 6	0	10
Polypropylene	0	10
Inorganic	0	5

All PCCB samples came from vendors located in Dalton, GA. The majority of reclaim most likely came from tufted carpet made in Dalton, GA since tufted accounts for 90% of manufactured carpet, Dalton supplies 70% of U.S. demand, and the USA recycles 97% of its own carpet waste [24, 26]. In general, the companies collected the material from carpet production selvedge and discarded post-consumer carpet (Table 4.3).

Table 4.3. PCCB Samples and Supplier Companies

Lot #	Date Received	Company
PCCB-1	September 8, 2008	Mohawk Industries, Inc.
PCCB-2	November 17, 2009	Mohawk Industries, Inc.
PCCB-3	August 19, 2011	Shaw Industries, Inc.
PCCB-4	October 21, 2011	Beaulieu of America
PCCB-5	April 6, 2012	Shaw Industries, Inc.

Although suppliers would not divulge the exact processing conditions used in the reclamation of PCCB, the heterogeneous mixture of short fibers and latex particles suggested ambient grinding of the composite backing after shaving off the face fibers followed by density separation of the fines from the larger bulk fibers. The small crumb in the resultant blend appeared to be random shaped particles with multi-colored filaments that tended to entangle with themselves.

The next polymer waste stream came from carpet tiles with thermoplastic backings made by InterfaceFLOR, LLC of LaGrange, GA. The company's recycling division divulged their reclaim came from post-consumer carpet from tile (PCCT) that underwent ambient milling after shaving off the face yarn. The salvaged tile crumb had

dark, random-shaped particles that looked more like amorphous rubber crumb than finer SBR particles, but lacked the elasticity of rubber (Fig. 4.5).

Figure 4.5. PCCT Crumb from Tile Carcass

The MSDS for the PCCT sample listed components such as PVC, calcium alumina silicate and respirable quartz, although percentage ranges of each component were not disclosed. Interface exclusively supplied a total of six PCCT lots, so special attention was paid to each ones composition and source (Table 4.4).

Table 4.4. PCCT Samples and Sources

Lot #	Date Received	Composition/Source
PCCT-1	February 13, 2009	Crumb from Production line
PCCT-2	February 13, 2009	Crumb from Pilot line
PCCT-3	October 12, 2009	Small crumb from proprietary line
PCCT-4	October 12, 2009	Pellets from Canadian line
PCCT-5	April 29, 2011	Crumb from Production line
PCCT-6	April 29, 2011	Finer crumb from Production line

The collected PCCT lots came from waste streams available at the time of request. Only lots PCCT-1, PCCT-5 and PCCT-6 had comparable source and composition. Lots PCCT-2, PCCT-3 and PCCT-4 came from special requests of the suppliers. As a result, the wide range of processes and forms provided a variety of PCCT materials for comparison of infill.

Finally, the last polymeric waste stream was green PET flake reclaimed from post-consumer drink bottles that were collected by Mohawk Industries. The PET was mainly green flakes with minor parts of colorless chips and flexible film that came from ambient chopping or milling of reclaimed plastic bottles (Fig. 4.6).

Figure 4.6. Mohawk Green PET Flake from Drink Bottles

For this study, the term “flake” applied to a flat shape with one dimension such as wall thickness significantly smaller than the other two dimensions, as opposed to a “crumb” with approximately equal length, width and height. The flake came from chopping the very thin walls of post-consumer drink bottles that resulted in only flakes in the green mixture without random shaped crumbs. Further modification to the flakes would add to the cost of material, so only the initial reclaimed form was tested.

Another form of PET came from bottle preforms produced by a PET vendor, Resilux America, LLC; located in Pendergrass, GA (Fig. 4.7).

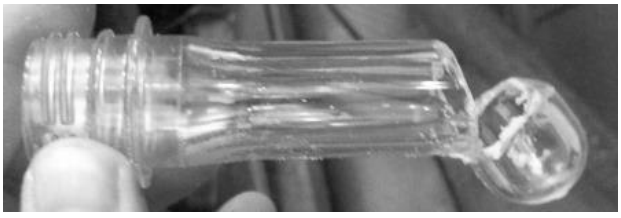

Figure 4.7. Resilux PET Preform

The Resilux PET preforms were made from molten thermoplastic extruded into thick-walled cylinders that served as precursors to thinner-walled PET drink bottles. The preforms underwent cryogenic grinding during the modification phase and created crumb particles, the resultant crumb provided a stark contrast to the Mohawk PET flake and GCRI in both form and composition.

4.2 Methods

4.2.1 Impact Measurements

Impact absorption was the main performance factor of this study, as it was the only performance-related specification in many field purchasing decisions [2, 21, 34]. The instrument described in ASTM F355 and F1936 was a portable unit applicable to field and laboratory measurements for a physical characteristic, but it was not a safety standard itself. ASTM F355 Procedure A described the instrument and methodology that was developed by Richard Breland [44]. For this study, the impact measuring device was purchased from Biomechanica of Portland, Oregon (Fig. 4.8).

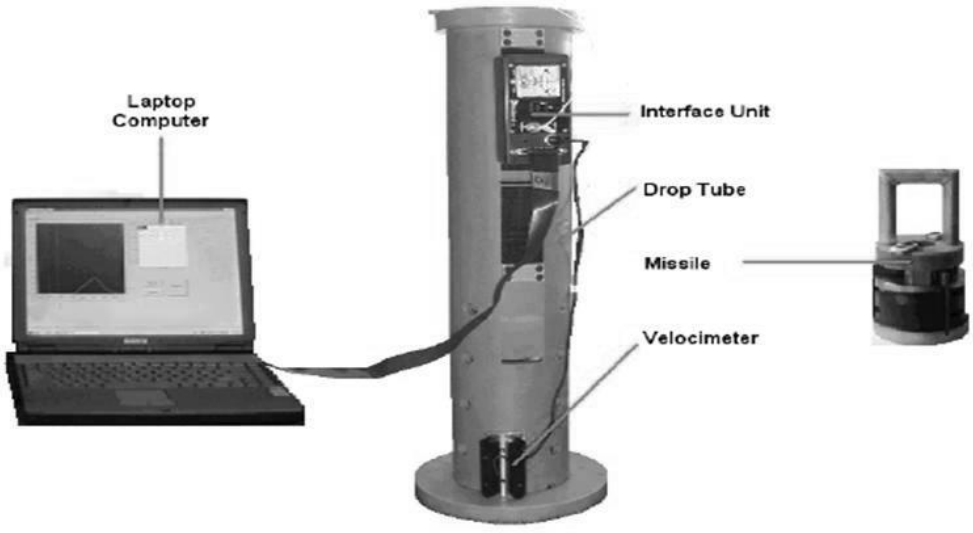

Figure 4.8. Biomechanica Impact Test System

The missile was 9.1 kilograms (20 pounds) with a flat base of 129 square centimeters (20 sq. inches) that simulated the average human head, although its reactions to impact forces was more linear than a cranium [21, 34]. After the missile dropped inside the tube for 0.6 meters (2 feet), the subsequent impact against the test surface was recorded by velocity and acceleration sensors that collected data every 50 microseconds. Next, the computer analyzed the impact data to determine Gmax, velocity and other results related to shock absorption during impact. The drop was repeated three times, and final values were obtained by averaging the last two results. Although operation of a test cycle was relatively simple, the end results depended on mathematical analyses as explained in Section 2.5.

Although the link between a hard impact and fatal head injury was controversial, physics still dictated the time, force and energy of the missile's fall (34) (Table 4.5).

Table 4.5. Physics of the Missile at Impact

Properties/Units	**English**	**Metric**
Distance	2.0	0.61
	Feet	Meter
Acceleration	32.2	9.81
	ft/(sq. sec)	m/(sq. sec)
Potential energy	40.0	54.4
	lbf-ft	Joules (N*m)
Time to impact	0.35	0.35
	Seconds	Seconds
Impact velocity	11	3.46
	ft/sec	m/sec
Kinetic energy	40.0	54.4
	lbf-ft	Joules (N*m)

Although the behavior of the missile was linear and measureable, the reaction of the human brain to the violent impact was less discernible. Impact-related research determined that strain on brain tissue caused various kinds of injuries such as hemorrhaging and MTBI, but quantifying a fatal injury was not so clear. Impact criteria such as Gmax, Severity Index, and HIC depended on previous studies of automobile-related crashes that created the Wayne State Tolerance Curve and Gadd Integral. These criteria were later applied to sports injuries, and Gmax became the most applied standard since it was a defined ratio of an object's peak deceleration to 9.81 m/s^2 [42, 44]. ATSM F1551 and F1936 recommend an average Gmax value below 200 for STF, while turf vendors required lower values around 80-110 [21, 34, 41]. According to Ed Milner, the president of the International Association for Sports Surface Sciences, the difference between a Gmax of 100 and 200 meant that a football player could experience six times the body damage [21]. The other indicators, SI and HIC, were originally recommended for transport vehicles and helmets, so utilization for sports surfaces required additional study [36]. Regardless, impact research correlated fatal head injuries to HIC values above 1000 to high Gmax.

According to ASTM F355, F1292, and F1551, the subscribed Impact Tester was designed for outside fields and indoor laboratory conditions. However, ASTM F1936 described laboratory conditions not available with a shared facility, but parameters such as temperature and relative humidity were monitored. One of the study goals was to create a baseline for impact for material comparison within a confined setup. Therefore, the synthetic turf setup needed sufficient area in the laboratory to support the Impact

Tester and the underlying STF. The missile had a 5 inch (12.8 cm) diameter as described in ASTM F355, and the base of the drop tube had to be large enough to maintain a 2-foot vertical drop during the impact event. To accommodate the missile and tube base, the minimum area of the synthetic turf was 12 by 12 square inches to support the Impact Test and accommodate 2.3-3.0 lbs of infill, which was recommended by STR for synthetic turf loading with GCRI. The turf inside the wooden frame required inner dimensions of 12 inch width, 12 inch length and 1.5 inch depth (Figures 4.9 and 4.10).

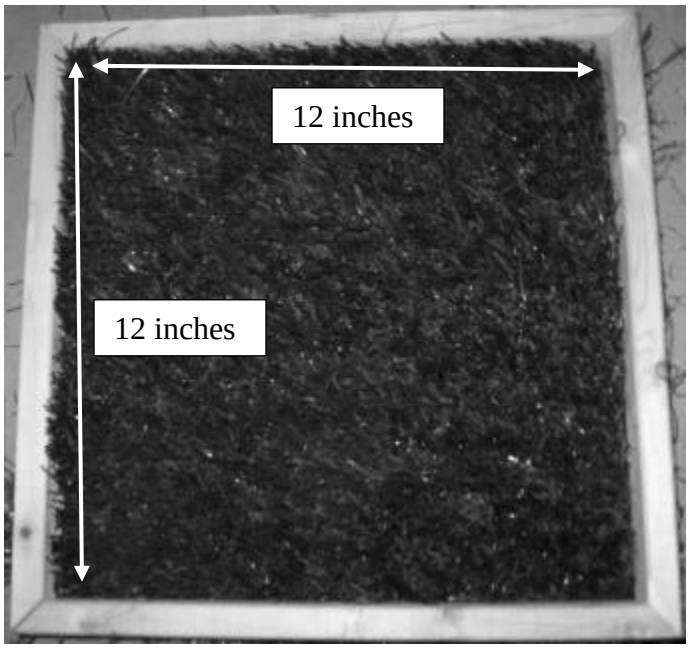

Figure 4.9. Laboratory Turf Platform

Figure 4.10. Impact Turf Test Setup

As mentioned in section 4.1.1, testing the GCRI and alternate infill required a laboratory turf setup to permanently contain the infill and was stackable in a closed container for long term storage. For study of fundamental turf properties, the infill was within the turf temporarily in order to test the same material in different turf. Regardless of long-term use, both test setups had to provide stable impact measurements.

4.2.2 Physical Conditions

The physical structure of the infill particles played an important role in filling the turf. The ideal amount of infill had to fit between the synthetic tufts while reaching a level at least two-thirds of pile height [7, 17, 39]. As referenced earlier, STF required 2.3-3.0 lbs of GCRI to fill the tufts and achieve acceptable impact performance. However, the variety of alternates did not have the same bulk density or particle size;

therefore the test samples required adjustments to pack turf to the same degree as GCRI. After filling the turf, other factors such as the shape of the infill could also affect interaction between each other and with the turf during an impact event, which was not well studied previously with GCRI [3, 21]. To help understand infill's ability to fill and add cushion to turf, pre-selected physical characteristics such as particle size, bulk density, crystallinity, and infill depth were included in the study.

After receiving several GCRI samples, analysis of granulated crumb rubber helped compare the samples to each other and to the background literature specifications. First, structural analyses of millimeter-sized particles required several tests. Random samples were examined using an Olympus BX51 Microscope. The high-resolution pictures were used to analyze particle structure and dimensions among the various lots, which related to filling the turf, infill migration and water drainage rate [1, 4, 21]. Next, the particle size was measured according to ASTM D5644, a method that used metal sieve meshes to mechanically separate particles according to size. The physical rotation and tapping within the meshes occurred via the Rotap Device (Fig. 4.11).

Figure 4.11. Rotap Device with Stacked Sieves

According to a GCRI vendors and available literature, the ideal infill size would fit between the synthetic tufts, which fell somewhere between 0.5 to 3.0 mm. To help narrow the range, the Rotap allowed measurements of the average particle size of each lot by weighing the mass of particles trapped between metal sieves [1]. Then a summary of these different sieve collections represented a distribution of different particle sizes that fell within the 0.1-2.35 mm range, although dimensions outside of this range were not precluded from further testing. Average particle size also came from the 0.1-2.35 mm sieves by weight averaging the trapped samples. An unavoidable error was the amount of material that fell through the sieves into the bottom pan, and then a significant loss would create a significant error in the average calculation. Nonetheless, the calculated size average at least could be related to the relative size distribution and the influence of any lot difference with a given sample. Although particles above 2.35-mm were beyond entrapment by available sieves, large particles were not precluded from infill impact testing. To sum up, only the vender recommendation offered a particle size range, so study of the actual rubber crumb would help determine the significance of size.

Next, the physical dimensions and shape were quantified in combination as bulk density (BD), which determined effective packing of infill in the turf according to ASTM D5603-01. BD measurements required dividing the mass of infill crumb by the volume of a standard density cup filled by the crumb, and then collect several samples for an overall average. Hence, the physical structure of infill particles was semi-quantified and helped calculate the volume filled by a given amount of infill, although it could not account for ease of penetration or compaction within the turf.

Another relevant physical property was the specific density of the samples: the amount of solid material that occupied the physical space minus empty voids. Specific density contributed to loading of infill in turf, but may also correlate with particle hardness due to higher crystallinity or filler content. Higher crystallinity in a homogenous polymer like PET would mean increased specific density of the particles, marginal increase of bulk density and higher glass transition. Analysis of this non-porous density utilized an Accupyc Gas Pycnometer from Micromeritics. The underlying principle was that the difference between amorphous and crystalline density correlated to the degree of crystallinity [45]. The detection of amorphous and crystalline polymer regions of infill materials also employed a wide angle X-ray diffraction (WAXD) scan conducted by a Rigaku Micromax-002 (Cu Kα radiation, Nickel filtered) SAXS/WAXS diffraction system operated at 45kV and 66 mA with a Rigaku R-AXIS IV++ detection system. Then crystallinity was quantified by integrating and subtracting the amorphous spectra from the crystalline spectra peaks [45]. Both methods gave approximate values for percent crystallinity of the various infill materials, which in turn related to both density and hardness of the infill particles.

After loading of the turf, physical conditions were monitored before and after impact testing to ensure consistent conditions and gauge the effects of impact. Temperature and humidity were part of a controlled test setting required by ASTM 355. A commercial thermometer and humidity gauge monitored the air surrounding the test bed and impact test. Conditioning of the turf and infill occurred in the testing laboratory for at least four hours before testing, and a long temperature probe measured the temperature of both after loading the turf like Figure 4.12.

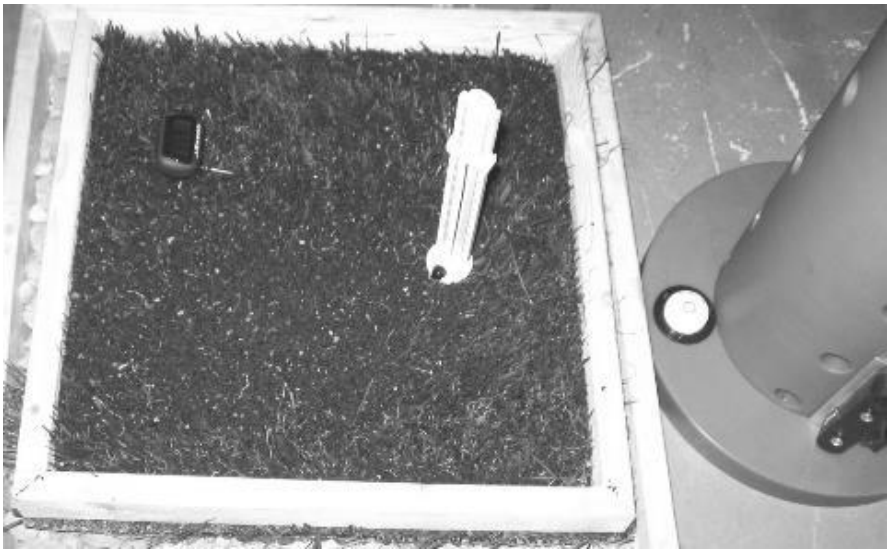

Figure 4.12. Infill Depth and Temperature Measurements

The precise control described by ASTM F355 called for 50±2% relative humidity and 23±2º C (73.5±3.5º F), which was not possible in the shared laboratory space. Nonetheless, both were stable for at least twenty-fours before impact testing and documented.

The interaction of turf and infill involved three additional variables that were monitored during normal STF: pile height, depth of infill and depth of root [4, 41]. All three properties were checked with a white modified ruler as seen in Figure 4.12. The modified ruler was supplied by Biomechanica that used a stiff wire to penetrate the turf. To measure the pile height of the tufts, the fully extended wire touched the backing while the upper portion had a wide circular base that touched the tufts with 0.7 per square inch of pressure, which was confirmed by a weight scale underneath the backing. Infill and root depth used the same scale ruler where the upper ruler portion went further into the tufts until approximately 2 pounds of force registered on the weight scale. The infill

depth incorporated both infill and the root zone of the turf as seen in Fig. 4.1, while the root depth came from compression off the top tufts to until reaching the empty root zone. For all three types of vertical dimensions, three measurements were taken before impact testing to determine the average value.

4.2.3 Chemical Compositions

With a variety of waste streams from disparate sources, comparing the alternates to rubber crumb required analyses of chemistry and internal infill particle structure, namely the polymer, filler and plasticizer. The first step was identifying organic compounds by Fourier Transform Infrared Spectroscopy (FTIR) and zinc selenide crystal for attenuated total reflectance (ATR). The FTIR-ATR instrument was a Bruker Vector 22 with a split-pea ATR that collected 64 scans of the surface at 4 cm^{-1} resolution without sample modification. After identifying the organic chemicals, thermogravimetric analysis (TGA) measured the relative amounts of filler and volatiles as detailed by ASTM D6370. The TGA instruments were a Seiko Instruments TG/DTA (differential thermal analyzer) 5200 and a TA Instrument Q5000. Both instruments utilized nitrogen during thermal decomposition in a platinum pan when heated from 30° to 750°C at 10°C per minute. The resulting thermal scan revealed discrete steps that were assigned to volatile chemicals, polymeric binder and residual filler/ash such as the following illustration from Reference 46 (Fig. 4.13).

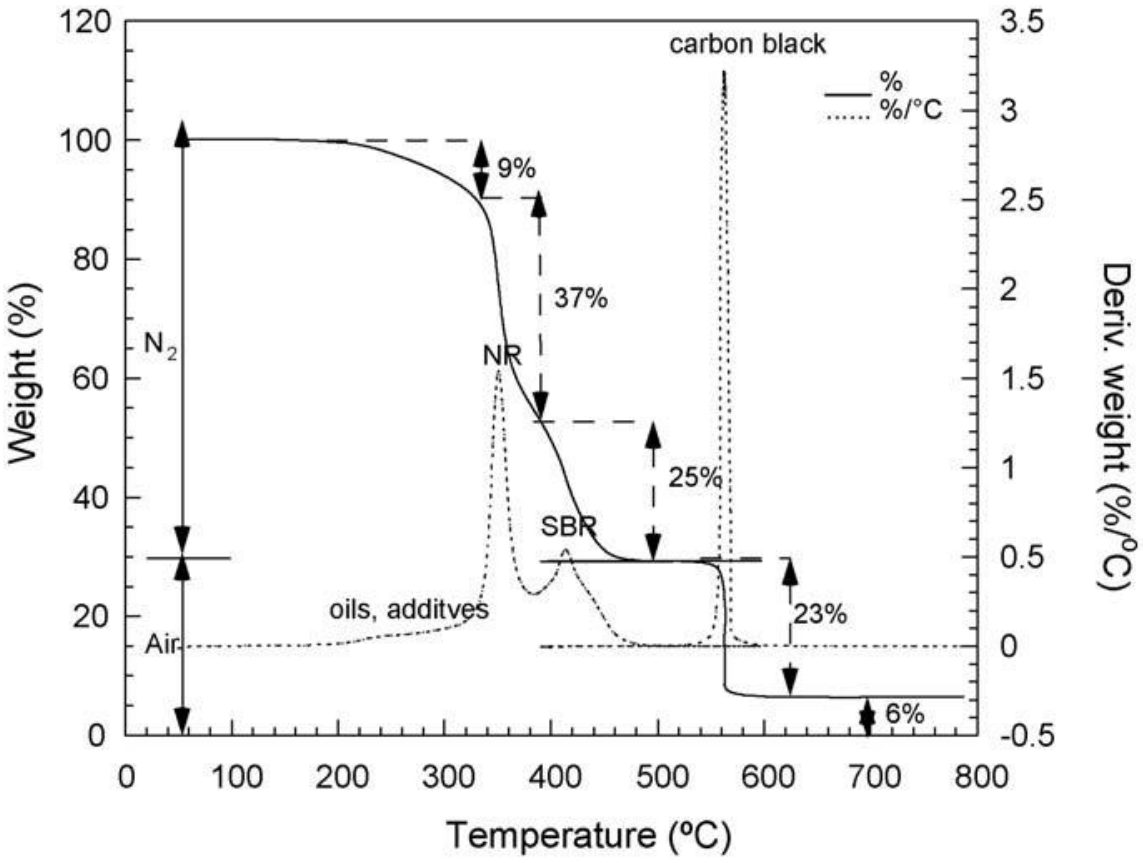

Figure 4.13. Literature Example of Tire Rubber TGA (Air to Nitrogen at 563°C) [46]

The central difference between the two instruments was the high-resolution variable heating rate capability of the Seiko (HR-TGA) that slowed heating rates at distinct mass losses of individual components, while the TA instrument ran a constant heating rate that shortened test time. The chemicals listed in Fig. 4.13 such as natural rubber (NR), styrene-butadiene rubber (SBR), carbon black and oils could be generally attributed to formulations for tire rubber. However, identification of the particular chemicals in the infill and its alternatives were secondary to the study's stated objectives, so only precursory analyses were performed to confirm the presence of ingredients listed in the

background research. Instead, the levels of additives, polymer and filler were more relevant since they related to densities and structure.

4.2.4 Modifications of Turf and Infill

The first experimental modification was for the turf itself with only tuft length modified to create test platforms and study the turf's interaction with rubber infill. The typical STF surface was designed to last for five years, and good maintenance could extend that life-span to 10 years. Therefore, the polyethylene tufts of modern turf were resistant to cutting by hand tools or conventional grass cutters, which was why a STF vendor recommended the Oster Clipmaster with variable-speed (Fig 4.14).

Figure 4.14. Oster Clipmaster

The Clipmaster used steel blades to shear across the width of each tuft without damaging the underlying backing, which matched closely with the clipper's original purpose trimming wool off sheep safely. Controlled shearing of the tufts completely off the

backing was essential to stapling the backing to a wooden frame while the remaining tufts within the inner dimensions of frame kept an unmodified pile height (Fig. 4.9). For the study of the interaction between turf and infill, pile height was controlled by cutting down to 0.5-inch tall wood spacers placed inside the turf (Fig. 4.15).

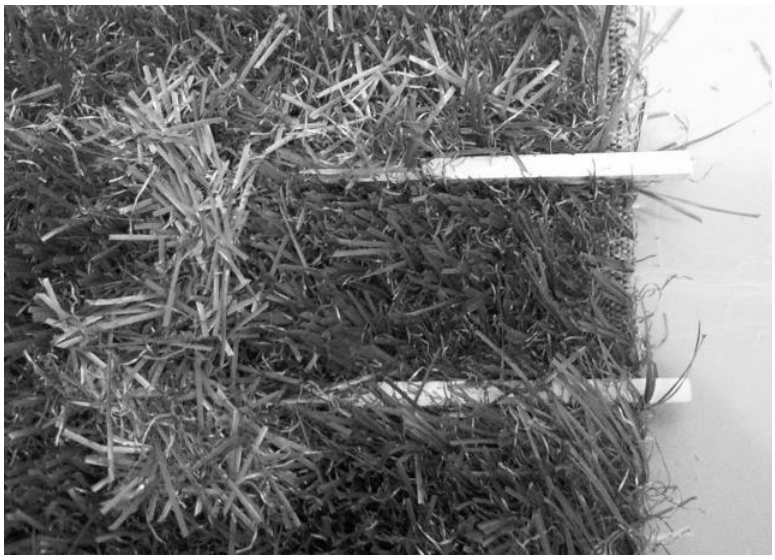

Figure 4.15. Modifying the Pile Height

Afterwards, pile height was measured with the modified ruler used for infill depth as seen in Fig. 4.12. Only the 3D-52 turf required such changes since it became the standard surface for infill testing.

After testing the alternate infill samples as received, selected attributes of each lot were adjusted as mentioned in Section 3.2.4. The primary adjustment was changing the particle size to match closer to GCRI and pack more efficiently within the turf. Adjusting the average particle size of the carpet infill required the Rotap (Fig. 4.11) to sift out fibers and dirt to reach the desired particle size distribution. Then PCCB-based infill used same size modification procedure to reach a specific size plus reduce loose fiber content. Next,

PCCT required size adjustment for testing in standard turf, plus unmodified PCCT in 4th generation turf. As for PET, the available forms included flakes from the reclaim and bottle preforms, both too large to effectively penetrate between the turf tufts. Therefore, the desired PET particle size was generated by cutting mill grinding both forms with a Wiley Mill Standard Model No. 3 with a preselected screen (2, 3 or 4 mm diameter gaps) beneath the rotating blades (Figures 4.16 and 4.17).

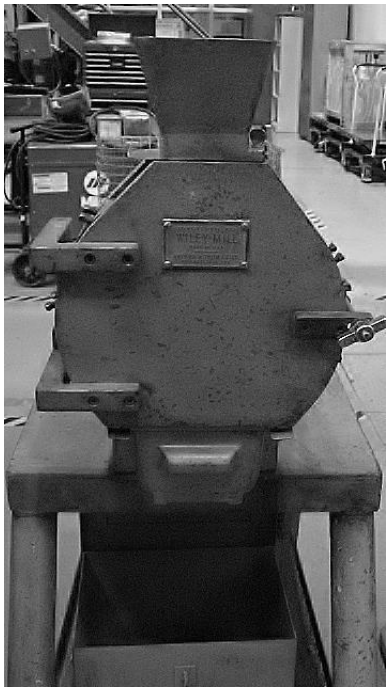

Figure 4.16. Wiley Mill

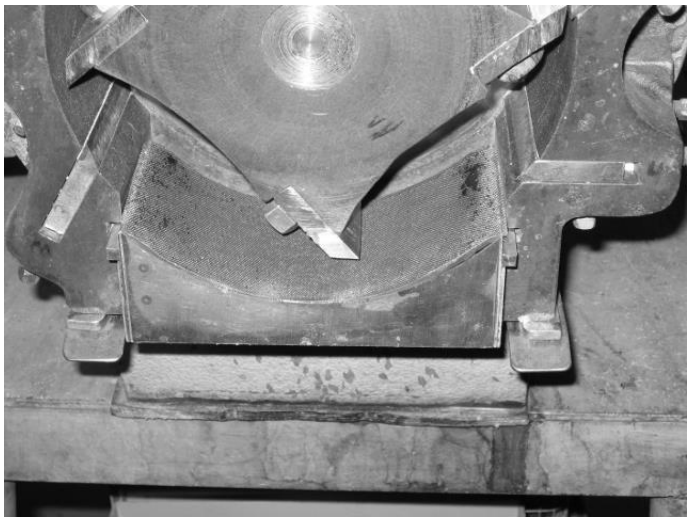

Figure 4.17. Wiley Mill Blade and Screen

The rate of blade rotation and size of the mesh screen correlated to a size range, while changing from ambient to cryogenic grinding affected particle shape due to change in ductility of the particle material. Adjusting each infill particle size also changed its interaction with the turf platform and helped verify the adjusted property's relationship to impact absorption if not outright improve it.

CHAPTER 5

RESULTS AND DISCUSSION

5.1 Granulated Crumb Rubber Infill (GCRI)

Without a published standard for optimum infill properties or performance, different samples of commercial crumb rubber were acquired to provide a survey of properties of available material. After comparing the test results, one of the lots served as the standard infill for the remainder of the research.

5.1.1 Chemical Composition of Tire Rubber

In the automotive market, tire components are made from many forms of rubber such as natural rubber (NR), isoprene (IR), butadiene (BR), ethylene-propylene-diene monomer (EPDM) and styrene-butadiene (SBR), all in combination with additives such as plasticizers and carbon black [1, 11, 16, 46]. For this study, the general types of chemicals and their relative amounts became the specific focus while the specific chemical components were secondary because customer demands for both tire and infill tended to place more emphasis on end product performance rather than formulation. For chemical analysis of tires, frequently used methods include Fourier Transform Infrared Spectroscopy (FTIR) with Attenuated Total Reflectance (ATR) capability and Thermogravimetric Analysis (TGA). Consequently, these methods were utilized in this study to compare properties of different GCRI lots.

As listed in Table 4.1, the granulated infill was produced by grinding the rubber components of tires from various brands and sources, and identifying every chemical present was impractical for this study. According to research on the recycling of tire

rubber, FTIR-ATR greatly facilitated identification of the major constituents of the infill particle's surface in a short amount of time [46]. The findings of this research were summarized in Table 5.1 to aid in chemical identification.

Table 5.1. FTIR Band Assignments for GCRI

Peak (cm^{-1})	Chemical	Component or Source	Ref #
2964	$-CH_3$	Rubber	47
2950, 2853	$-CH_2-$	Rubber	47
1739	C=O	Thermal oxidation	48
1540	Zinc Stearate	Anti-adherent	48
1461	$-CH_2-$	Rubber	47
1430	$=CH_2$	Rubber	48
1376	$-CH_3$	Rubber	47
1076	-C-S- (sulfur)	Crosslink	47
1026	Carbon Black	Filler	48
960	Trans Butadiene	Rubber	46,47
875	Trans Isoprene	Rubber	48
815	Isoprene	Rubber	46
722	$-CH_2-$	Rubber	47

FTIR-ATR analyses focused on samples from the first two lots of GCRI that came from Synthetic Turf Resources (STR), which procured the infill from Liberty Tire Recycling (LTR). The references and chemical groups summarized in Table 5.1 came from research specific to automotive tire rubber [46, 47, 48]. Consequently, the most prominent peaks in the following spectra confirmed tire ingredients such as rubber, a release agent, and carbon black (Figures 5.1 and 5.2).

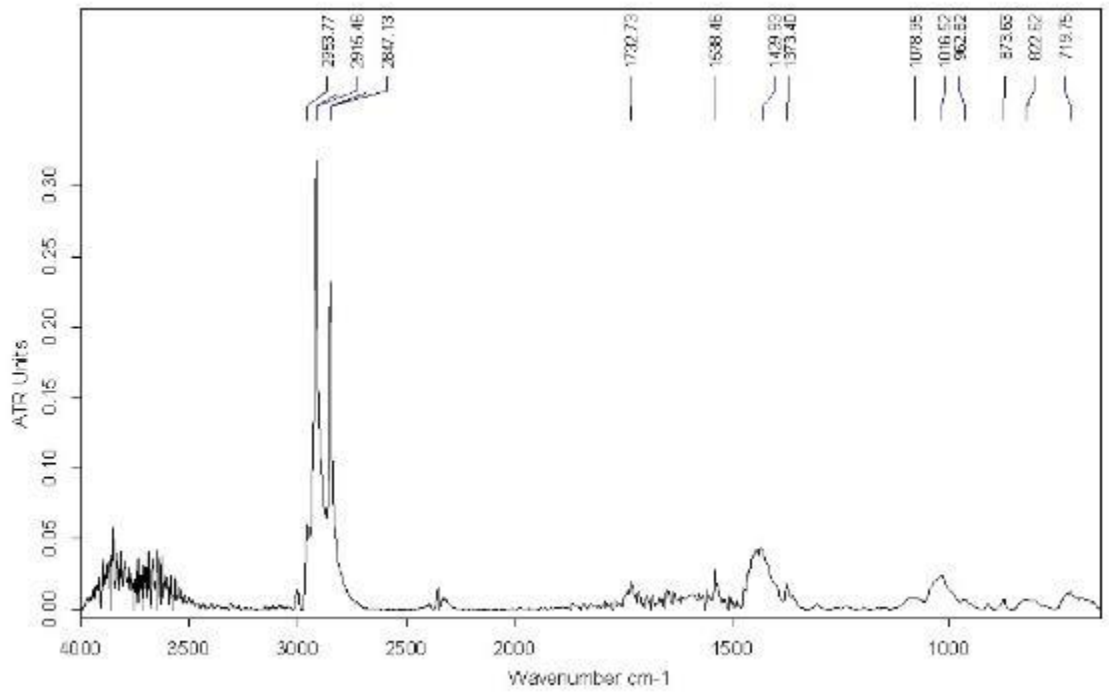

Figure 5.1. FTIR of GCRI-1

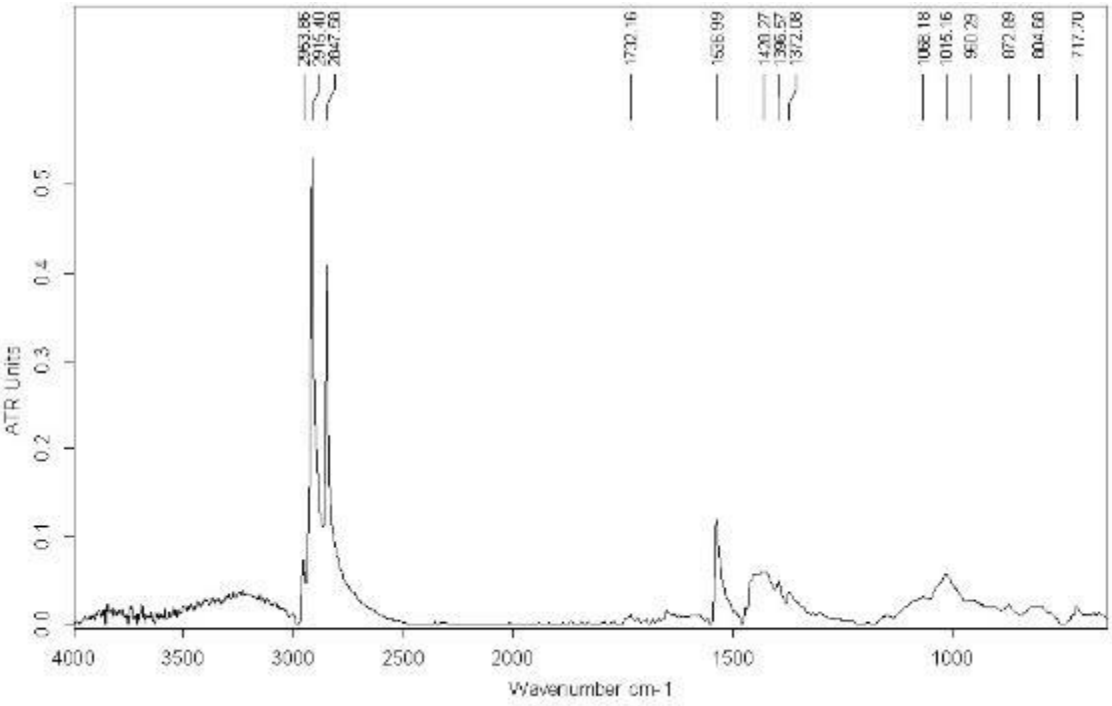

Figure 5.2. FTIR of GCRI-2

Among the possible rubber components, The FTIR spectra of the two lots shared several prominent peaks belonging to the chemical groups of isoprene (815 and 875 cm^{-1}) and butadiene (960 cm^{-1}). Other possible rubber ingredients, such as styrene (704 and 756 cm^{-1}) and EPDM (1376 and 1461 cm^{-1}), were absent from both spectra; and therefore not present in the infill [47]. Other peaks in Table 5.1 belong to zinc stearate and carbon black, which are rubber additives. The differences between the two samples were only the amounts of chemical groups, such as GCRI-2 containing more zinc stearate and thermal oxidation. Overall, these components closely matched the type and levels found in previous studies while the lots matched each other [46, 47, 48, 49].

To find the approximate levels of these components in tire rubber, previous experiments used TGA-based tire decomposition, such as Fig. 4.13, to measure specific mass losses assignable to individual tire components (Table 5.2).

Table 5.2. Tire Components from Fig. 4.13 [46]

Temperature (Celsius)	Percentage	Component
300	9	Volatiles
350	37	NR
424	25	SBR
563*	23	Carbon black
600	6	Inorganic filler

* Under oxygen flow instead of nitrogen

The TGA of the two GCRI lots produced curves under nitrogen gas, which consolidated inorganic filler with carbon black as the total filler content. Then the temperature was

determined for each mass loss in Fig. 5.3 and assigned to a component according to previous descriptions in literature for volatiles, polymers and fillers (46, 49).

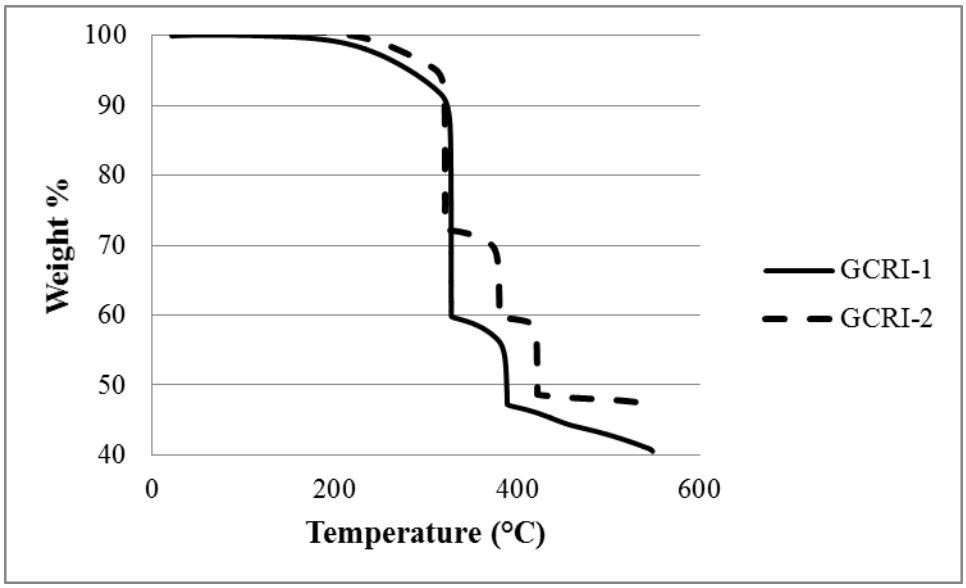

Figure 5.3. TGA of GCRI Lots 1 and 2

Table 5.3. Components in GCRI-1 TGA

Temperature (Celsius)	Weight Percentage	Component
200	9	Volatiles
327	31	NR
386	13	BR
400	47	Total Filler

Table 5.4. Components in GCRI-2 TGA

Temperature (Celsius)	Weight Percentage	Component
200	5	Volatiles
320	23	NR
380	12	NR or BR
422	12	BR
430	48	Total Filler

The rubber supplier of the two lots (LTR) reclaimed the rubber from tires used for tractors and trailers, which would account for similar chemistries between FTIR and TGA analyses. The differences in specific component quantities came from variations within the tire and between different tire lots. After separating the particles by mesh size, TGA showed deviations of the rubber component amounts, but still had consistent types of components (Figures 5.4 and 5.5).

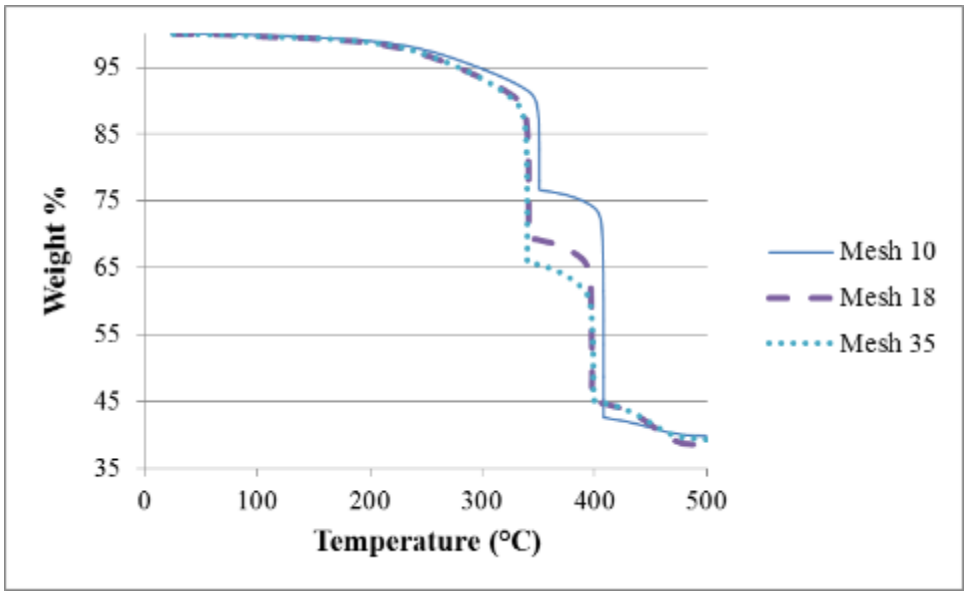

Figure 5.4. NR and BR in GCRI-1 According to TGA

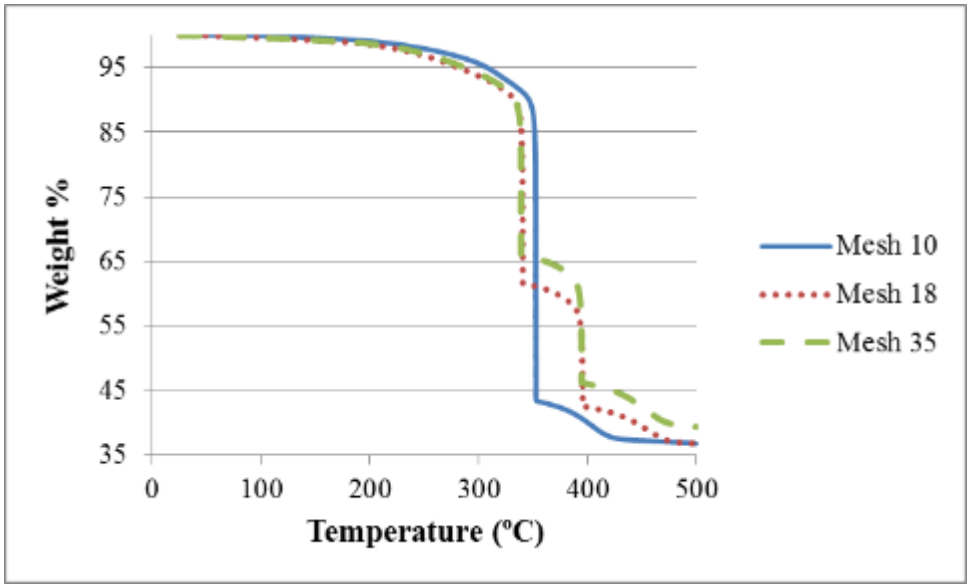

Figure 5.5. NR and BR in GCRI-2 According to TGA

Overall, particle size did not show significant differences in total rubber content between the lots or within each lot, although the mesh 10 rubber component in Figure 5.5 is almost all NR. The other ingredients had consistent levels for oils at less than 10% and total filler at 45% based on Tables 5.3 and 5.4. The remaining 45% belonged to the rubber in both initial lots, which is close to the approximately 40% mentioned in academic and product literature [11, 17, Appendix 1]. Furthermore, the 41% of a truck tire could be divided into 27% for NR and 14% for synthetic rubber, butadiene in this case, both percentages close to the ones shown in Tables 5.3 and 5.4. Since the composition of the first two lots matched information from previous studies, further chemical analyses were unnecessary unless subsequent impact performance showed significant differences between the GCRI lots.

5.1.2 Physical Conditions of GCRI

While the chemical composition came from the original tire, the physical structure of GCRI came from the subsequent production grinding process. According to the literature and vendors, the two major grinding processes utilized for rubber infill are cryogenic and ambient [16]. Therefore, both processes were represented by samples of rubber infill lots.

Table 5.5. Grinding Process for GCRI

Lot #	Grinding Process	Company
GCRI-1	Ambient	Liberty Tire Recycling
GCRI-2	Ambient	Liberty Tire Recycling
GCRI-3	Ambient	Genan Inc.
GCRI-4	Ambient	Liberty Tire Recycling
GCRI-5	Ambient	Liberty Tire Recycling
GCRI-6	Cryogenic	Liberty Tire Recycling
GCRI-7	Cryogenic	Lehigh Technologies
GCRI-8	Cryogenic	Lehigh Technologies

The literature described the ambient-generated crumb as torn, irregular shapes with a rough, oxidized surface from thermal degradation while cryogenic grinding created a smooth fractured surface with minimum oxidation [16]. These descriptions matched visual analysis of both ambient and cryogenic samples as shown in Figs. 5.6 and 5.7.

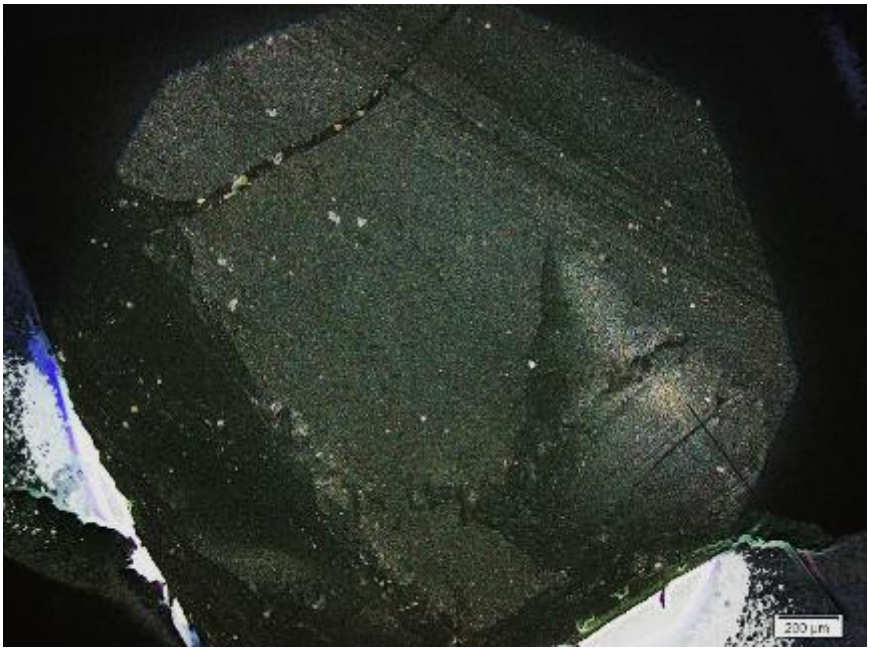

Figure 5.6. GCRI-4 Ambient Ground Crumb with Rough, Torn Edges

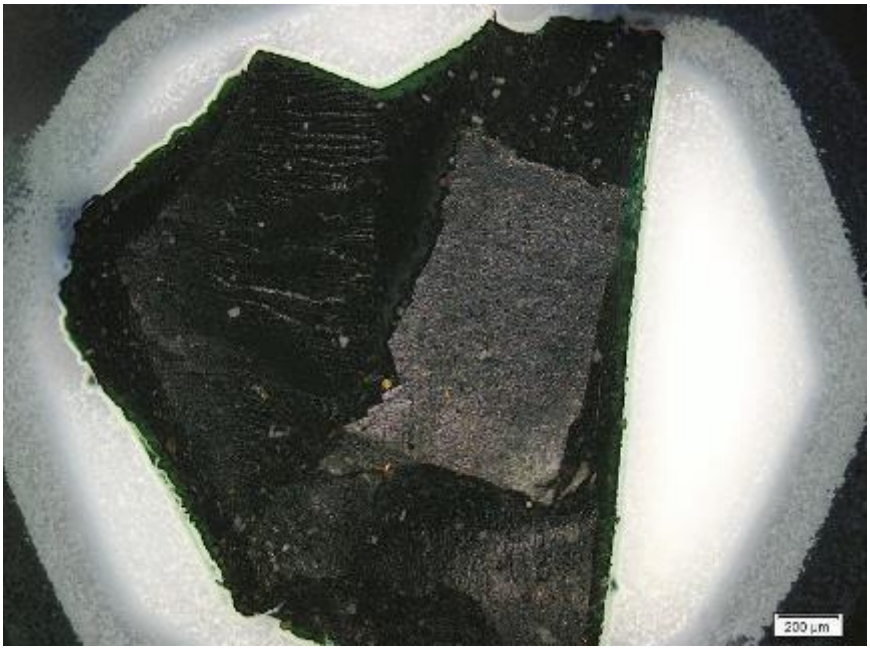

Figure 5.7. GCRI-6 Cryogenic Ground Crumb with Smooth, Angular Edges

The sample of GCRI-4 in Fig. 5.6 came from particles retained at mesh 8 (2.35 mm), while GCRI-6 sample in Fig. 5.7 was retained by mesh 12 (1.70 mm). Although both types of grinding processes affected surface roughness and shape of edges, questions remained about crumb packing and infill interaction with its own neighboring particles and with turf.

Despite the lack of particle size standards for infill, the only recommendations for efficient packing of turf were between 0.5 to 1.5 mm. The turf vendor, STR, relayed the importance of small particles fitting between the long tufts while remaining too large to slip through perforations in the turf backing. Based on this reasoning, Liberty Tire Recycling and other rubber suppliers made ground crumb specifically as turf infill by sifting the material with appropriate mesh sizes to meet the 0.5-1.5 mm particle size criterion (Figs. 5.8 and 5.9).

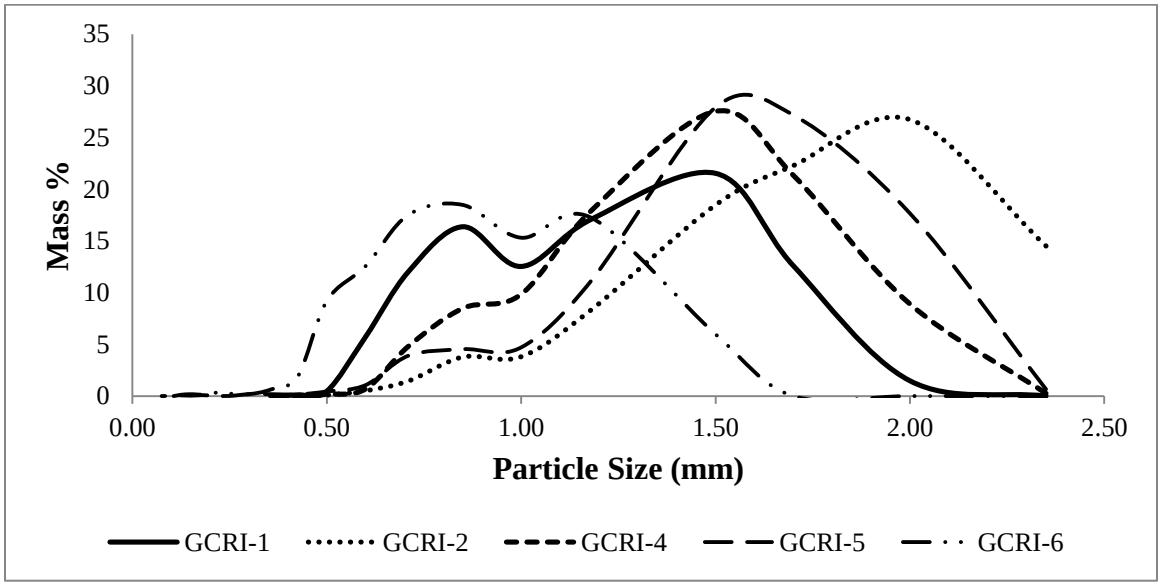

Figure 5.8. Size Distribution of LTR Infill

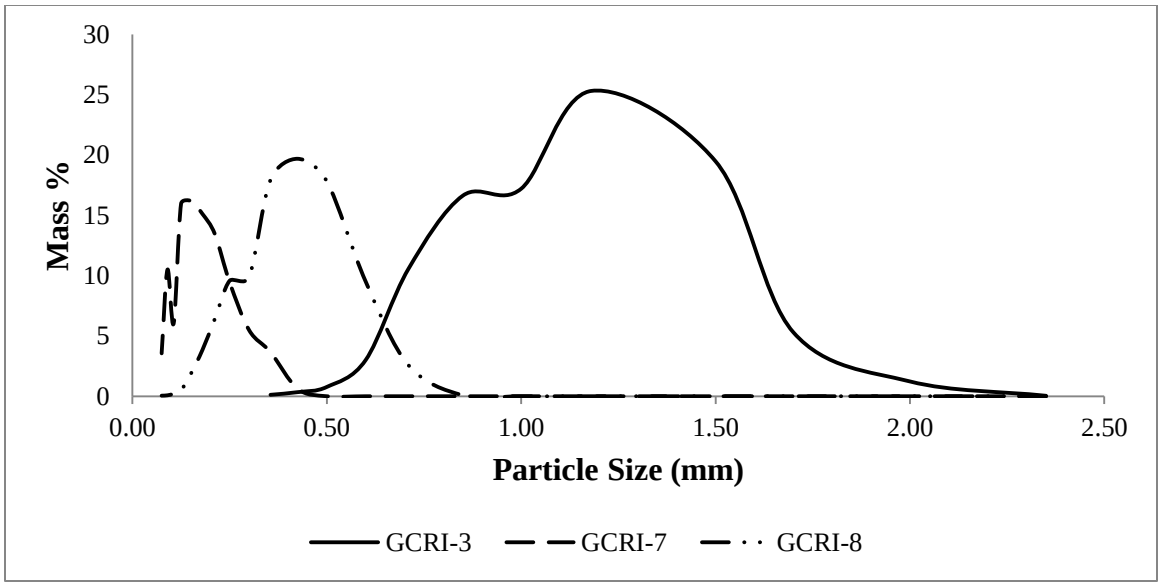

Figure 5.9. Size Distribution of Genan (GCRI-3) and Lehigh (GCRI-7 & 8) Infills

LTR and Genan produce ground rubber made specifically as turf infill, but the size distribution curves fell below 1.0 mm. In contrast, Lehigh specialized in fine powder made by cryogenic milling and produced a more narrow, small particle size without sifting through mesh [11]. Whether by incident of the process or intended purpose, all the tested cryogenic crumbs possessed narrower size distributions than ambient, which was reflected in the calculated average particle size (Table 5.6).

Table 5.6. Average Particle Size and Bulk Density of GCRI

Lot#	Average Particle (mm)	SD (mm)	Bulk Density (gm/cc)
GCRI-1	1.16	0.37	0.43
GCRI-2	1.71	0.43	0.48
GCRI-3	1.12	0.32	0.41
GCRI-4	1.38	0.37	0.50
GCRI-5	1.51	0.39	0.46
GCRI-6	0.86	0.28	0.48
GCRI-7	0.17	0.07	0.57
GCRI-8	0.39	0.13	0.44

Each lot had over 90% of its crumb trapped by sieves sized between 0.075 to 2.35-mm, so any given sample would lose at least 10% of material even if the overall particle size distribution was above 0.5-mm. In the worst case, 100% of the cryogenic micro-particles from GCRI-7 were below 0.5-mm and would not be effectively retained by the turf backing, thus precluding impact testing. When considering the extra production cost of liquid nitrogen and the resulting low particle size, cryogenically-ground crumb rubber was not chosen as a representative sample for comparison to alternate infill.

When estimating the optimum amount of infill, the bulk density became central to calculating the amount of crumb material needed to fill the empty space within the turf and reach optimum impact performance. Overall, the average particle size, distribution range or particle shape of each lot did not correlate to the bulk density packing of the rubber particles: average ambient crumb was 0.46 ± 0.04 grams per cubic centimeter, average cryogenic was 0.50 ± 0.07 gm/cc, and the overall average was 0.47 ± 0.05 gm/cc. Based on the vendor's minimum recommended amount of GCRI at 2.3 lbs. (1043 grams) to fill a 12 by 12 square inch of turf (929 sq. cm), the overall BD average of 0.47 gm/cc density equals a turf fill volume of 2235 ± 223 cubic centimeters (approximately 0.59 gallons). Initial impact testing utilized a random rubber sample from lot GCRI-2 that was calculated to fill 2136 cc (0.56 gallons), a value still within the 2235 ± 223 cc range. Therefore, the initial fill volume of 2136 cc was retained as the standard empty turf volume for estimating possible alternative infill amounts to aid comparison to the crumb rubber.

5.1.3 Impact Measurements of GCRI

Despite available impact-related test methods and criteria, the lack of a standard product required establishing one for this study. GCRI suppliers were from Georgia, Texas and Pennsylvania; the acquired samples provided a regional survey of commercial infill products. For each lot, the first impact test of the crumb rubber without turf served as comparison to the eventual turf-based results (Figs. 5.10-11).

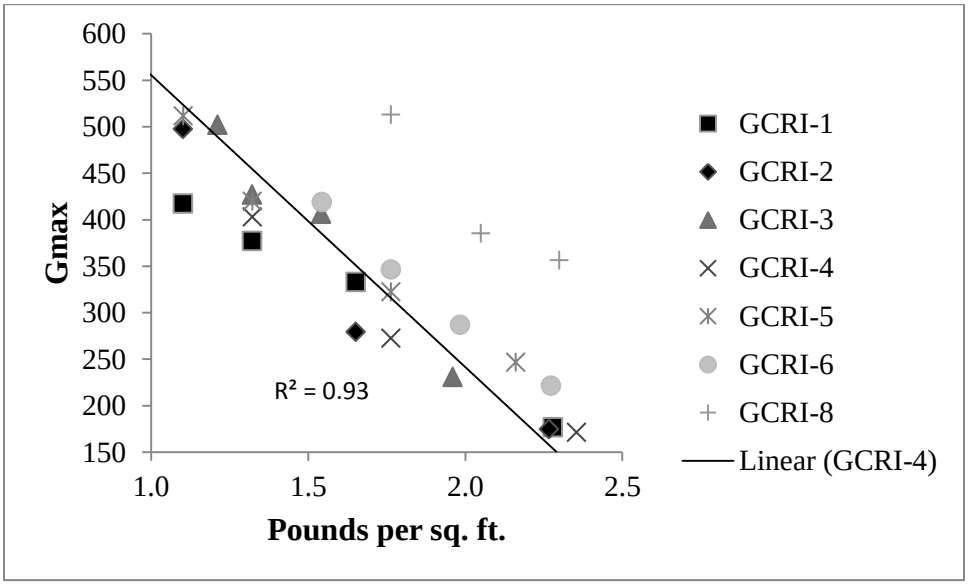

Figure 5.10. Non-turf Gmax Values vs. Loading of GCRI

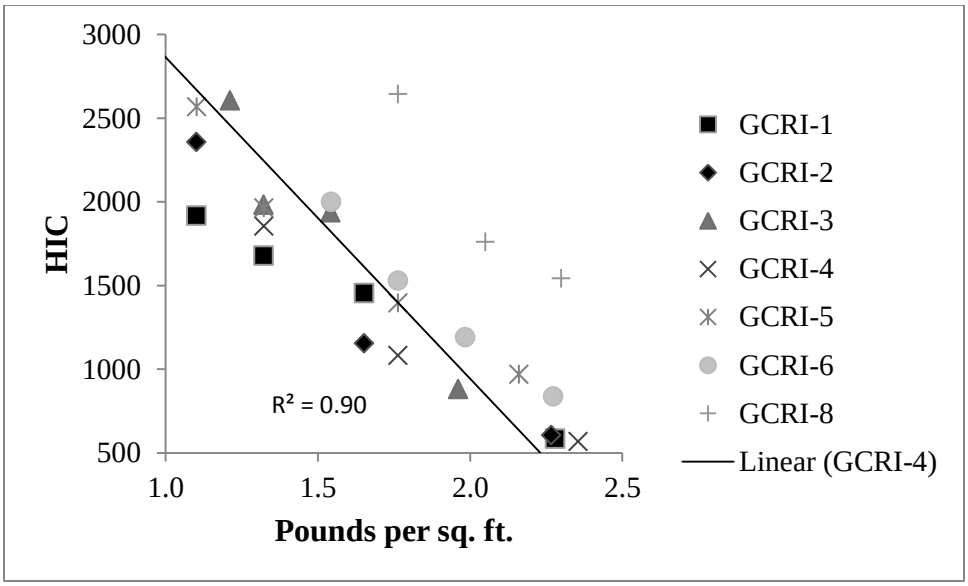

Figure 5.11. Non-turf HIC Values vs. Loading of GCRI

An operational STF required Gmax values below 200 to be considered safe by impact test methods, and HIC had to be below 1000 to prevent life threatening injuries [34]. During loading of one square foot area of concrete flooring without turf, all GCRI lots demonstrated a linear decrease of impact hardness readings with similar R^2 correlation values such as the ones shown in Figures 5.10 and 5.11. At 2.3-lb loading, the recommended infill amount would supposedly saturate the turf, and most of the lots trended towards similar Gmax and HIC values except for GCRI-8 possibly due to exceptionably small particles. The other cryogenic sample, GCRI-6, also had high impact values and low particle size, but both properties remained close to the ambient samples probably due to an overlapping distribution. Aside from similar bulk densities and subsequent turf loading between the rubber samples, particle size distribution may play a central role in impact absorption besides efficient filling of the turf.

After measuring non-turf impact performance for all GCRI samples, the next step was the incremental loading of the standard turf setup (Fig. 4.9). In the following Figures 5.12-13, the zero loading point was impact testing of the turf itself without infill.

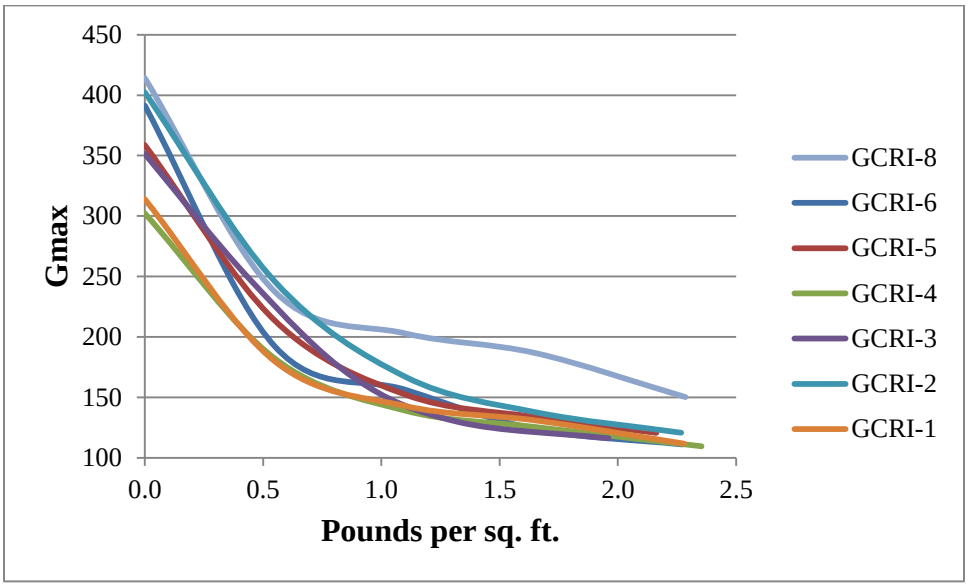

Figure 5.12. Gmax Values of GCRI in GameDay Turf

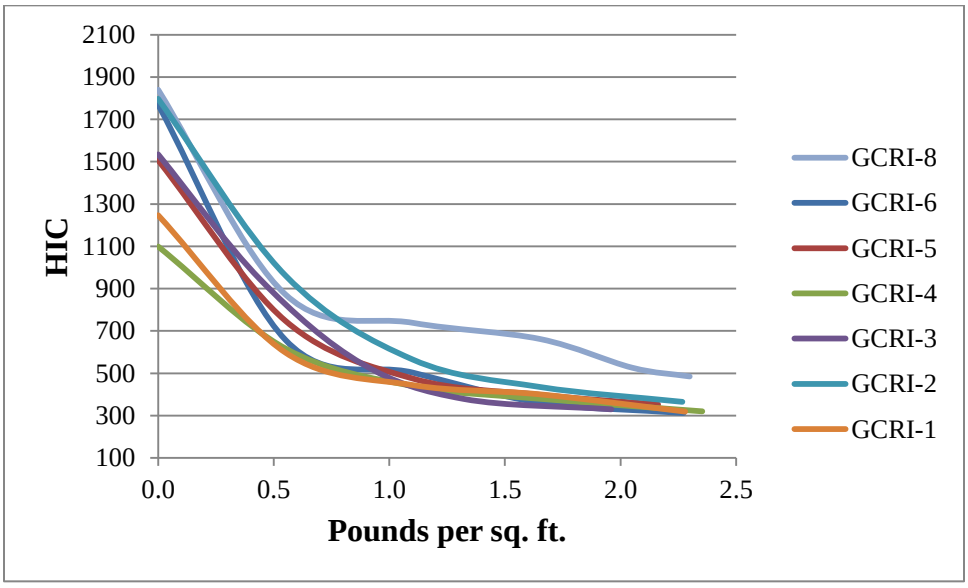

Figure 5.13. HIC Values of GCRI in GameDay Turf

Without infill, the turf proved unsafe during falling impact with a high Gmax range of 300-400 g and HIC of 1100-1900. The wide variation in the non-filled impact values also indicated deviations within the turf product. Without infill to support the tufts, the backing likely absorbed most of the impact forces with the tuft playing a less significant role. Then at infill levels around 1.0 pound per sq. ft., impact hardness of all tested rubber samples underwent a major decline towards both safety thresholds, Gmax and HIC. Additional infill loading improved impact absorption with a less steep, linear slope until all but one lot closely converged at approximately 2.3 lbs. per sq. ft. The only non-converging rubber sample, GCRI-8, had the highest impact values suggesting a limit to particle range of the acceptable infill product, but the impact-vs-loading curve still followed the same trend towards its own low impact reading (Table 5.7).

Table 5.7. Impact Readings with 2.3 lbs. / sq. ft. GCRI Filled Turf

LOT#	**GMAX**	**HIC**
GCRI-1	112	319
GCRI-2	121	365
GCRI-3	116	329
GCRI-4	110	320
GCRI-5	121	353
GCRI-6	111	312
AVERAGE*	**115**	**333**
GCRI-8	**150**	**485**

* Excluding GCRI-8

After excluding the micro-powder GCRI-8, the convergence of the impact curves indicated similar infill behavior despite differences in the underlying turf and GCRI. In

other words, the Apparently, the rubber particle interaction with the turf masked deviations within the turf construction while creating a synergistic improvement in overall impact performance better than the infill or turf alone.

Upon discovering this synergistic interaction, unknowns remained about the convergence of impact values at 2.3 lbs. per sq. ft. of infill, which was also when the GCRI filled the turf and began overwhelming the height of the tufts. Another interesting point was that all but one GCRI sample reached similar impact readings while possessing various overlapping particle sizes. Particle size going below the range recommended in Section 5.1.2 likely caused one GCRI-8 to have the highest impact readings, thus confirming the lower limit of 0.5 mm. Figure 5.8 showed GCRI-2 might have particles above 2.5 mm, but not significant enough to test. Instead, the acceptable particle size range could extend to 0.5 – 3.0 mm (0.02 – 0.12 in) judging by the overlap of particle size and impact absorption performance. Among the available lots, GCRI-4 had sufficient material for the next study phase to produce a more definitive particle size range for improved interaction between rubber crumb particles and turf.

5.2 GCRI-Turf Fundamental Study

While establishing a baseline for GCRI impact performance, several samples of rubber infill demonstrated similar impact absorption behavior and values despite disparities in sources, processing, surface roughness and particle size distribution. Yet similarities in bulk density, shape and/or chemical composition could explain overlapping impact results. Integration of infill into synthetic turf further improved impact performance despite variation in the underlying turf. The next step was thus to study the interaction between infill and turf in order to understand the degree of influence each

component had on the other while operating synergistically in the STF system to absorb impact energy.

5.2.1 Impact Performance of Refined GCRI

With the exception of GCRI-8 (Table 5.7), the crumb rubber infill samples demonstrated similar trends and overlapping values for impact performance (Figs. 5.12 and 5.13), thus any obtained lot could represent commercially available GCRI products in further testing. Due to availability of material, ambient infill lot GCRI-4 became the standard infill for the remainder of the experiments in this work. Previous testing of GCRI-4 revealed particles with rough edges (Fig. 5.6), a bulk density of 0.50 gm/cc and an average particle size of 1.38±0.37 mm, and a tested particle size distribution range of 0.50-2.35 mm. The infill also provided a near-unimodal distribution of particle size (Fig. 5.14 and Table 5.8).

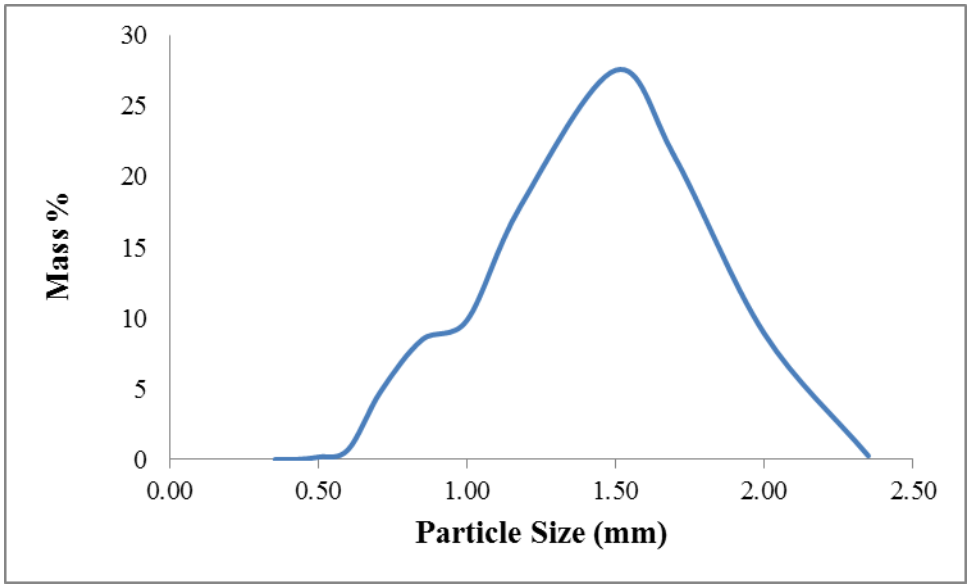

Figure 5.14. Particle Size Distribution of GCRI-4 Crumb Rubber Infill

Table 5.8. GCRI-4 Mesh Distribution

Mesh	Size (mm)	Mass %
8	2.35	0.3
10	2.00	8.9
12	**1.70**	**21.3**
14	**1.50**	**27.5**
16	**1.18**	**17.9**
18	1.00	9.8
20	0.85	8.5
25	0.71	4.8
30	0.60	0.7
35	0.50	0.2
40	0.425	0.0
45	0.355	0.0

The highlighted portions of Table 5.8 encompassed nearly 67% of total mass of available infill, so a series of test cycles via Rotap produced significant quantity of particles between 1.18 – 1.70 mm for further impact analysis (Fig. 5.15).

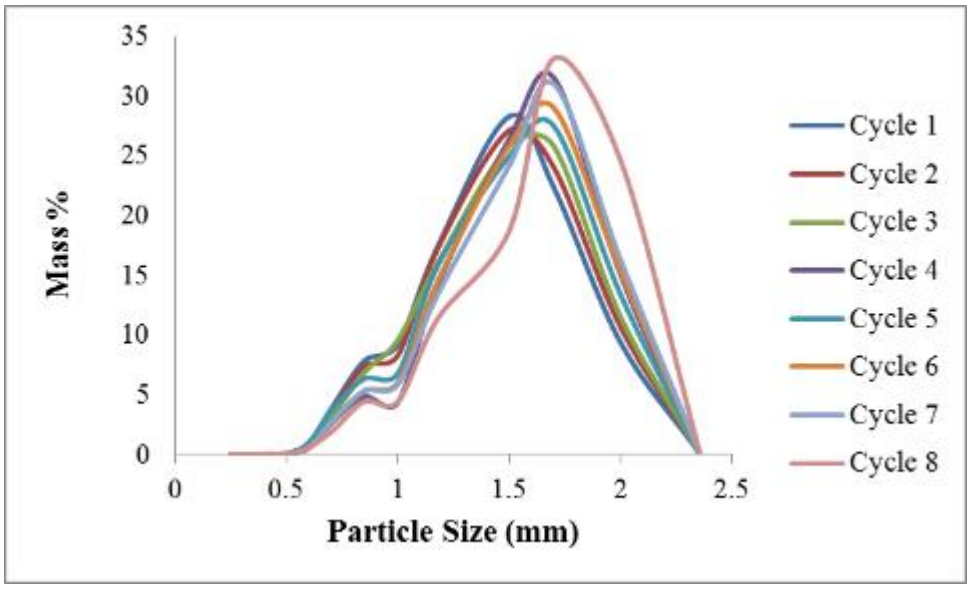

Figure 5.15. Rotap Separation of GCRI-4 Crumb Rubber Infill

Each cycle isolated particles between 0.5 to 2.5 millimeters, but the peaks shifted from unimodal to bimodal with the desired mesh components still encompassed by the largest peak. With each cycle, the individual components at mesh 12 (1.7 mm), mesh 14 (1.5 mm), and mesh 16 (1.18 mm) accumulated to reach 2.3 pounds each for the impact setup. A noted observation was that bulk density increased with higher particle size going from 0.48 gm/cc for mesh 12 to 0.46 gm/cc for mesh 16. However, none of the refined samples with bulk densities lower than the original lot displayed improved Gmax in Fig. 5.16.

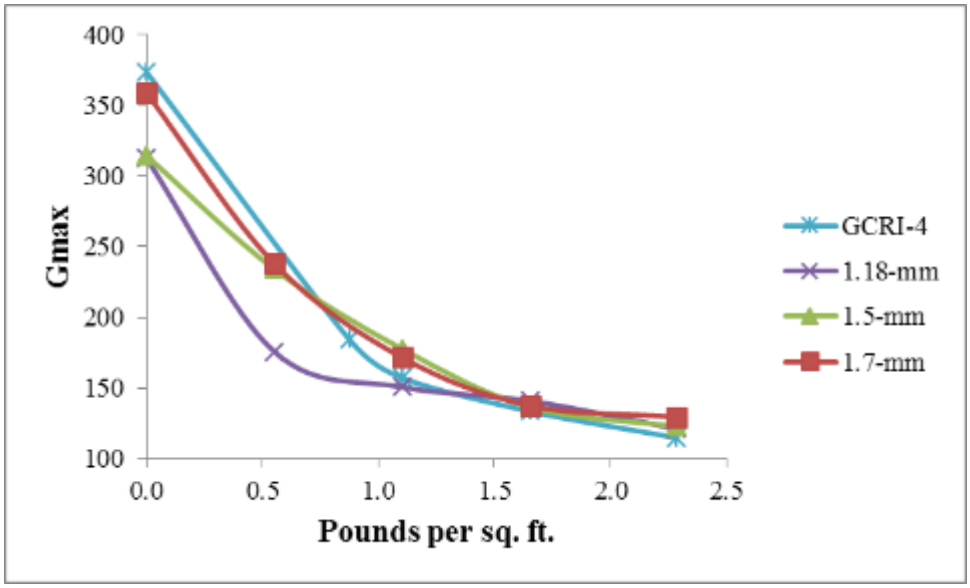

Figure 5.16. Gmax Values of Various GCRI-4 Mesh Samples in Turf

The turf sample showed impact between 300 to 400 Gmax, and all rubber samples showed non-linear converging to overlapping Gmax trend-lines that achieved a plateau below 150. The non-linear plot lines and the end results mimicked the behavior of previous GCRI samples shown in Fig. 5.12. Refinement of GCRI particle size might

therefore change the curve of Gmax impact values versus loading of turf, but the best impact absorption remained the same at the optimum loading level of 2.3 lbs. of infill / sq. ft. of turf.

5.2.2 Fundamental Turf Variables

Concerning the rubber infill, the majority of lot samples (GCRI-1 to 6) displayed converging impact values when loaded in synthetic turf, and then refinement of the GCRI-4 showed little variation in the end results. The focus shifted to the turf itself, which had already demonstrated impact absorption variability before loading the infill (Figs. 5.12-13). For the GameDay Grass™ 3D-52, the polyethylene blade tuft length and the woven backing were the selected aspects to investigate.

5.2.2.1 Turf Setup

To account for product variability, numerous one foot square samples were cut from the same roll of 3D-52 turf. Then by utilizing the method mentioned in section 4.2.2, four sets of different pile heights were prepared by using a mechanical shearer to hand-trim tufts off the turf with the aid of 0.5-in wooden spacers (Figure 5.17).

Figure 5.17. Four Different Pile Heights for 3D-52 Turf

Going from right to left, the first set was unaltered turf with an average pile height of 40 mm, the next set had reduced pile heights aided by wood spacers to 19 mm, another set cut to ten mm, and the remaining left-side set had the tufts removed to a remaining three millimeters of punched-thru yarns. Each sample was assigned a number from one to twelve, and each set was measured for average tuft height as summarized in Table 5.9.

Table 5.9. Modified Turf Height

Sample #	**1 to 3**	**4 to 6**	**7 to 9**	**10 to 12**
Pile Height Average (mm)	3	11	20	43
SD (mm)	0	1	3	2

The non-sheared control set (Samples No. 10, 11 and 12) showed larger deviations of the average pile height than the remaining samples (Samples 1 to 9). The shears and spacers maintained effective control over pile height during modification. Next, each turf sample was tested for impact performance with the same infill material. Each cut sample was fit

inside the wood frame with the metal bottom and filled with the standard GCRI as illustrated in Figure 5.18.

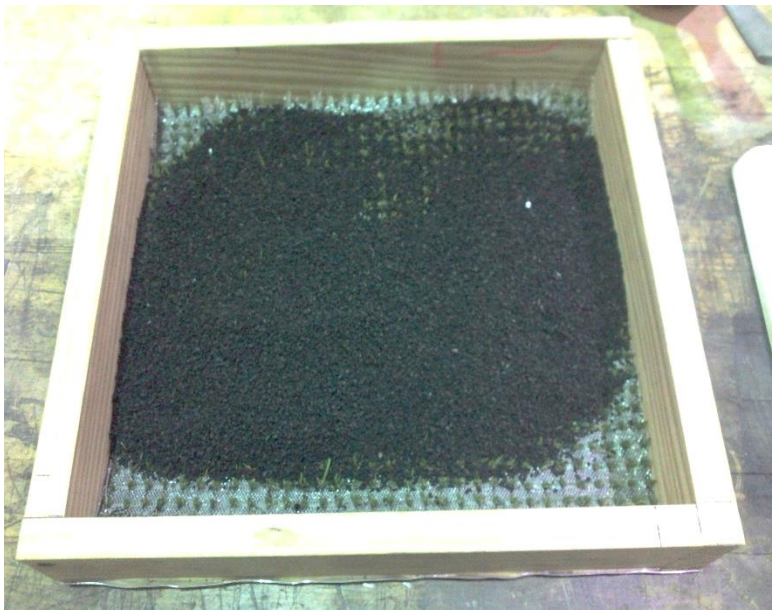

Figure 5.18. Setup for Turf Impact Study

The amount of loaded infill increased after each impact test up to the lowest recommended GCRI amount, 2.3 lbs. / sq. ft. Finally, the infill was recollected for the reuse in the next impact test, and the cleaned turf was replaced with the next sample.

5.2.2.2 Turf Impact Results

In the background research, one of the keys to improved synthetic turf was longer tuft lengths, which also increased overall pile height. Testing the GameDay turf by itself displayed reduced cushioning with decreasing pile height (Figs. 5.19 and 5.20).

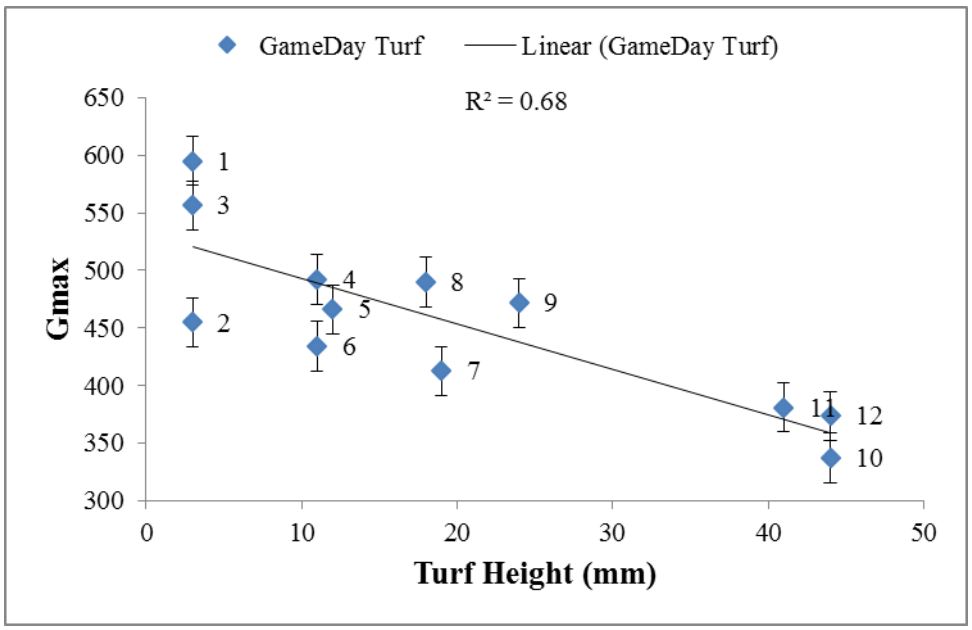

Figure 5.19. Gmax Values of Non-filled Turf at Varying Blade Yarn Pile Heights

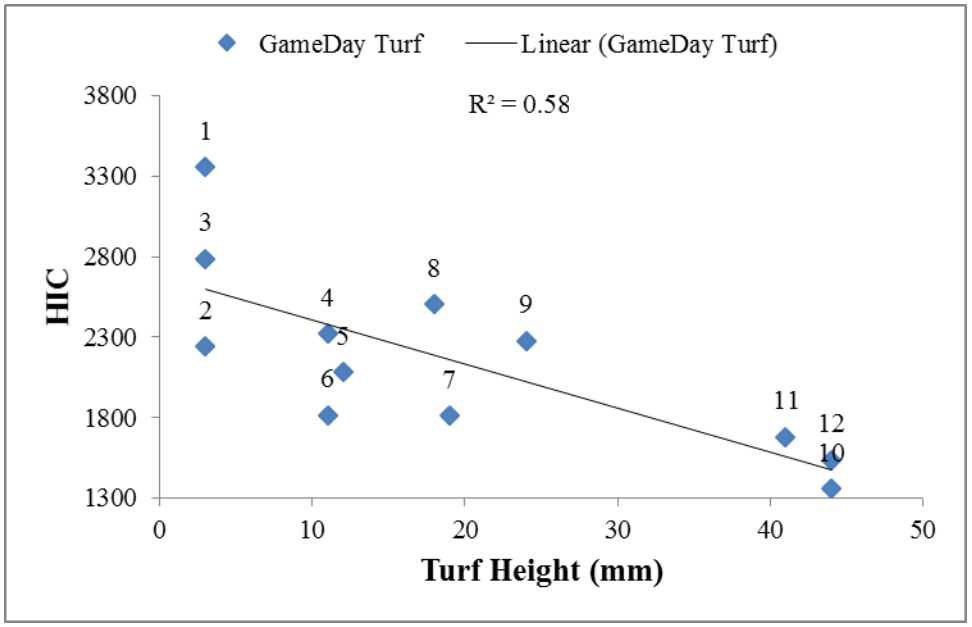

Figure 5.20. HIC Values of Non-filled Turf at Varying Blade Yarn Pile Heights

Compared to initial readings in Figs. 5.12 and 5.13, the control samples Nos. 10, 11 and 12 with the maximum tuft height showed similar results of between 300-400 Gmax and

1100-1900 HIC. The remaining turf samples with reduced pile height showed increased values for both types of impact readings, although impact readings versus pile height were not linear according to the correlation coefficient (R^2) of the individual values. However, curve linearity of the turf sets made for Table 5.9 showed statistically direct correlation when using average values (Table 5.10).

Table 5.10. Average Impact of Modified Gameday Turf

Sample #	**1 to 3**	**4 to 6**	**7 to 9**	**10 to 12**	
Pile Height (mm)	3	11	20	43	
SD (mm)	0	1	3	2	**R^2**
Gmax	535	464	458	364	0.95
SD	73	29	40	24	-
HIC	2795	2073	2197	1526	0.84
SD	558	252	354	161	-

The average of all three samples were more linear than the individual samples likely due to variation within the product. For further impact testing with GCRI and turf, four observations were deemed important:

1. Pile height made a direct, linear contribution to impact absorption.
2. For a given pile height, at least three turf samples were required for a representative average due to variability found in the turf and GCRI samples.
3. HIC and Gmax impact tests showed linear trends when testing GCRI without turf (Section 5.1.3), and then the curves became less linear in combination with the turf due to interaction between the tufts and GCRI.
4. Since HIC reached acceptable levels before Gmax in every sample (Figure 5.12 versus 5.13), Gmax was therefore deemed sufficient to gauge impact absorption for the remainder of the study.

5.2.2.3 GCRI Impact Results

Lot GCRI-4 crumb rubber material was tested in a 3G STF brand named GameDay (Section 4.1.1) with each turf sample designated a number from 1 to 12 as listed in Table 5.9 with variable infill loading up to the vendor-recommended amount of 2.3 lbs. (1043 grams) / sq. ft. of turf. Pile height was also fixed before loading. The resulting data quantified the synergistic effects of pile height and infill loading levels of the turf on attained Gmax values (Table 5.11, Figs. 5.21-22).

Table 5.11. Dual Variable Impacts on Gmax Values

Turf#	Pile Height (mm)	0.0	0.6	1.1	1.7	2.3	GCRI (lbs.)
1	3	595	387	263	208	173	Gmax value per pile height per GCRI load
2	3	455	408	300	196	175	
3	3	556	420	271	231	180	
4	11	492	378	257	181	130	
5	12	466	383	284	208	153	
6	11	434	384	279	192	149	
7	19	413	339	209	166	127	
8	18	490	347	242	177	142	
9	24	472	274	217	166	134	
10	44	337	209	151	132	119	
11	41	381	197	151	128	111	
12	44	374	184*	157	134	115	

*Infill loading reached 0.9 lbs. instead of 0.6 lbs.

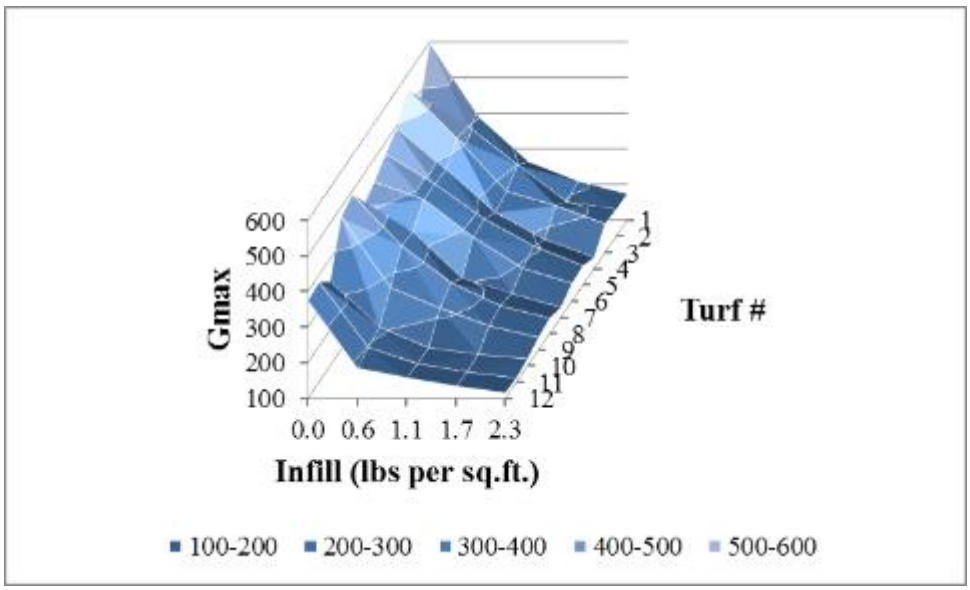

Figure 5.21. Gmax Trend per GameDay Turf Sample

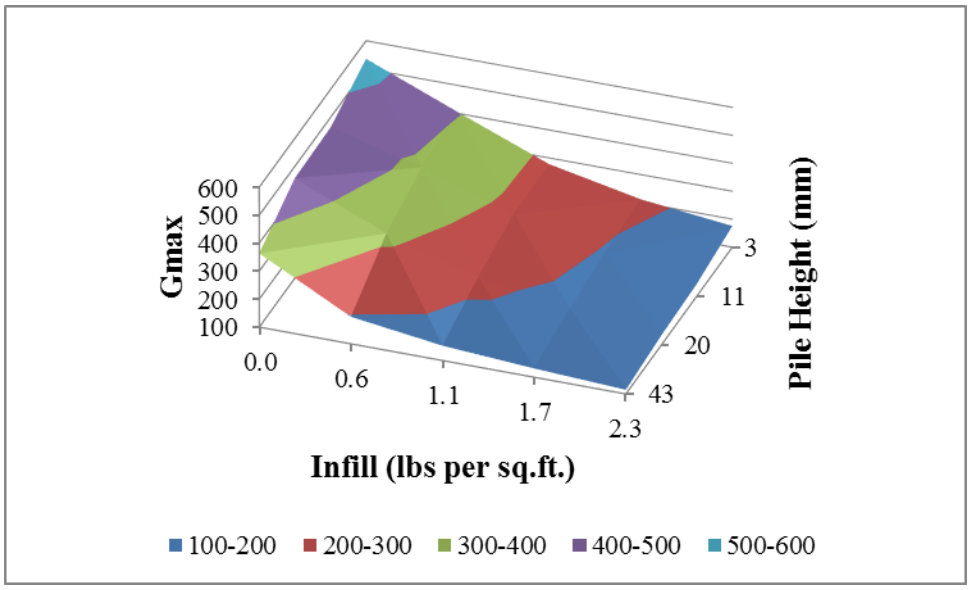

Figure 5.22. Gmax Value Average vs. GameDay Turf Pile Height Average

As indicated in Table 5.11, the turf samples exhibited Gmax values less than 200 when loaded at 2.3 pounds of infill per sq. ft. of turf. The highest Gmax value occurred with turf containing only the backing carcass (i.e., with all the face pile sheared off) and no

GCRI, while the lowest Gmax value occurred with the highest (original) turf pile height and highest GCRI loading. Figure 5.21 illustrates the continuity of this trend despite variances among the 12 samples, while Fig. 5.22 incorporates average values to smooth out the variances. The Fig. 5.22 contour plot exhibits non-linear slopes along the GCRI loading axis, and the slopes along the pile height axis is more linear. However, each variable's linearity and contribution to shock absorption required further analyses.

5.2.2.4 Multiple Regression of Impact Data

The Fig. 5.22 contour plot of both independent factors vs. Gmax values showed the pile height of turf in a negative linear relationship with impact absorption values while the GCRI loading effect appeared non-linear. Previously, both factors underwent single variable linear regression analysis with Microsoft Excel, a method designed to match data to a mathematical equation to find trends or predict values. The pile height showed an R^2 value of 0.95 with respect to Gmax values (Table 5.10), indicating a very strong negative linear relationship between the two variables [50, 51]. Figure 5.10, which shows a plot of GCRI loading levels versus Gmax values, also shows an R^2 value of 0.93, again indicating a strong negative linear relationship. When GCRI was integrated with unaltered turf (Figure 5.12), the resulting Gmax values became less linear (Table 5.12).

Table 5.12. R^2 Values for Linear Correlations to the Data of Fig. 5.12

Lot#	GMAX	R^2 of Linear Trend Line
GCRI-1	112	0.77
GCRI-2	121	0.83
GCRI-3	116	0.86
GCRI-4	110	0.78
GCRI-5	121	0.82
GCRI-6	111	0.74
GCRI-8	150	0.79

The lower R^2 values in Table 5.12 suggest that the data points of Fig. 5.12 were less likely to follow linear trend lines than the infill or turf factors alone. Logically, the next question was how the two factors interacted synergistically to generate filled-turf Gmax values lower than that of either factor alone.

Further regression analysis incorporated both independent (explanatory) variables pile height and infill loading into one linear regression equation, the general format of which is shown below [50].

$$Gmax = b_0 + (b_1 * infill\_loading) + (b_2 * pile\_height)$$

Equation 5.1. Multiple Linear Regression Equation for Gmax

The ideal equation would be a linear model that directly correlate**s** changes in the impact results to an equal change in the factors. However, the factors contain differences in magnitude such as 3 to 43 mm for pile height and 0 to 2.3 lbs. for infill loading, which might skew the relative significance of coefficients b_1 and b_2. Normalizing the data with the highest value of each factor would thus negate the factors' magnitude differences and

create comparative readings in Appendix 3. Another potential issue was the variability of the turf backing previously noted in section 5.2.2.1. If the combination of infill and turf created a unique mechanism during impact absorption, then testing the turf alone may introduce unrelated variations that detract from fitting the data to a linear equation. To minimize the effects of the scattering from non-filled turf on regression analysis, data points based on turf with zero amount of infill were eliminated so the remaining data came from filled (non-zero) turf (data shown in Appendix 4). After regression of these three data types, the raw data and normalized data produced the best fit to a mathematical model with coefficients that explained the significance of the independent factors contribution to Gmax.

Before combining the factors into one equation, the first step was to use analysis of variance (ANOVA) to determine if the factors had statistical significance for the end result, or was it simply the result of random chance [50]. One-way ANOVA tests the significance of each individual predictor (independent) variable. The data was analyzed by the MINITAB program from Minitab Inc. (www.minitab.com) to reach several statistical results listed in Appendices 2 to 4. One-way ANOVA was applied to each data table to determine the adjusted R^2 (Minitab version of R^2 that accounted for the number of explanatory variables) and P-value (the probability that the data was random and the factor not significant at a 95% confidence level) in Table 5.13.

Table 5.13. One-Way ANOVA for Impact Data

Data Source	Statistics	GCRI (lbs.)	Pile Height (mm)
Raw impact data from Appendix 2	Adjusted R^2 (%)	80.43	3.18
	P-Value (%)	0.0	28.0
Normalized data from Appendix 3	Adjusted R^2 (%)	80.43	3.18
	P-Value (%)	0.0	28.0

Non-zero data from Appendix 4	Adjusted R^2 (%)	66.66	14.87
	P-Value (%)	0.0	5.8

From the raw data, the GCRI loading mass into the turf was a significant factor for the Gmax values attained with a 0.0% chance of a random result, while the pile height had a very low correlation to Gmax values with a low R^2 value of 3.18%, i.e., changing pile height did not have a significant effect on impact absorption. Normalizing the data revealed that the factors showed the same significance as non-normalized data, i.e., regression analysis of normalized data could still proceed since the fit of the resultant model equation would be equal to the raw data. Finally, ignoring the non-manipulated data points from zero-loading of infill reduced the R^2 value of GCRI loading mass vs. Gmax values to 66.66% and increased the R^2 value for pile height vs. Gmax values to 14.87%, although random noise was still higher for pile height than the infill weight in the turf. At this point, manipulation of the raw data did not improve the P-value significance of either loading or height, but normalization did gauge relative significance within the model equation.

In all cases of data types, both factors made synergistic contributions to the impact results when regression analysis determined the coefficients for Equation 5.1 (Table 5.14).

Table 5.14. Coefficients from Linear Regression

Data Type	**b_0 (Constant)**	**b_1 (Loading)**	**b_2 (Height)**	**Adj. R^2**	**P-Value**
Raw	481	-137	-3.12	88.7	0.0
Normalized	481	-313	-137	88.7	0.0
Non-zero	425	-106	-2.93	86.7	0.0

In the b_0 column of Table 5.14, the calculated Gmax values are within range of other non-filled turf results such as Figure 5.19 and Table 5.10. In columns for b_1 and b_2, both coefficients show negative slopes as the result of the inverse relationship that exists between the explanatory factors and Gmax. When the independent factors were combined into one model, the R^2 of the resultant linear equation is 89% at a 95% confidence level, indicating the regression results were not due to chance. Within the raw data analysis, the coefficient of the loading variable is much higher than that of the height variable, which suggests that loading has a greater influence on Gmax values. For the normalized data, the coefficients are raised according to the maximum parameter of each factor: (-137 * 2.286 = -313) for infill loading and (-3.12 * 44.0 = -137) for pile height. The new coefficients now account for difference of magnitude between the factors, and infill loading is still higher and more significant to Gmax than pile height. When applied to Equation 5.1, both coefficients and variables require parameter adjustments that create a dimensionless model.

$$\text{Gmax} = b_0 + [(b_1 * \text{infill\_loading\_max})(\text{infill\_loading}/\text{infill\_loading\_max})] + [(b_2 * \text{pile\_height\_max})(\text{pile height}/\text{pile\_height\_max})]$$

Equation 5.2. Parameters for the Multiple Linear Regression of Gmax

Then the model can be simplified to account for the new coefficients (b_1` and $b_2$`) and maximum parameters (2.3 lbs. for maximum infill loading and 44 mm for maximum pile height).

$$Gmax = b_0 + [(b_1`)(\text{infill loading}/2.3)] + [(b_2`)(\text{pile height}/44)]$$

Equation 5.3. Dimensionless Form of the Multiple Linear Regression of Gmax

In the last two columns of Table 5.14, the adjusted R^2 and P-value were also equal between the non-manipulated data and the normalized data, which led to three observations regarding the linear model equations:

1. Normalizing the data was unnecessary to producing a better fit model equation, but the resulting factor coefficients offered improved comparison of relative significance.
2. Correlation of the model linear equation was high enough to preclude further regression analyses.
3. Both factors were significant to the model equation, although the infill mass per unit area loading factor had greater influence than pile height on the attainment of Gmax values.

The regression of the non-zero data set still showed a higher coefficient for the loading variable than for the pile height variable with a high level of confidence in their significance to the impact data; however the adjusted R^2 was lower for the non-zero loading data set compared to the previous two data sets. In conclusion, the multiple regression analyses of the unmodified Gmax and normalized data revealed the significance of GCRI loading and turf pile height, with greater emphasis placed on the infill-based independent factor of mass per unit area of turf.

5.2.2.5 Infill Loading vs. Pile Height

Two factors, loading and pile height, proved statistically significant in influencing Gmax. The higher coefficient for infill loading (Table 5.12) also indicated greater influence on impact absorption than pile height, at least for GCRI infill. Nonetheless, the fundamental study of the GCRI-turf interaction found two important factors governing the effects of the turf: increased turf pile height helped improve impact absorption, and a wide disparity in cushioning by the turf alone was masked by sufficient infill loading. By themselves, each factor had linear effect on Gmax (Fig. 5.11 and Table 5.10). Ultimately, GCRI loading of the synthetic turf lead to convergence of impact results at high loading even after altering the pile height (Figure 5.23).

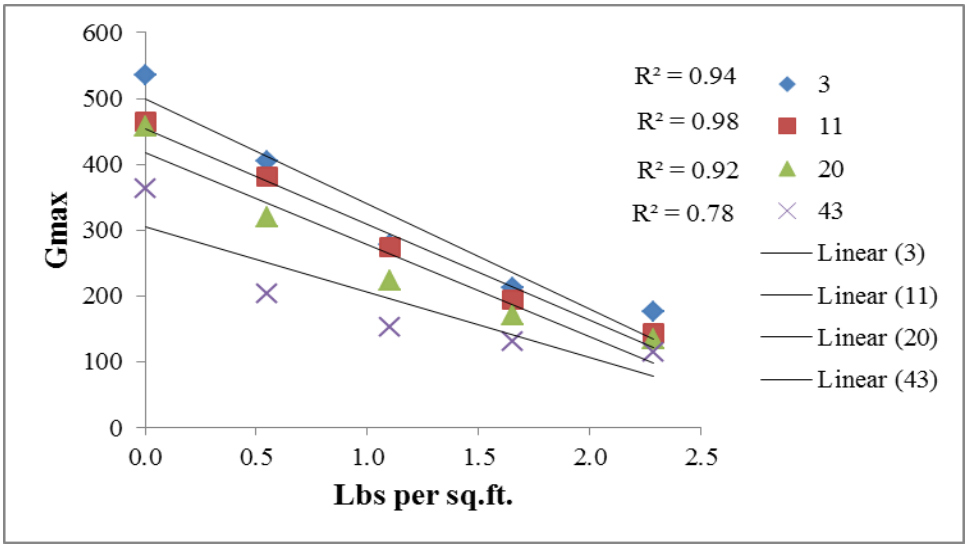

Figure 5.23. Average Gmax Value vs. GCRI Loading Affected by Pile Height (mm)

Starting at low pile heights, the g-vs-loading curves were linear then became non-linear with increased tuft height, which indicated an interaction between the infill and tufts that contributed to impact absorption. At low infill loading, increased pile height reduced Gmax values significantly, e.g. 535 to 364 at 0.6 lbs. / sq. ft., but at optimum infill load of

2.3 lbs. / sq. ft., Gmax reached only 61 g difference between maximum and minimum pile height. Consequently, the combination of the tallest pile and highest infill loading yielded the lowest Gmax by somehow masking the variations within the turf and infill while adding non-linear interaction between turf and infill.

5.2.3 Fourth Generation Turf

Although Fig 5.23 demonstrated impact improvement with increasing pile height, Section 4.1.1 noted that fourth generation turf utilized a shape-modified tuft to improve turf performance. The GameDay brand 3D-60H had tufts with an H-shaped cross-section in contrast to the diamond-shaped tufts of standard brand 3D-52. Another difference between the brands was denoted by the numeric part of their designations that indicated the weight of the face fibers in ounces per yard squared. Regarding 3D-52 versus 3D-60, Table 3.2 listed the different face fiber weights (52 oz/yd^2 vs. 60 oz/yd^2) and nominal tuft heights (57 mm vs. 51 mm). Yet pile height measured for this study showed little difference between the brands: 40±3 mm for 3D-52 and 42±3 mm for 3D-60. To clarify, nominal pile height according to ASTM D-5823 came from cutting tufts from the backing and measuring its length, while the pile height utilized in this study meant distance from backing to top of the turf pile as described in Section 4.2.2. Despite the smaller tuft length in 3D-60H, the turf had a higher number of tufts per turf area than 3D-52 that created a higher face weight in the turf, and these closer tufts acted as reinforcement for each other and for the infill. This reinforcement was proven when the non-filled, 4th generation turf demonstrated improved cushioning values that did not overlap the standard 3rd generation turf (Figures 5.24 and 5.25).

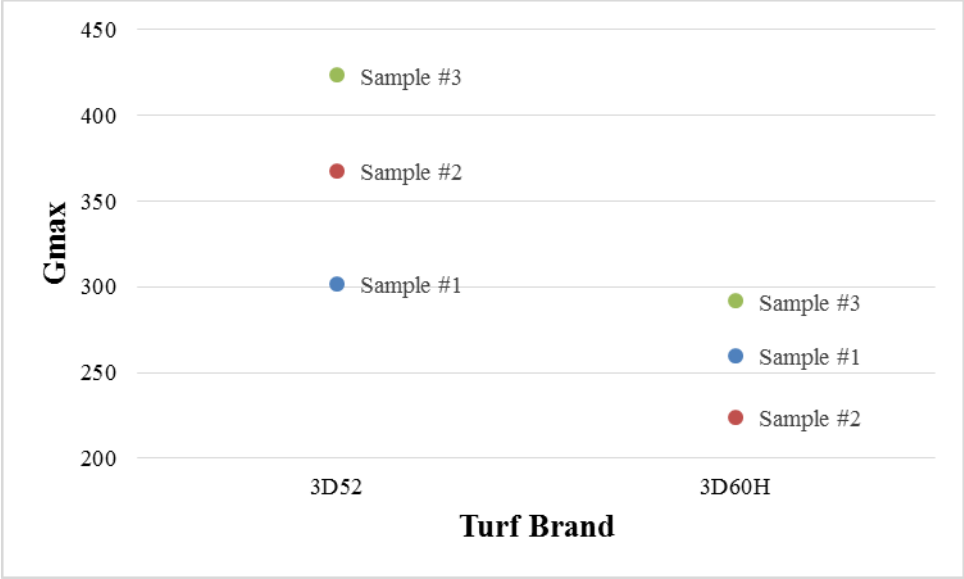

Figure 5.24. Gmax Values of Non-Filled Turf (3rd vs. 4th Generation)

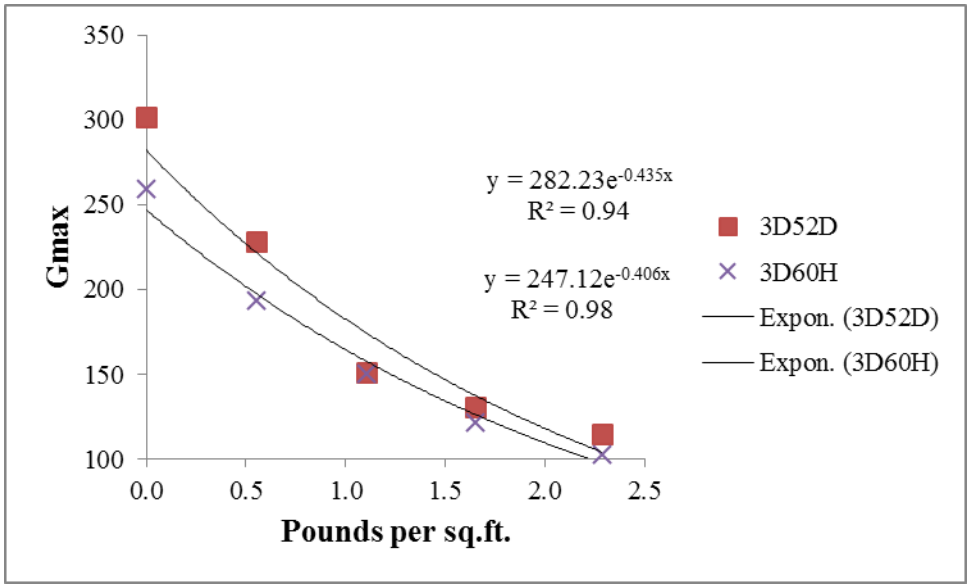

Figure 5.25. Gmax Values vs. GCRI Loading (3rd vs. 4th Generation)

Both Figs. 5.24 and 5.25 demonstrated a lower Gmax for the 4th generation turf 3D-60H than 3rd generation 3D-52. Loading the turf provided one overlapping point in the Gmax vs. loading curves; otherwise, impact values of the 3D-60H remained lower from turf

alone to ultimate fill. Consequently, the new turf lowered Gmax from 115 to 103, and HIC from 342 to 284. Even the behavior of the impact curves correlated better to the raw data with 4th generation turf. Turf Gmax improvement was thus demonstrated with denser, different-shaped tufts that maintained interaction with the rubber infill.

5.3 Post-Consumer Carpet Broadloom Infill Alternative

Since development in the 1950's, the commercial-scale production of modern carpet has led to issues with carpet-related waste disposal that spurred the creation of the Memorandum of Understanding for Carpet Stewardship (MOU) by 2002. The MOU encouraged reuse of material derived from post-consumer, discarded carpet that would otherwise occupy space in landfills. By 2008, the recycling effort could only successfully reclaim the face fiber from the pile that was made of synthetic thermoplastic and composed 50% of the carpet's mass as a rule of thumb [27]. The remaining carpet was the carcass, which was a mixture of latex, filler and trapped fibers that hindered reclamation efforts to achieve successful diversion of waste away from landfills. With a substantial base of U.S. carpet production and reclamation located in Georgia, carpet-related waste was a potential source with logistical and social incentives from the MOU to produce an alternate infill product.

5.3.1 Chemical Composition of Broadloom Carcass

As mentioned in section 4.1.3, the post-consumer carpet samples from broadloom (PCCB) came from several venders located in Dalton, GA. The material came from ambient grinding of the latex-based carcass after the removal of the face fibers. The heterogeneous mix of short fibers and random shaped ground particles contained major components of styrene-butadiene (SBR) and calcium carbonate ($CaCO_3$) according to

vender sources and background research (Table 4.2 and Figure 4.4). The individual particles contained chemicals that displayed FTIR bands attributable to both SBR and $CaCO_3$ (Figure 5.26 and Table 5.15).

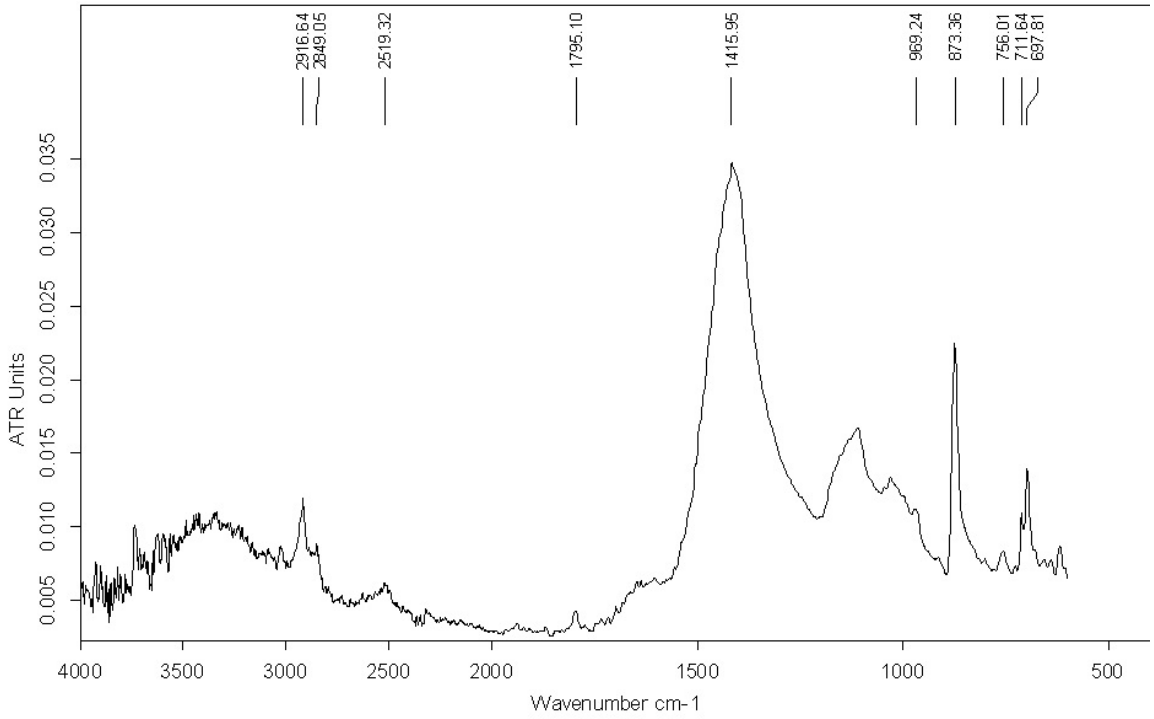

Figure 5.26. ATR-FTIR of PCCB Lot 1 Particle

Table 5.15. FTIR Band Assignments for PCCB

Peak (cm^{-1})	Chemical	Function	Ref #
2917, 2849	$-CH_2-$	Fiber, Backing	47
2519, 1795, 1416	$CaCO_3$	Filler	52
969	Butadiene	Latex	46,47
873	$CaCO_3$	Filler	52
756	Phenyl ring	Latex	46
712	$CaCO_3$	Filler	52
698	Phenyl ring	Latex	46

The spectrum of PCCB Lot 1 (Fig. 5.26) was considered typical of the other broadloom samples. The prominence of the calcium carbonate peaks indicated a high concentration of the filler relative to the amount of SBR latex. The unrecovered, remaining fibers were not the focus of the research, but signature peaks of nylon and polypropylene could not be distinguished from the latex FTIR bands. According to the height of the spectrum peaks, SBR and $CaCO_3$ were major components of the recovered PCCB particle mix.

To determine actual amounts of SBR and $CaCO_3$ in the carpet reclaim, random particles from two lots were subjected to thermal decomposition via TGA. Akin to the GCRI analysis summarized in Table 5.2, samples from different sources sieved by 70 and 200 mesh displayed the following sequential thermal steps (Fig. 5.27).

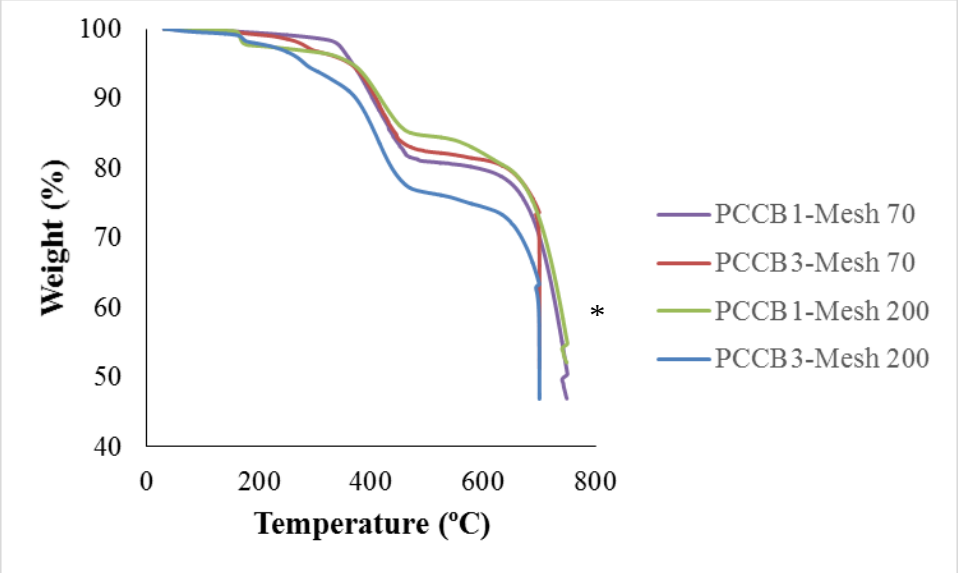

*CO_2 loss above 600° C from $CaCO_3$

Figure 5.27. TGA of PCCB Lots 1 and 3

Both lots had similar thermally-driven losses and matched other curves found in literature concerning carpet backing; therefore assignable to volatiles, latex, and filler (Tables 5.16 and 5.17) [53].

Table 5.16. Decomposition Temperatures and Mass Percentages of PCCB-1

Carpet Component	Mesh 70 (Cº/Mass %)	Mesh 200 (Cº/Mass %)	Temperature Average (C)	Mass Average (%)
Volatiles	340 / 2	166 / 4	250	3
SBR	402 / 17	420 / 11	411	14
$CaCO_3$	745 / 77	741 / 75	743	76

Table 5.17. Decomposition Temperatures and Mass Percentages of PCCB-3

Carpet Component	Mesh 70 (Cº/Mass %)	Mesh 200 (Cº/Mass %)	Decomposition Average (C)	Mass Average (%)
Volatiles	285 / 3	283 / 6	284	4
SBR	414 / 14	414 / 17	414	15
$CaCO_3$	694 / 73	695 / 68	694	70

The beginning of mass losses between 402º - 420º C matched the SBR curve that ended at 435º C in the literature, and decompositions that began between 694º - 745º C belonged to $CaCO_3$, which also occurred at 775º C [53]. After the volatiles and polymers degraded below 500º C, material loss afterwards came from remaining $CaCO_3$ filler that degrades into carbon dioxide and calcium oxide. The percentages of calcium carbonate in both PCCB lots (Tables 5.16 and 5.17) were much larger than the carbon black filler in rubber infill (Tables 5.3 and 5.4). Conversely, the polymeric components in PCCB were lower than in GCRI. Therefore, within the same synthetic turf, the $CaCO_3$ filler would thus play a significant role in the impact performance of PCCB, possibly larger than the analogous carbon black filler would with GCRI.

5.3.2 Physical Conditions of PCCB

According to the PCCB venders, the goal of the carpet grinding process was reclamation of the carpet fibers and reduction of the carcass to small particles. The samples summarized in Table 4.3 showed the bulk of particles to be below 0.5 mm, the minimum of preferred infill size (Figure 5.28).

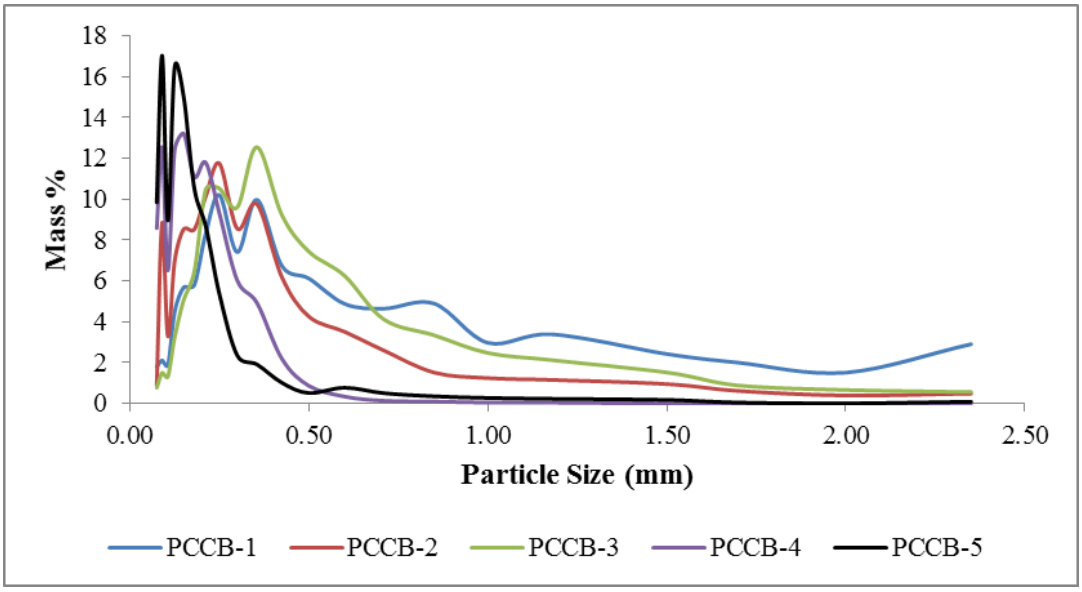

Figure 5.28. Size Distribution of PCCB Particles

In contrast to the bimodal distribution of GCRI in Fig. 5.8 and 5.9, the PCCB curves showed multiple peaks that trended toward smaller particle sizes. More physical differences between GCRI and PCCB became apparent after examination of the particles under magnification.

Figure 5.29. PCCB-1 Crumb from 2.35-mm Sieve

Figure 5.30. PCCB-1 Crumb from 0.212-mm Sieve

The particle in Fig. 5.29 was a visibly distinguishable composite of latex, filler and fibers that were a contrast to the more homogenous appearance of rubber infill seen in Figures 5.6 and 5.7. Further grinding of the PCCB carcass reduced the particles to a loose mixture of fibers and latex crumb (Fig. 5.30). The change from composite to physical mix created an assortment of average particle size and bulk density (Table 5.18).

Table 5.18. Particle Size and Bulk Density of Ground/Sieved PCCB

Lot#	Source	Average Particle (mm)	SD (mm)	Bulk Density (gm/cc)
PCCB-1	Mohawk	0.53	0.51	0.25
PCCB-2	Mohawk	0.33	0.31	0.66
PCCB-3	Shaw	0.43	0.35	0.41
PCCB-4	Beaulieu	0.18	0.10	0.74
PCCB-5	Shaw	0.17	0.15	0.31

The calculated values in Table 5.18 had a degree of uncertainty since the Rotap sieves could not trap all the test material with the loss reaching between 4% to 28% from test to test. When putting this uncertainty aside, the first four samples followed a negative correlation between increased particle size and reduced bulk density, which suggested greater recovery of the fiber from the latex particles. The remaining lot, PCCB-5, had a low bulk density with the lowest average particle size, possibly due to a large amount of loose fiber not bonded to the latex particles. Neither a standard reclamation process nor test method was available that could measure the amount of unclaimed fiber in a given sample, thus the precise ratio of SBR particles to loose fiber was unknown for all the PCCB samples. Assuming bulk density and particle distribution were important factors that governed infill loading, then each PCCB lot would penetrate at different levels than rubber infill since their particle size averages were below the GCRI-4 standard of 1.38 ±

0.37 mm, and all but one PCCB lot were outside the 0.41 – 0.57 gm/cc range of all the GCRI (Table 5.6). In summary, PCCB interaction with the turf during impact testing would thus demonstrate how these physical parameters detract or enhance performance.

5.3.3 Impact Measurements of PCCB

In Table 5.18, each PCCB lot had lower average particle size than the GCRI-4 standard and wide variations of bulk density. For PCCB samples below 0.43 gm per cubic centimeter, turf filling went below 2.3 pounds per square foot, while higher densities filled the turf. To compensate for different bulk densities, each PCCB had an initial fill calculated based on filling an empty turf volume of 2136 cc calculated in Section 5.1.2 (Table 5.19).

Table 5.19. Infill Loading for PCCB

Lot#	Bulk Density (gm/cc)	Estimated Infill Load (lbs. / sq. ft.)
PCCB-1	0.25	1.2
PCCB-2	0.66	3.1
PCCB-3	0.41	1.9
PCCB-4	0.74	3.4
PCCB-5	0.31	1.4

The loading values in Table 5.19 served as amounts for filling the turf at similar volumetric levels as the rubber infill in order to maintain similar conditions during impact testing.

In the following impact tests, PCCB samples were evaluated at estimated infill amounts from Table 5.19 except for PCCB-5 from Shaw that was excluded due to limited material (Fig. 5.31).

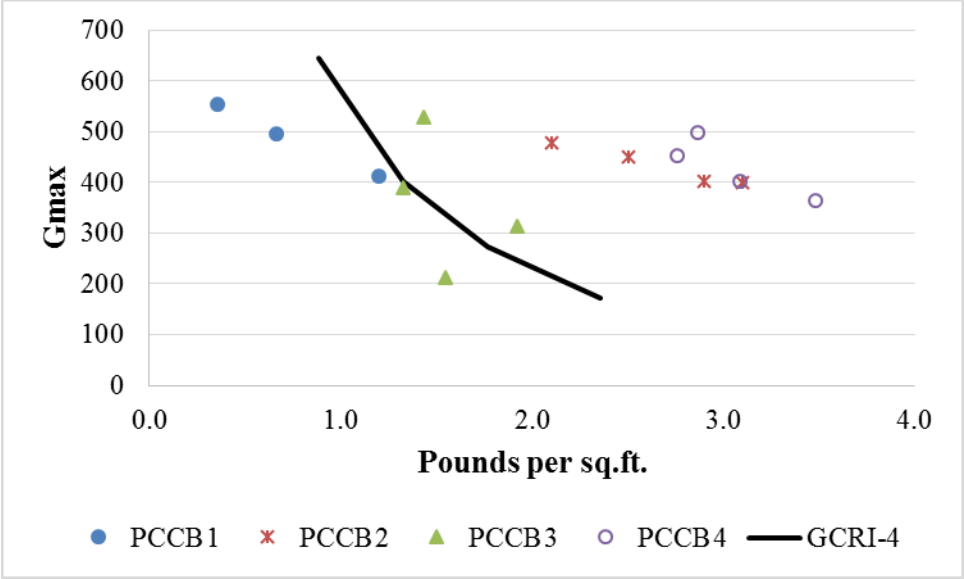

Figure 5.31. Non-turf Gmax Values of PCCB

Overall, the behavior of PCCB showed stark contrasts to rubber based infill. The first observation was that GCRI lots without turf in Fig. 5.10 reached almost 150 Gmax at the recommended amount of infill, while none of the PCCB in Fig. 5.31 went below 200 Gmax even at loading levels above 2.3 lbs. / sq. ft.. Previously, most of the GCRI exhibited similar linear trend behavior with overlapping impact values, but only a few of the PCCB samples had linear trends plus none of them exhibited similar impact values. When tested in turf, PCCB lots 3 and 4 displayed random data points that did not correlate predictably, while PCCB lots 1 and 2 exhibited declining Gmax values with increasing amounts of infill like GCRI-4 (Fig. 5.32).

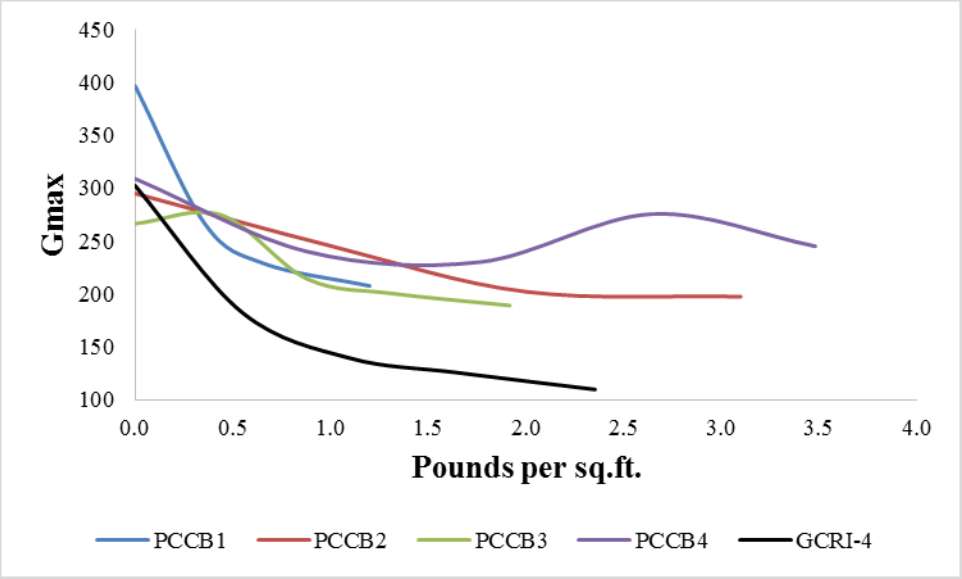

Figure 5.32. Gmax Values of PCCB in Gameday Turf

Overall, the most apparent difference between rubber and broadloom carcass was the wide variation in the physical properties of the carpet lots (Fig. 5.32) in contrast to overlapping properties between the GCRI that lead to overlapping Gmax values (Fig. 5.12). The PCCB samples had improved Gmax performance in the turf and achieved plateaus at optimum filling despite impact absorption variation of the unfilled turf, i.e. from 240 to 397 Gmax in turf with 0 lbs. of infill. However, the PCCB samples only reached Gmax values above 180 while the GCRI-4 achieved a 110 Gmax in the same brand of turf. The difference of impact performance between GCRI and PCCB became more apparent with HIC comparisons (Table 5.20).

Table 5.20. Impact Values of PCCB at Optimum Loading

Lot#	Gmax	HIC
GCRI-4	110	320
PCCB-1	208	705
PCCB-2	197	636
PCCB-3	189	623
PCCB-4	245	924

All PCCB samples achieved HIC values below 1000 but at approximately 2-3 times that of GCRI, and Gmax fared no better. In the current composition of loose fibers and minute size particles, none of the PCCB-based infills matched GCRI structure nor matched the behavior of the impact curves.

5.3.4 Modification of PCCB

Among the PCCB samples, only the PCCB-1 sample had an average particle size above 0.5 mm, the minimum particle size recommended for infill. With only 36% of its particles above 0.5 mm, the other 64% major portion of PCCB-1 mass would slip through the perforated backing of the synthetic turf. The infill loss would hinder impact absorption of the turf and block the drainage channels of the underlying STF foundation. Hence, the grinding process for broadloom carpet carcass would have to shift the particles to replicate the 0.5-3.0 mm range of GCRI in order to prevent loss of infill and to protect the turf foundation from drain blockage. Towards that end, the central question would be how adjusting the particle size distribution would affect impact performance.

For isolating particle sizes above 0.5 mm, the Rotap sieves sifted through the PCCB-1 particles via meshes 35 (0.50 mm) and larger. Then recombining the particles produced a refined infill. This Rotap method was applied repeatedly to accumulate a sufficient amount for infill. The previous Rotap analysis (Fig. 5.28) determined a

possible 36% yield of particles in the unrefined PCCB-1 sample that could achieve the desired size range. The actual yield by repeated Rotap isolation reached 25% of particles at 0.50 mm and higher to achieve the refined version of PCCB-1. Additional analysis of the isolated and remaining particles confirmed sizes above and below 0.5-mm (Fig. 5.33).

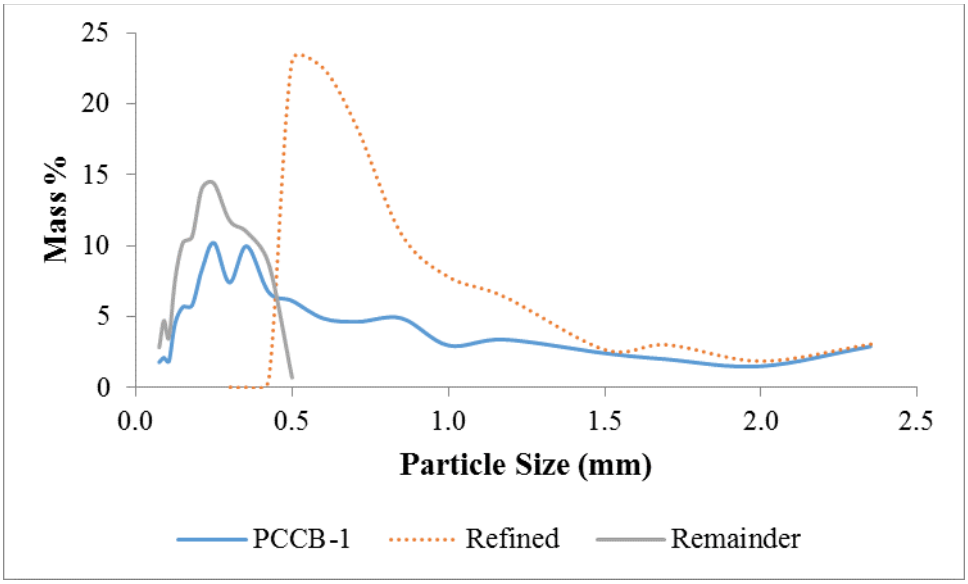

Figure 5.33. Size Distribution of Refined PCCB-1

Fig. 5.33 illustrates isolation of the "Refined" latex particles above 0.5 mm via Rotap, while the smaller particles were designated as the "Remainder" group. The Rotap method also affected the overall bulk density of each group (Table 5.21).

Table 5.21. Particle Size and Bulk Density of PCCB-1 Fractions

PCCB-1 State	Average Particle (mm)	SD (mm)	Bulk Density (gm/cc)	SD (gm/cc)
Bulk	0.53	0.51	0.49	0.09
Refined	0.83	0.43	0.44	0.06
Remainder	0.23	0.10	0.66	0.02

The “Bulk” results came from the repetitive use of the Rotap method and illustrated a wide variation of distribution within the material regarding particle size and density. While the unrefined bulk PCCB-1 had higher average bulk density than the initial result of 0.25 gm/cc (Table 5.18), the measured test samples went from 0.30 to 0.63 gm/cc in the same batch. As for the separated batches, the refined particles (≥0.50 mm) achieved a higher particle size average with a standard deviation of size almost as high as the bulk material. In addition, the bulk density of the refined PCCB-1 was lower than bulk BD, which suggested the removed particles contained more filler than the refined. The remainder of PCCB-1 particles were below 0.50 mm, a lower average particle size with a single peak distribution curve and a higher bulk density than the original PCCB-1. Because the smaller size of the remaining PCCB-1 would flow through the perforated turf backing, only the refined version was tested for impact absorption.

Compared to the initial PCCB-1 sample, the turf was filled with a refined version. Although the exact difference in loose fiber content between samples could not be quantified, the impact turf setup did show visual differences (Figures 5.34 and 5.35).

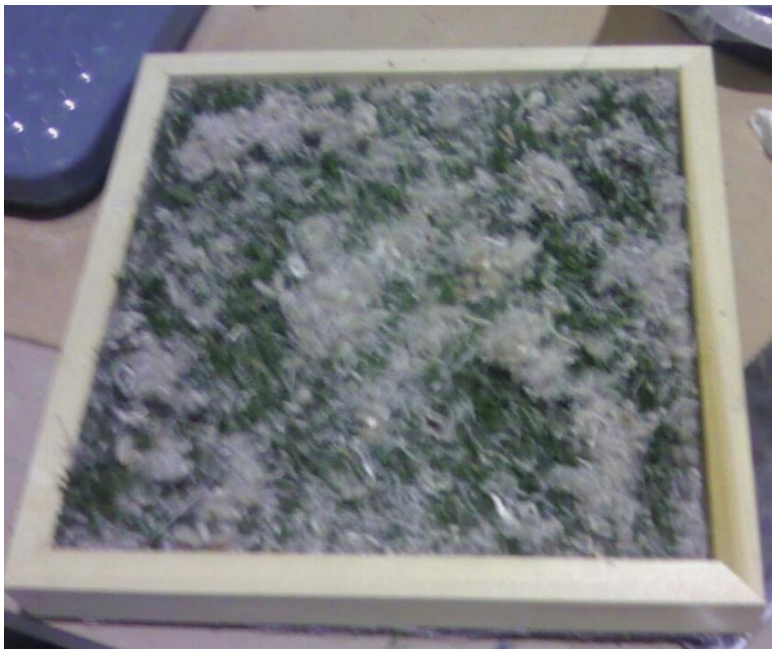

Figure 5.34. Fiber Clumps in Impact Turf Setup for PCCB-1

Figure 5.35. Fiber Clumps in Impact Turf Setup for Refined PCCB-1

In Fig. 5.34, the aggregations or clumps of fibers were difficult to break down manually into individual fibers that might aid integration into the turf. After the refining process, the fiber clumps were smaller and more easily penetrated the tufts in Fig. 5.35. As for impact performance effects, the "Refined" and "Remainder" PCCB-1 samples showed changes before addition to turf (Figures 5.36 and 5.37).

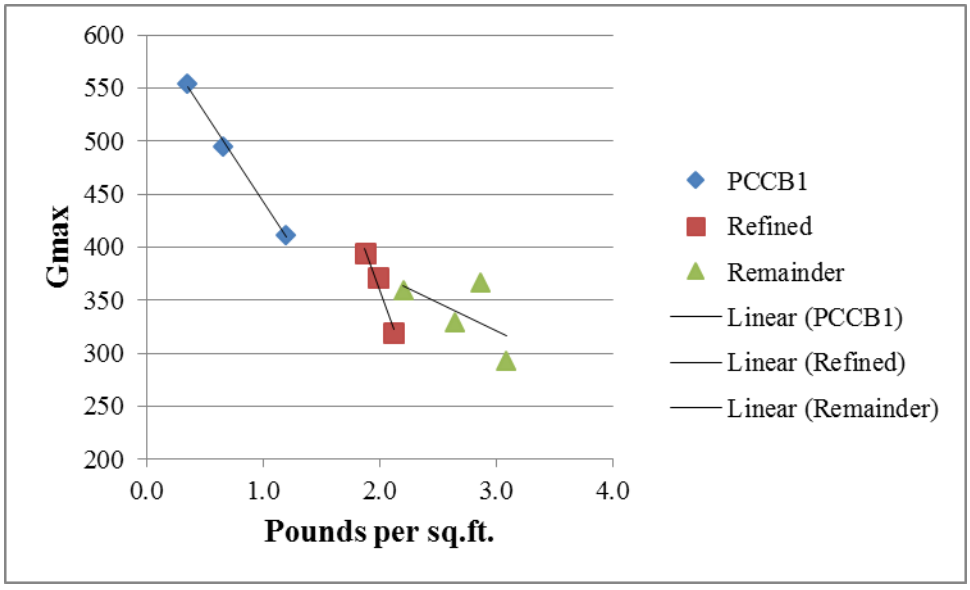

Figure 5.36. Non-turf Gmax Values vs. Infill Loading for PCCB-1

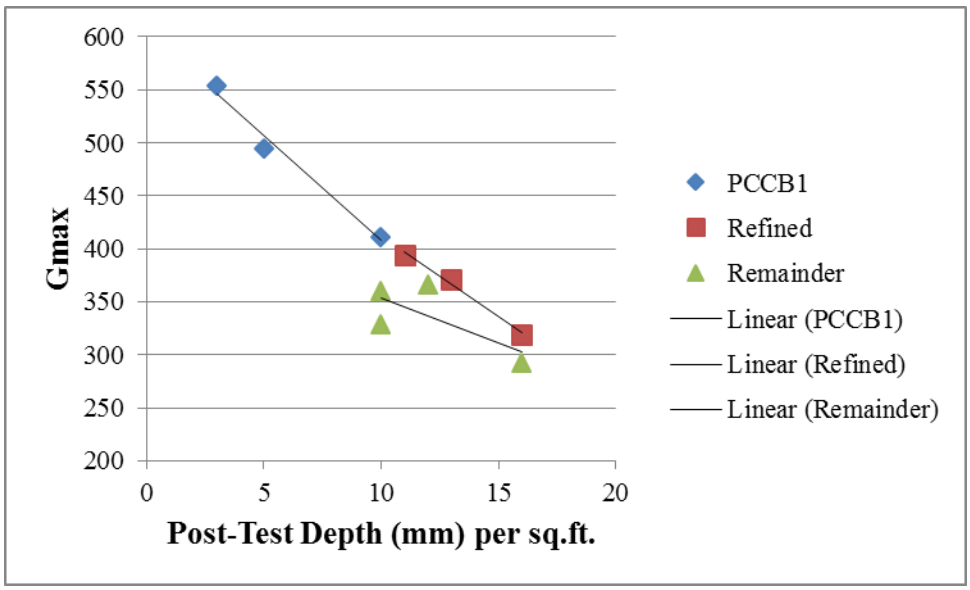

Figure 5.37. Non-turf Gmax Values vs. Infill Depth for PCCB-1

The "Refined" form of PCCB-1 had a similar bulk density (0.44 gm/cc) to the original bulk material (0.49 gm/cc), but Gmax testing yielded lower values along with higher turf loading of bulk PCCB-1. The data slopes were linear in Fig. 5.36 with the trend lines of both bulk and Refined PCCB-1. When plotting Gmax against the infill depth post-impact testing in Fig. 5.37, both Refined and Remainder PCCB had aligned slopes. Since the Refined infill had large SBR particles above 0.5-mm from the original lot, then the aligned slopes in Fig. 5.37 meant that large SBR latex particles had a strong linear influence on performance of the original bulk material.

As for the Remainder PCCB-1 made of particles below 0.5-mm, the Gmax followed a declining trend for both the amount of loading and post-test infill depth without turf. However, the data points did not closely follow the trend lines found in the Refined or bulk forms. The Remainder PCCB-1 particles achieved a bulk density of 0.66 gm/cc that shifted the Gmax trend to higher infill weight while achieving the lowest

Gmax values in Fig. 5.36. When plotted at post-test infill depth in Fig. 5.37, the Remainder PCCB-1 Gmax went lower than the Refined while both modified forms showed downward trend lines. However, the lower Gmax values were moot since the small particle sizes of the Remainder PCCB-1 would not be retained by the synthetic turf. Therefore, impact testing with synthetic turf was not practical if the particles would slip through the turf backing and foul the drainage system.

When incorporated into the 3D52 turf, the Refined PCCB-1 penetrated between the long turf tufts deeper than the bulk form, but clumped fibers remained visible (Fig. 5.34 vs. Fig. 5.35). The higher bulk density of Refined PCCB-1shifted the impact values to lower Gmax at higher infill loading in the turf than bulk PCCB-1 (Fig. 5.38).

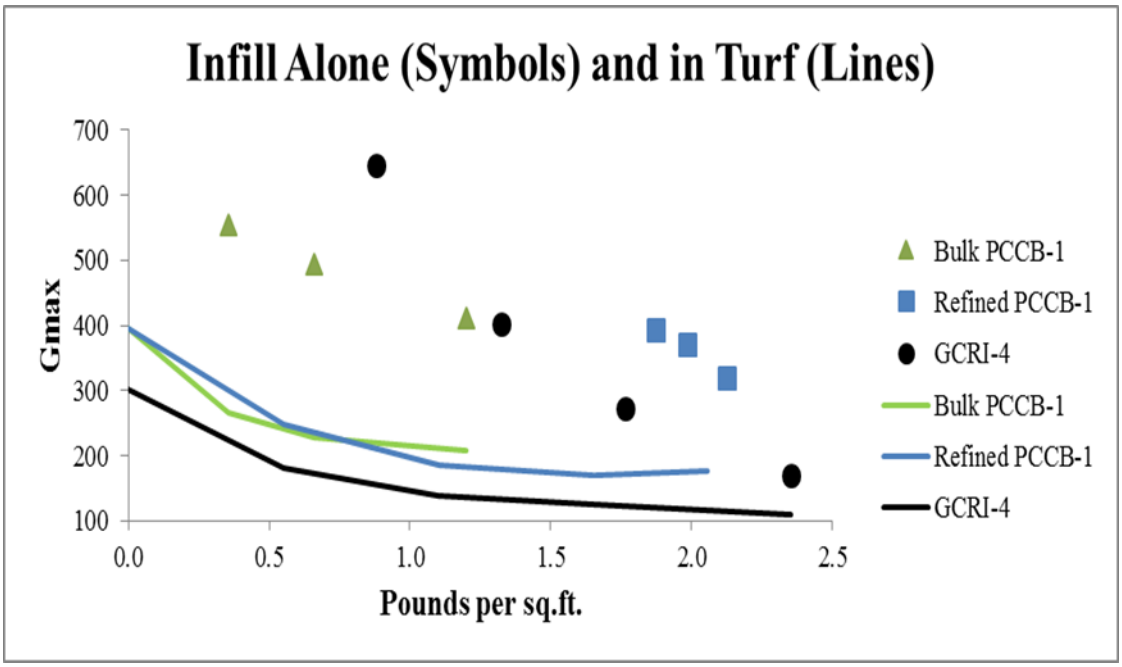

Figure 5.38. Bulk and Refined PCCB-1 versus GCRI Gmax

Whether testing different lots of GCRI or PCCB, the non-turf Gmax vs. infill amount curves were approximately linear and became non-linear when integrated with the turf. In Fig. 5.38, all infill samples without turf showed linear or near-linear curves. Then all impact values were higher than GCRI at the highest weight. When incorporated with turf, the original PCCB-1 achieved a plateau reaching 208 Gmax, and then Refined PCCB-1 lowered the plateau to 177, a 15% improvement. Therefore, the bulk density of the Refined PCCB lead to greater infill loading, easier turf integration and lower resultant Gmax. Whether by particle size modification or by bulk density change through reduction of fiber content, the refined PCCB particles improved control over infill Gmax performance, but not enough to match the impact absorption properties of standard rubber-based product.

5.4 Post-Consumer Carpet Tile Infill Alternative

Unlike the cross-linked latex of broadloom carpet, the carcass of tile carpet was already recyclable into other tile products due to its partial thermoplastic composition. Consequently, tile back reclaim came in several forms even from one source. With several forms of this reclaim available, the overall goal was to find the most desirable structure and reclaim method.

5.4.1 Chemical Composition of Tile Carcass

In contrast to the numerous PCCB vendors, reclaim from post-consumer carpet tile (PCCT) came from one supplier, InterfaceFLOR, LLC of La Grange, GA. As detailed in Section 4.1.3, the first three lots were dark, random-shaped, flattened particles from a production line (Lot 1), a pilot line (Lot 2) and a reduced particle size line (Lot 3) respectively (Figs. 4.5 and 5.39). Finally, Lot 4 came from tile carcass that was melt

extruded into pellets (Fig. 5.40). The remaining Lots 5 and 6 came from the same production line as Lot 1. However, Lot 5 material had a crumb structure more like rubber crumb than flat particles, and Lot 6 was finer crumb caught by particle traps placed along the processing line (Figs. 5.41 and 5.42).

Figure 5.39. PCCT Crumb of Lot 1

Figure 5.40. PCCT Lot 4 Extruded Pellets

Figure 5.41. PCCT Lot 5 Production Line Crumb

Figure 5.42. PCCT Lot 6 Production Line Fines from Traps

While broadloom backing arrived only as fine particles that required sieves to isolate the large material, the tile-based reclaim came in multiple forms and sizes from the same supplier.

InterfaceFLOR collected the post-consumer carpet and first shaved the face fibers for recycling. The tufted carpet face layer was composed of the fibrous tuft back-loop and primary backing, while the remaining tile carcass was made of a thermoplastic binder layer of PVC that contained phthalate-based plasticizer, a nonwoven fiberglass layer adding stiffness to the tile structure, and quartz sand (silica) filler. In an informational report, the PCCT supplier described plasticized PVC as the ideal binder for its carpet tile product due to its dimensional stability and non-toxic chemistry under ambient conditions [61]. The plasticizer in the PVC of PCCT was reported to be di-isononyl phthalate, and a 2006 European study was referenced in the report that found no hazards from exposure to this chemical for humans or the environment [62]. The PVC binder and plasticizer were confirmed to be present in the PCCT infill

particles as reported herein by FTIR and TGA. FTIR also detected silica that were visually evident as physical sand particles and fibers under high magnification of crumb particles from PCCT-1 (Figs. 5.43-5.44 and Table 5.22).

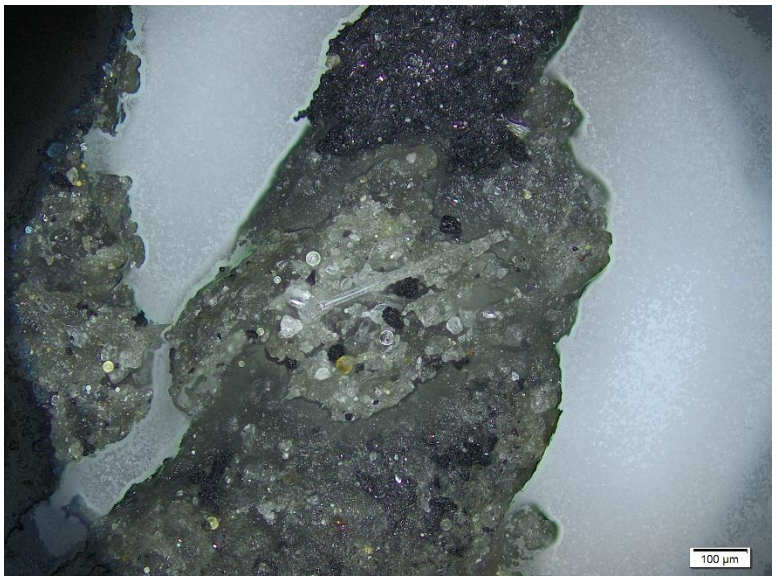

Figure 5.43. Glass Fibers and Silica in PCCT-1

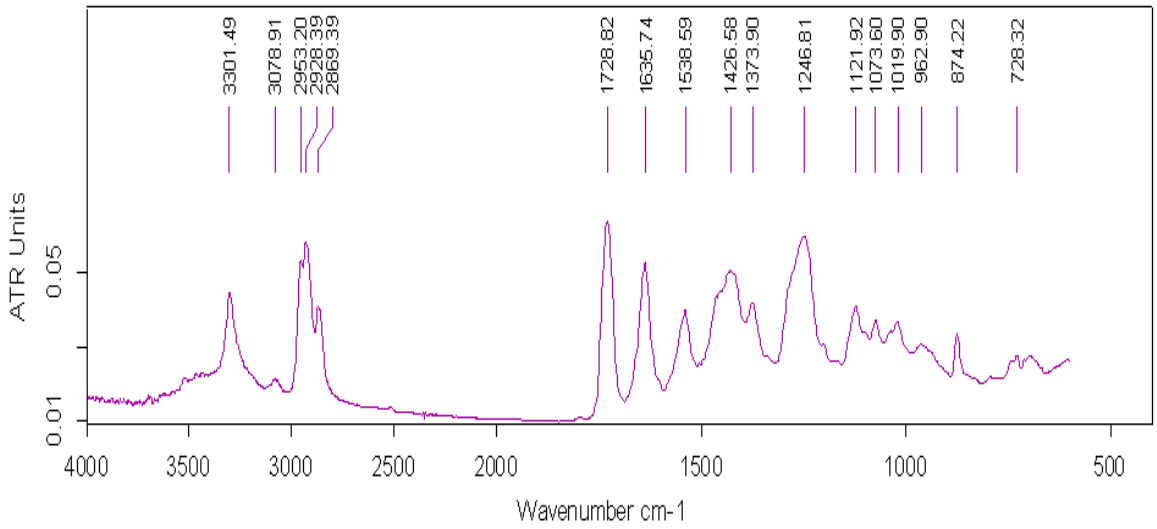

Figure 5.44. FTIR of PCCT-1

Table 5.22. FTIR Band Assignments for PCCT

Peak (cm^{-1})	Chemical	Function	Ref #
3302 & 3068	Polyamide	Fiber	54
1795	$CaCO_3$	Filler	52
1729	Phthalate	Plasticizer	54
1636	Polyamide	Fiber	54
1539	Polyamide	Fiber	54
1427	PVC	Backing	54
1415	$CaCO_3$, CaO	Filler	52
1247	PVC	Backing	54
1121, 1073 & 1019	Silica	Backing, Filler	54
963	PVC	Backing	54
874, 711	$CaCO_3$	Filler	52

Since polyamide is not listed as backing material for tile carpet, residual nylon face fibers were the likely source of the polyamide peaks. The remaining samples that came from different reclaim lines (Lots 2, 3 and 4) had similar FTIR peaks but at various relative heights (Figures 5.45, 5.46 and 5.47).

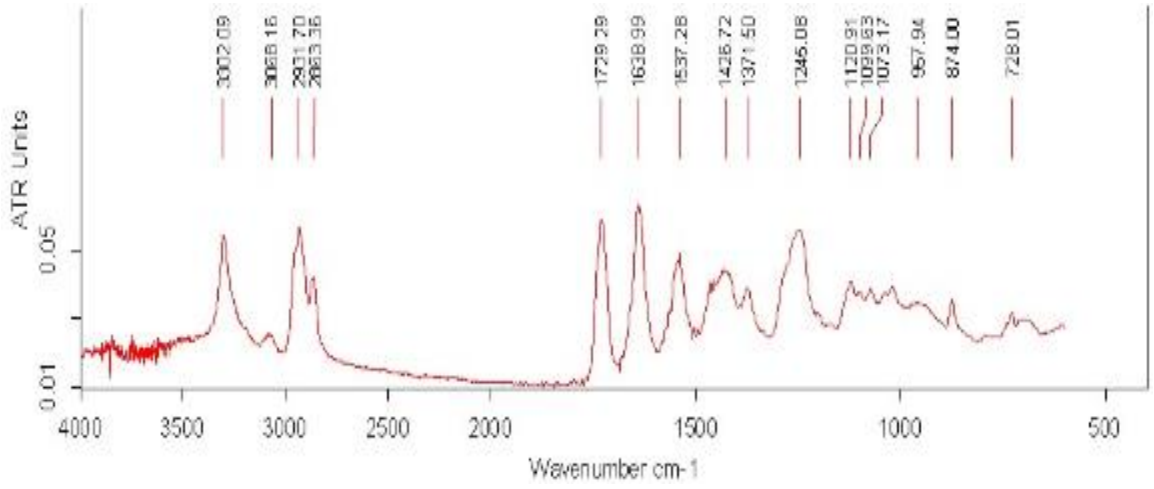

Figure 5.45. FTIR of PCCT-2

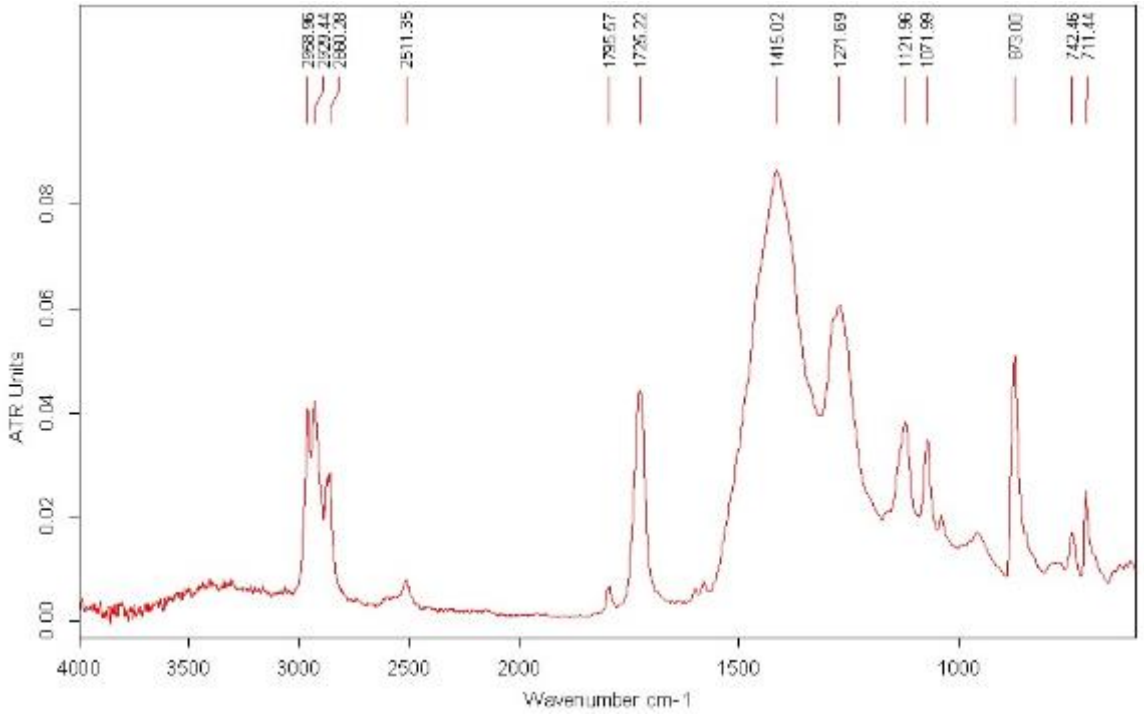

Figure 5.46. FTIR of PCCT-3

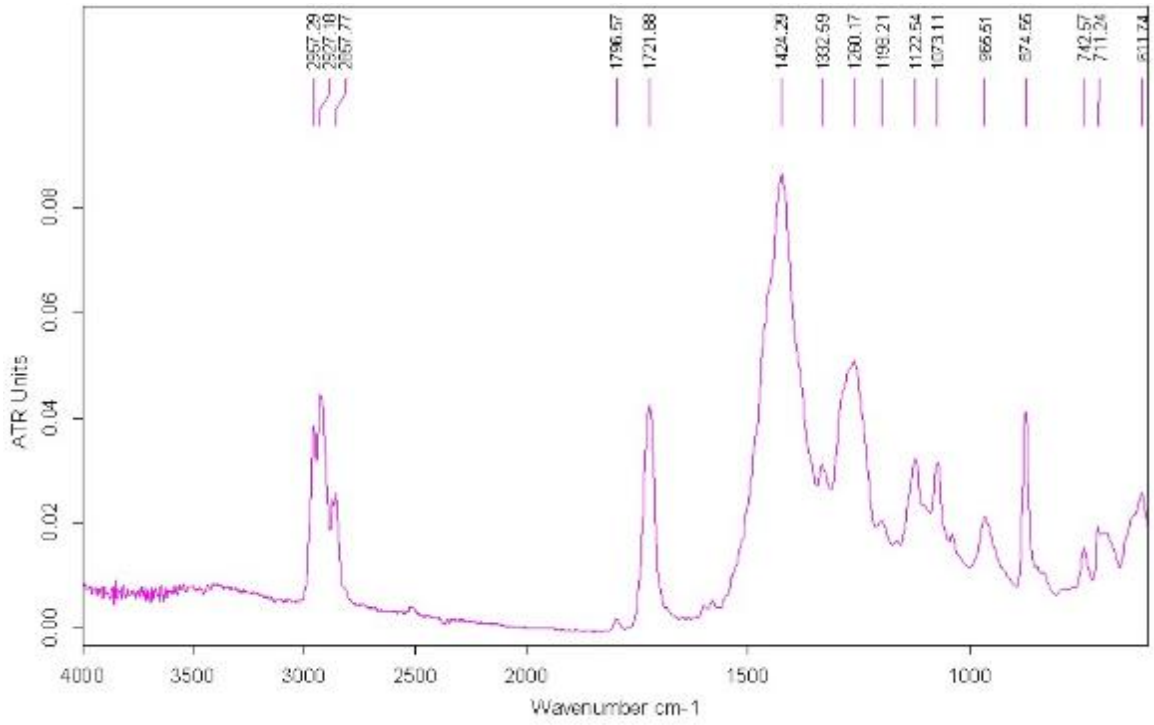

Figure 5.47. FTIR of PCCT-4

In FTIR analysis, both lots PCCT-1 and PCCT-2 had similar chemical composition levels of nylon, PVC and phthalates. The other lots PCCT-3 and PCCT-4 showed levels of phthalates, filler and PVC similar to each other but different from Lots 1 and 2. The absence of polyamide peaks (1539, 1636, or 3302) in Lots 3 and 4 indicated that very little or no nylon was present in the particle. Even though the presence of nylon was not consistent between the FTIR samples, all lots had PVC binder, plasticizers and fillers such as calcium carbonate and silica.

With the aid of TGA analysis, the chemical components in a given polymeric sample could be quantified by measuring the thermal degradation. However, PVC presented a challenge due to a two-stage decomposition that may overlap other chemicals [45]. The following TGA curves of the first three lots originated from samples separated with a mesh 10 sieve (2.0 mm) that isolated large particles, and a pellet was randomly selected for PCCT-4 (Fig. 5.48).

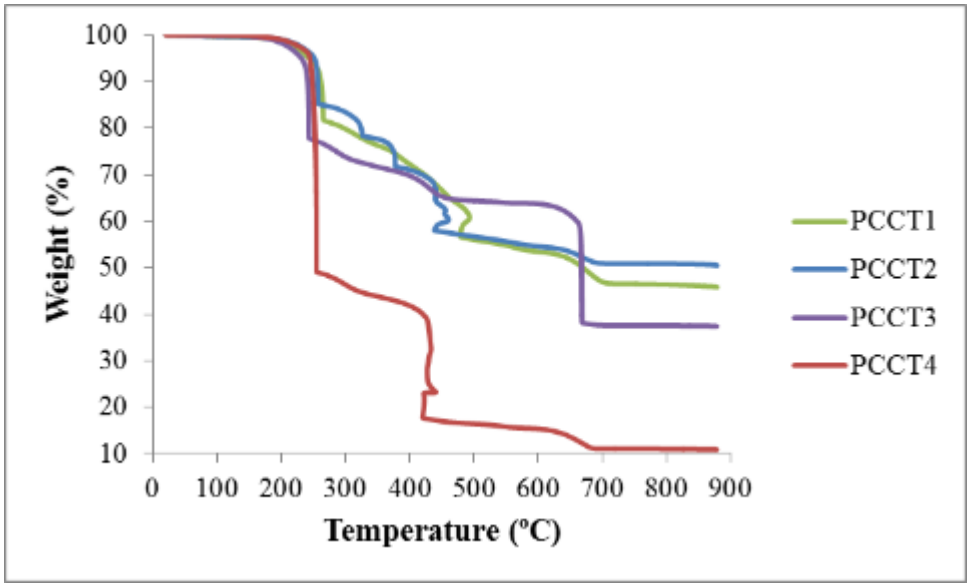

Figure 5.48. TGA of PCCT Lots 1 to 4

The first mass loss before 300º C was usually due to low boiling volatiles such as the phthalate-based plasticizer. However, the next curve drop between 300º to 500º C came from thermoplastic degradation of polymers like PVC, nylon or both. Another complication was the two-step decomposition of PVC that likely overlapped the weight loss of the plasticizers. The Production and Pilot Lots 1 and 2 had multiple curve drops assignable to PVC or nylon, but the Reduced and Pellet Lots 3 and 4 had fewer curve drops indicating the absence of polyamide fibers in them. Finally, the remaining mass loss came after 500º C due to calcium carbonate thermally degrading to carbon dioxide and calcium oxide, but the hydrochloric acid from the initial decomposition would have skewed this percentage as well. Therefore, the presence of the PVC played a role in every major decomposition and reduced the quantification of the other components to only estimates.

Even though PVC or nylon could not be discerned individually, the 300° – 500° C step was still polymeric. With a faster TGA test of PCCT Lots 5 and 6, the sections of mass loss become less distinct but still discernable enough to determine general composition. Like the first four lots, samples came from large particles isolated with an 8 mesh sieve (2.35 mm) and thermally decomposed under nitrogen to confirm the presence of plasticizers, thermoplastics and filler. Due to the PVC overlapping several steps, only estimates of the particle composition for comparisons of the samples was determined and summarized in Table 5.23.

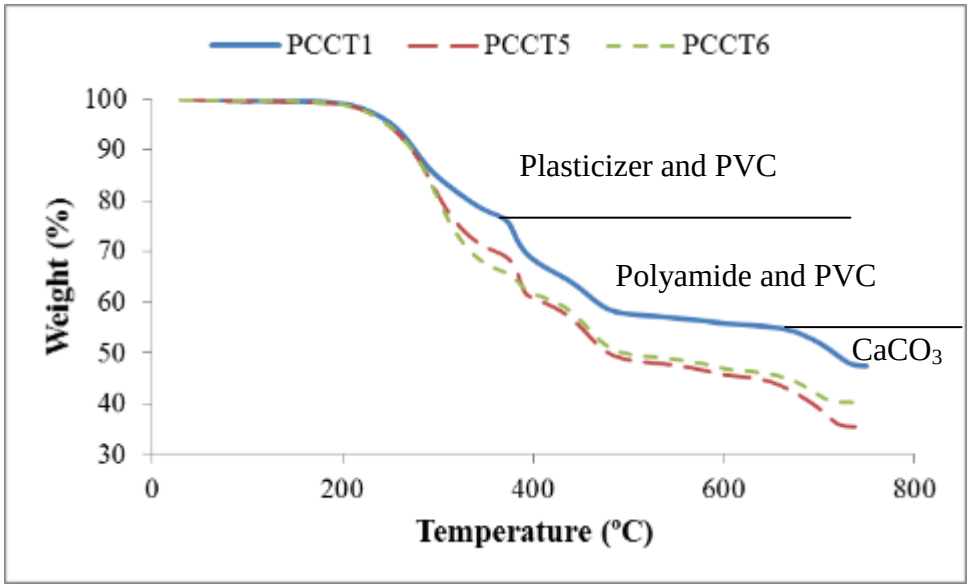

Figure 5.49. TGA of PCCT Lots 1, 5 and 6

Table 5.23. Estimated Components of PCCT Lots

Lines	**Production**	**Pilot**	**Reduced**	**Pellets**	**Production**	**Production**
Lot #	**PCCT-1**	**PCCT-2**	**PCCT-3**	**PCCT-4**	**PCCT-5**	**PCCT-6**
Plasticizer	18%	15%	23%	51%	28%	33%
Polymer	26%	27%	13%	32%	23%	17%
$CaCO_3$	16%	9%	59%	9%	23%	14%
Ash	40%	49%	5%	8%	26%	36%

Although the samples shared similar components, none of the volatiles, thermoplastics or fillers were apportioned the same in every lot. The polymer content that served as binder in the tile backing formed a relatively minor component between 13% - 32%. The other components, plasticizer and filler, showed large variations in overall mass probably due to several mitigating factors such as varying source material, the particular reclaim process used and the resultant particle structure. Overall, the exact composition was dubious with the available test methods, but the relative differences between the lots were significant.

5.4.2 Physical Conditions of PCCT

When loading synthetic turf, structural factors such as the particle size and shape of the GCRI particles affected penetration of the tufts and optimum infill load. These factors would thus extend to tile crumb utilized as infill. The external shape of the PCCT particles were illustrated in Figures 5.39 to 5.42, which included flat crumb, fine granules and round pellets. When examined by microscopy, as in Fig. 5.43 for PCCT-1, the other samples had various fibers and micro-particles embedded in the plastic matrix (Figs. 5.50 and 5.51).

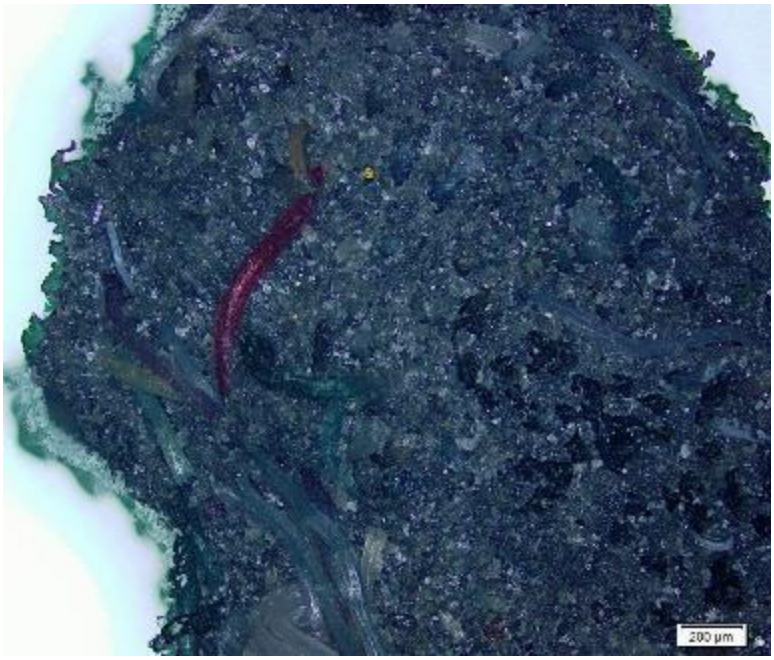

Figure 5.50. Embedded Fibers in Random Shaped PCCT-5 Crumb

Figure 5.51. Fibers Extending from PCCT-6 Crumb

Based on the previous research and testing, PVC was the likely binder for this reclaimed material that contained the filler and fibers. The coiling fibers were remnants of the dyed nylon fibers that could not be reclaimed by the initial recycling of the face fibers. The clear, straight fibers were silica-based fiberglass used as backing reinforcement (Figure 2.7). The remaining component was the chemical plasticizer that was already confirmed by FTIR and TGA. Overall, the tile crumbs were an agglomeration of disparate structures and chemistry.

To gauge which lots matched the particle size properties of the GCRI, the distribution and average particle sizes were quantified physically via ASTM D5644 Rotap, and the bulk densities via ASTM D5603-01. The Rotap method found a wide particle size distribution between the samples (Figures 5.52 and 5.53).

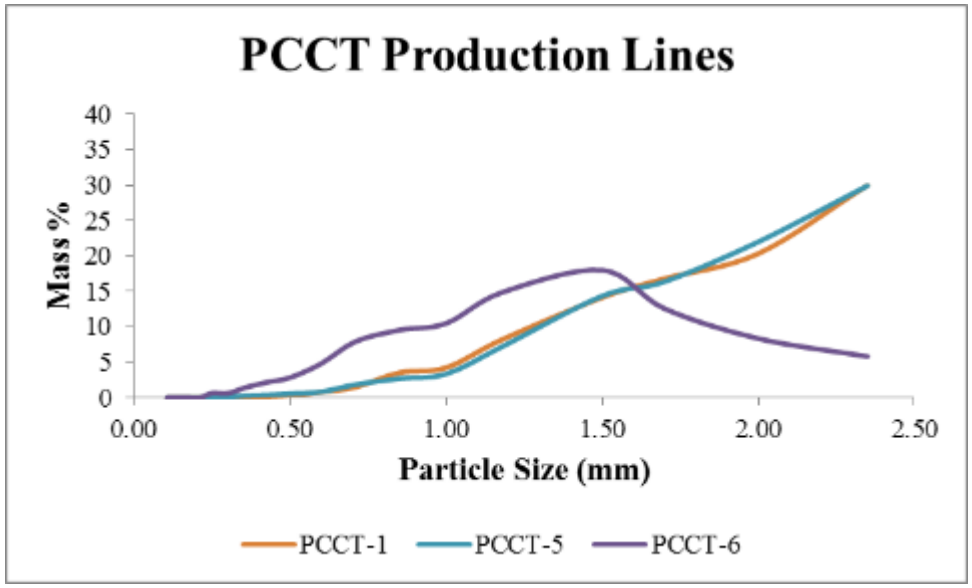

Figure 5.52. Particle Size Distribution of PCCT Production Lots 1, 5 and 6

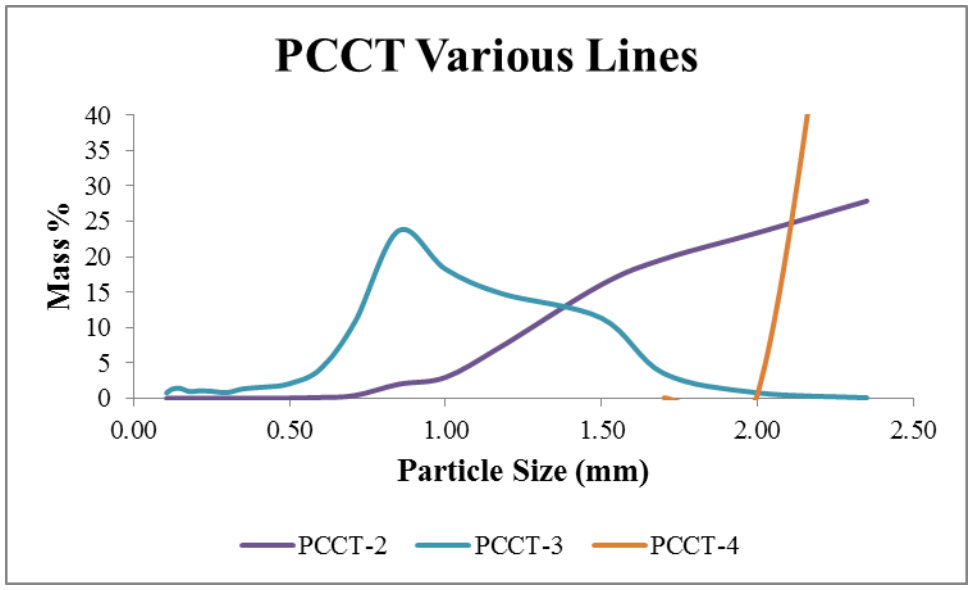

Figure 5.53. Particle Size Distribution of PCCT Lots 2 to 4

Table 5.24. Particle Size and Bulk Density of PCCT

Lot#	Lines	Average Particle (mm)	SD (mm)	Bulk Density (gm/cc)
PCCT-1	Production	>1.80	0.49	0.45
PCCT-2	Pilot	>1.84	0.43	0.53
PCCT-3	Reduced	0.94	0.38	0.35
PCCT-4	Pellets	>2.35	0.03	0.82
PCCT-5	Production	>1.80	0.50	0.35
PCCT-6	Production	1.27	0.52	0.34
GCRI-4	NA	1.38	0.37	0.50

The calculated size average for each lot was close to the actual values since the sieves trapped at least 88% of the material tested. Overall, comparison of average particle size to bulk density showed low correlation. The most notable difference came from the pellets of PCCT-4 with its large dimensions, designed spherical shape and high bulk density relative to the other samples. The majority of particles in sample lots 3 and 6 had significant amounts within the 0.5-3.0 mm range, but bulk densities were lower than the 0.43-0.57 gm/cc range of GCRI (Fig. 5.6). Overall, physical disparities of the PCCT samples were not equivalent to the structure of GCRI.

5.4.3 Impact Measurements of PCCT

When testing rubber infill in 3D52 brand turf, the vendor recommended a loading of 2.3 lbs per sq. ft. for filling the empty space between the tufts. The resulting cushioning effect achieved an impact performance of 110 Gmax under lab conditions, a safe level below the lethal threshold of 200 Gmax. With an average bulk density of 0.47 gm/cc, the rubber particles with a 1.38 ± 0.37 mm average size filled the empty turf space, which was calculated to be approximately 2136 cubic centimeters. To fill an

equivalent volume with alternate infill, calculations based on the PCCT bulk density of the individual lots provided the following calculated loads (Table 5.25).

Table 5.25. Infill Loading of PCCT per Square Foot

Lot#	Bulk Density (gm/cc)	Estimated Infill Load (lbs. / sq. ft.)
PCCT-1	0.45	2.09
PCCT-2	0.53	2.45
PCCT-3	0.35	1.61
PCCT-4	0.82	3.77
PCCT-5	0.35	1.59
PCCT-6	0.34	1.56

In the subsequent testing, infill loading was varied to evaluate the infill interaction with turf up to the infill amounts of Table 5.25, which actually served as guidelines for optimum filling of the turf to prevent over- or under-filling.

Starting with the samples without integration in turf, all PCCT samples underwent impact evaluation for comparison to the GCRI sample (Figures 5.54 and 5.55).

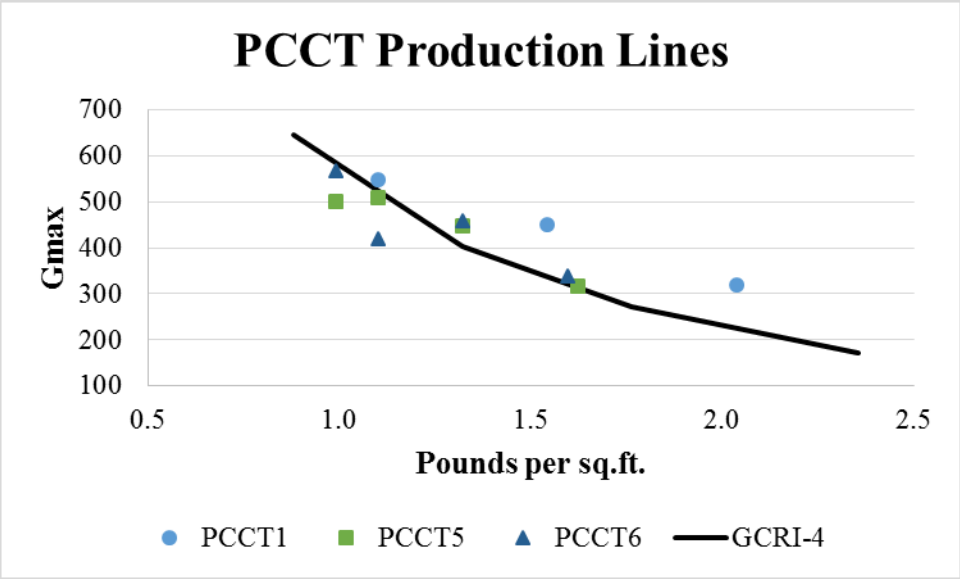

Figure 5.54. Non-turf Gmax of PCCT Production Lines

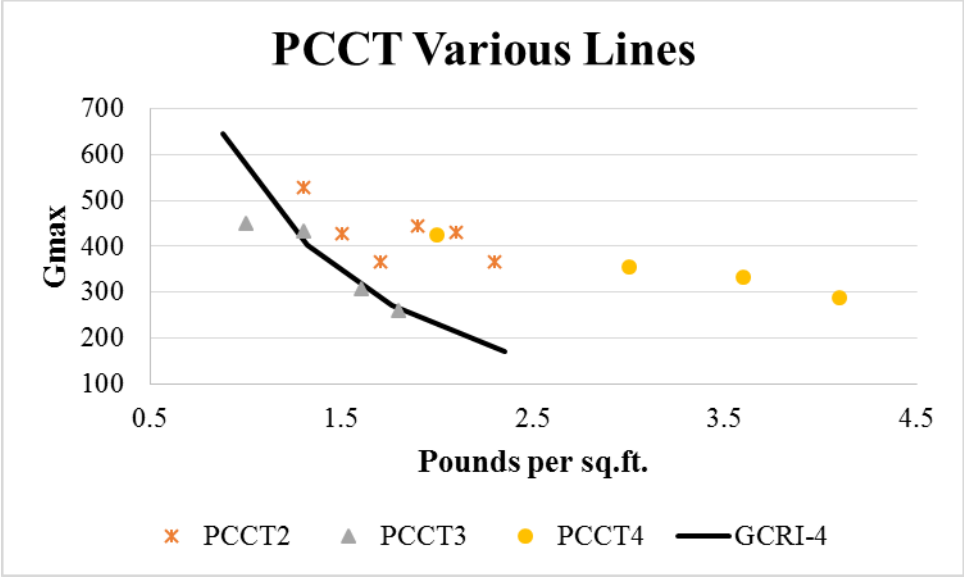

Figure 5.55. Non-turf Gmax Values of PCCT Lots 2 to 4

Between the above two figures, PCCT particles from the Production-based lines and the reduced particle line PCCT3 showed Gmax trends that overlapped the rubber standard but did not reach optimum impact absorption. The common factor between those PCCT lots were a bulk density at 0.45 gm/cc and below. However, none of the lots reached below 200 Gmax, and only PCCT-3 achieved a HIC below 1000 at 849. The overlap between PCCT-3 and the GCRI curves in Fig 5.55 indicated similar mechanical behavior. When integrated into the 3D52 turf, PCCT-3 came closest to matching the behavior of GCRI-4 (Fig. 5.56 and 5.57).

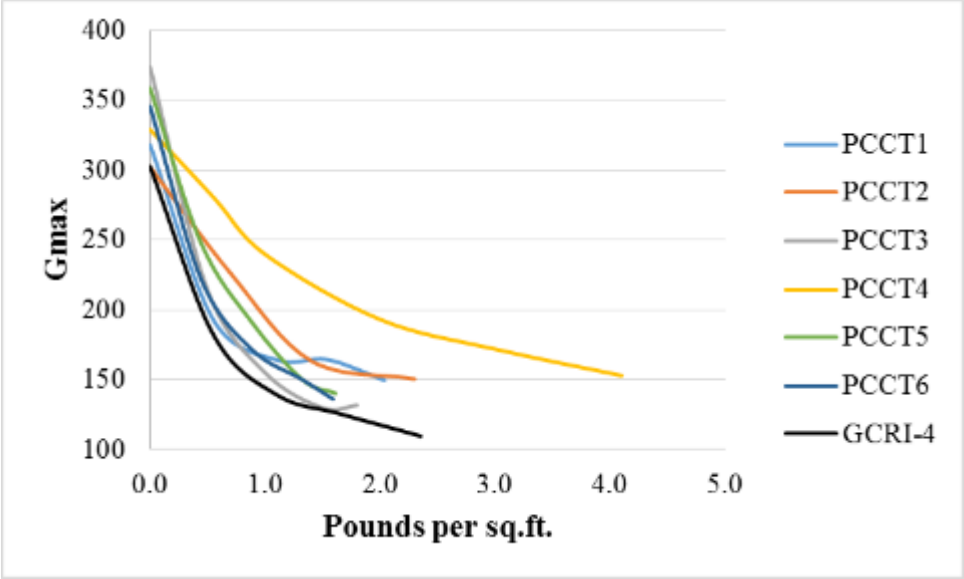

Figure 5.56. Gmax Values of PCCT Infill in Turf

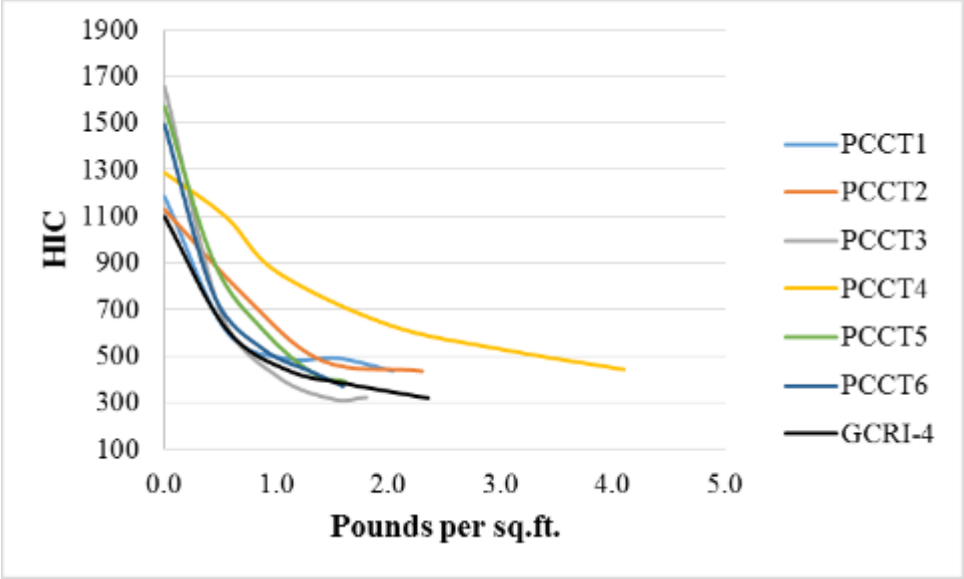

Figure 5.57. HIC Values of PCCT Infill in Turf

The similarities between PCCT-3 and GCRI particles such as random shape, high filler content and low bulk density might have translated to comparable turf performance for some of the PCCT. For concussion-related Gmax, PCCT-3 came closest to matching the

non-linear behavior of rubber infill after overcoming a higher initial Gmax that originated from the turf only to achieve a Gmax of 130 versus 110 for GCRI-4. As for HIC that gauges long-term cognitive trauma, the PCCT-3 curve exceeded GCRI-4 (316 versus 320 respectively) at the optimum filling of turf. Higher loading of PCCT-3 would not improve impact performance since the final amount of infill in the turf already exceeded the calculated guideline (1.8 lbs. instead of 1.6 lbs./sq. ft from Table 5.25) and visually extended over the tops of the tufts (Figure 5.58).

Figure 5.58. Turf 3D52 with PCCT-3 Infill

As for the remaining PCCT lots, their Gmax values were higher (Fig. 5.56), although PCCT-5 and PCCT-6 almost reached similar HIC values of GCRI (Fig. 5.57). Overall, most PCCT lots demonstrated non-linear responses versus infill loading that ended with

performance plateaus at optimum turf filling, but only PCCT-3 matched the rubber infill in terms of performance with and without the turf.

5.4.4 Modification of PCCT

One lot, PCCT-3, nearly matched GCRI impact absorption performance, and two other samples (PCCT-5 and PCCT-6) reached the next lowest Gmax and HIC values. Although these lots had similar bulk densities and hence infill loading of the turf (Table 5.25), their disparate particle ranges did not appear to affect the overall impact curves. To verify that particle size was not a significant factor, the next step taken was eliminating particles above 2.5 mm from PCCT-5 in order to obtain a closer particle distribution match to PCCT-6 (Fig. 5.52) by using mesh 8 (2.35-mm) in the Rotap. The resultant 823 grams (1.81 lbs.) was designated at PCCT5M8. The physical modification reinforced the average particle size of 1.8-mm, and retest of the bulk density stayed at 0.35 lbs./cc, which dictated a near equivalent amount of infill loading in the turf (Fig. 5.59).

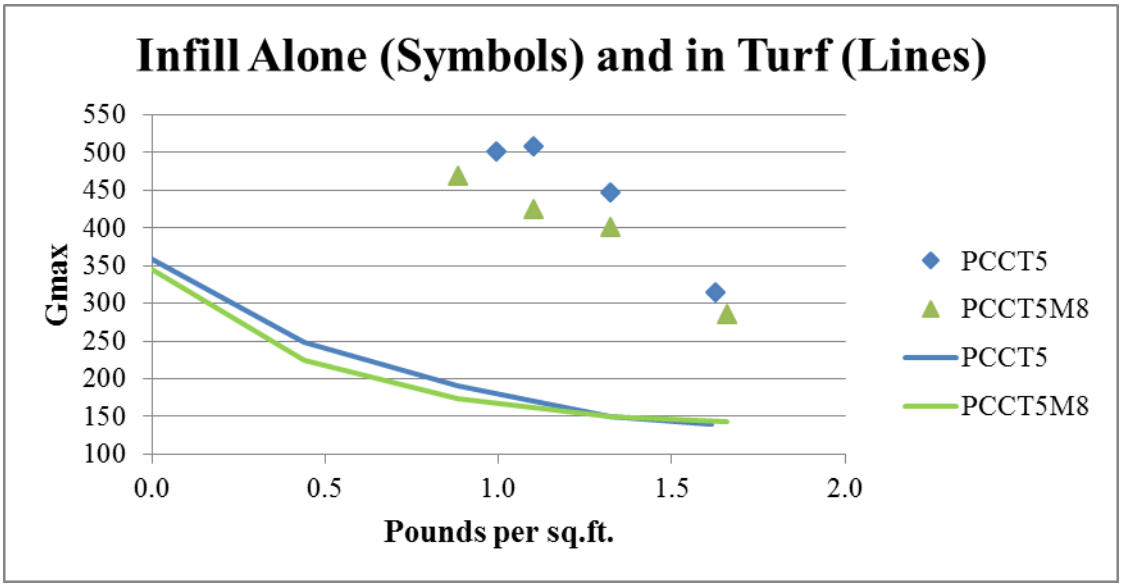

Figure 5.59. Bulk PCCT5 and Refined PCCT5M8 Gmax Values

Table 5.26. Lowest Gmax Impact Values of PCCT-5 Samples

Sample	**PCCT5**	**PCCT5M8**	**GCRI4**
Gmax (no turf)	315.3	285.1	171.2
HIC (no turf)	1248.7	1088.2	568.4
Gmax (in turf)	140.2	142.4	109.6
HIC (in turf)	390.9	398.1	320.0

The altered PCCT-5 showed improved impact performance when tested without turf. When loaded in turf, PCCT5M8 initially showed lower impact values. However, at maximum loading, the turf raised the altered PCCT5M8 impact curve slightly higher than PCCT5 despite reaching a load higher by 0.1 lb. The particle size of PCCT-5 thus exerted some influence on performance of the turf.

Although particle size variation of PCCT-5 did not have a large effect for the 3rd generation turf at maximum loading, the Gmax versus loading curve still followed a similar non-linear behavior to the unmodified PCCT, which may be extended to enhanced turf such as 3D-60H. In further Gmax testing, the turf from both 3D-52 and 3D-60H utilized bulk samples from GCRI4, PCCT5 and PCCT6 (Figure 5.60).

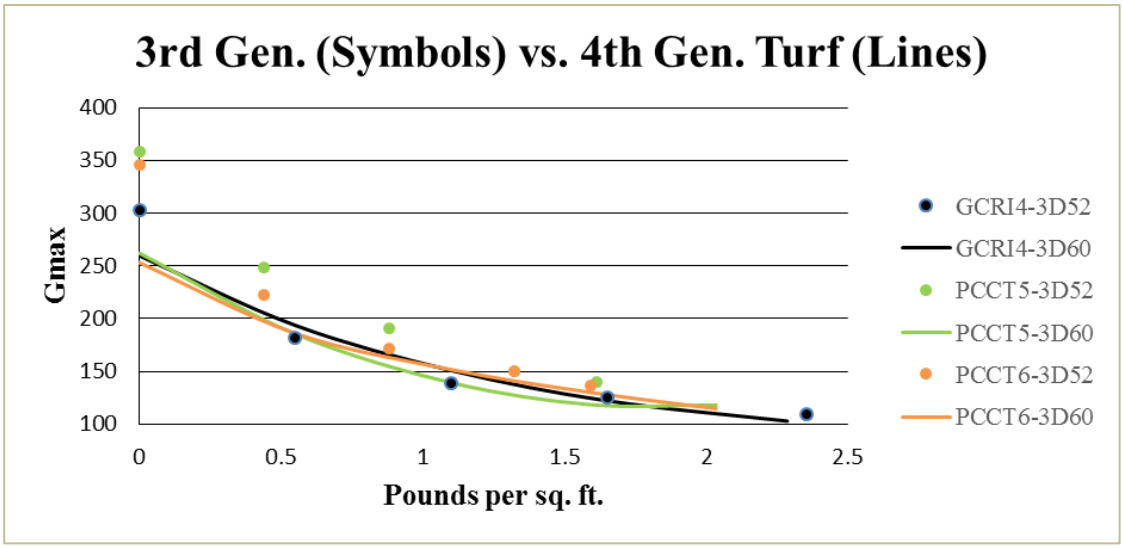

Figure 5.60. Different Turf Brands with GCRI and PCCT

Table 5.27. PCCT Gmax Values in GameDay Turf Brands

Lot#	GCRI4	PCCT5	PCCT6
3D-52	110	140	136
3D-60H	103	118	115

Upon review of Figures 5.25 and 5.60, 4th generation 3D-60H achieved lower Gmax than 3D-52 without infill, and then the Gmax of GCRI-4 was reduced in 3D-60H. In Table 5.27, both PCCT lots showed even greater improvement. Overall, the standard GCRI infill produced the lowest Gmax result, but the PCCT lots progressed by at least 15% with 4th generation turf while the rubber changed by 6%. In conclusion, the PCCT infill demonstrated interaction with the turf that exceeded the standard rubber infill, and future infill development may have to include adjustment of the turf with the infill.

5.4.5 Economic Feasibility

According to literature research, the feasibility of reclaiming tile-based carpet depends on an analysis of the reverse production system (RPS) [55]. The RPS methodology is collecting information on variables such as number and locations of recollection sites; routes and modes of transportation; and the amount of reclaimed material. Then variations can be minimized to create a steady waste stream and maximize return. Unfortunately, very little information existed about this type of carpet tile recycling. Therefore, the next step is determining the costs of collecting discarded tile carpet and producing the crumb. Then a RPS model based on using PCCT as infill may reduce the mentioned expenses below the cost of landfill diversion. By 2000, 5 billion tons of post-consumer carpet, both broadloom and tile, went to landfills, and cost of storage was estimated to be $40/ton while transportation over a 20-mile trip added $0.05/ton-mile. By 2011, only 9% of reclaimed carpet was diverted away from landfills, therefore reclaim costs were still too high [26]. When confining the cost estimate to carpet tile, InterfaceFLOR estimated the cost of PCCT production to be $0.75 per pound or $1,500/ton, which was broken down to the following: sequestration at $0.06 – 0.08/lb; transportation to Interface at $0.06 – 0.08/lb; labor at $0.30/lb; and finally processing and sizing at $0.30/lb [56]. Even if the landfill cost was higher than $0.75/lb, the reclamation costs of PCCT still needs to be comparable to those of GCRI, which the vender quoted to total $0.22/pound or $440/ton [11, 57]. The viability of PCCT infill thus requires more detailed modeling such as reverse logistics analysis for further cost reduction as it was applied to broadloom carpet reclamation [27, 55].

Another potential cost factor is the in-turf durability of the PCCT that will require repeated cyclic impact testing. Heavy use and/or weathering degradation should not substantially reduce impact-absorbance performance before replacement of the material becomes necessary due to off-field migration of particles, e.g., through player uniform attachment and rain water run-off. If either repeated impact use and/or or weathering proves sufficiently detrimental to the impact properties of the PCCT infill, then further physical, thermal and/or chemical modifications may extend its life in the turf and probably increase the final cost/lb.

Finally, the biocidal efficacy of the surface has to be comparable to GCRI. To prevent MRSA-type infections in outdoor surroundings, surface modifications of the polymeric PCCT crumb by various chemical antimicrobial treatments currently on the market (e.g., silver nanoparticles, AEGIS® ammonium alkyl "spear" chemistry or other routes) can be utilized. However, such chemical treatments will add further expense to the final PCCT infill product. In all future work, the protocol developed around the Gmax impact test method detailed herein should be applied after any chemical and/or material changes are made to the PCCT infill to ensure safety of the end product.

5.5 Post-Consumer PET Infill Alternative

Polyethylene terephthalate (PET) flake was viewed as a third potentially-viable alternative infill. This consumer-grade PET was present in soft drink/water bottles and carpet fibers with a high percentage of the post-consumer bottle stream still going to landfills. Carpet companies such as (Mohawk Ind., Rome, GA plant) recycles PET bottle flake into melt extruded carpet fiber. The incoming compacted bottle stream consists of a mixture of clear bottles (from water and soda markets) and green soda bottles (from soda

brands (e.g., Sprite®, Mountain Dew®, 7 Up®, etc.). The green color was achieved by adding green pigment concentrates to the PET in the melt blow molding process for UV protection and marketing purposes. Mohawk can effectively use the segregated "clear" PET bottle stream that can be dyed to any desired shade once it is melt extruded into fiber form, whereas the segregated "green" PET stream can only be over-dyed in fiber form to six acceptable shades for the commercial carpet market. As a result, the majority of the PET green bottle stream purchased by Mohawk Ind. for its carpet fiber production is, after separation from the clear PET bottle stream, either land filled or sold at a fraction of the purchase price to manufacturers of low-end extruded products such as tape tie-down straps for cardboard boxes [28]. Since the green PET flake stream came from an already-established, large-scale reclaim system and supply source, it represented a low-cost material candidate as an infill replacement for GCRI with a uniform polymeric chemistry and structure, in contrast to the carpet-based and rubber-based crumbs that consisted of multiple components.

5.5.1 Chemical Composition of PET

As noted in Section 4.1.3, the two lots of PET utilized in this research came from different sources. The first lot was green reclaimed soda bottle flake supplied by Mohawk Industries of Rome, GA (Fig. 4.6). A second source of PET came from a clear preform (Fig. 4.7) made by Resilux America, LLC of Pendergrass, GA. The Resilux preform (PETRE) was chemically the same PET used in the production of drink bottles, but was in a low crystalline form compared to the high crystalline form of the green PET flake. Although the Mohawk lot (PETMH) consisted of green pigmented material, other

colors plus clear flakes existed in the mixture that matched the chemical composition of the green flakes according to FTIR analyses (Figs. 5.61 and 5.62).

Figure 5.61. Mohawk PET Flake Mixture (as Received)

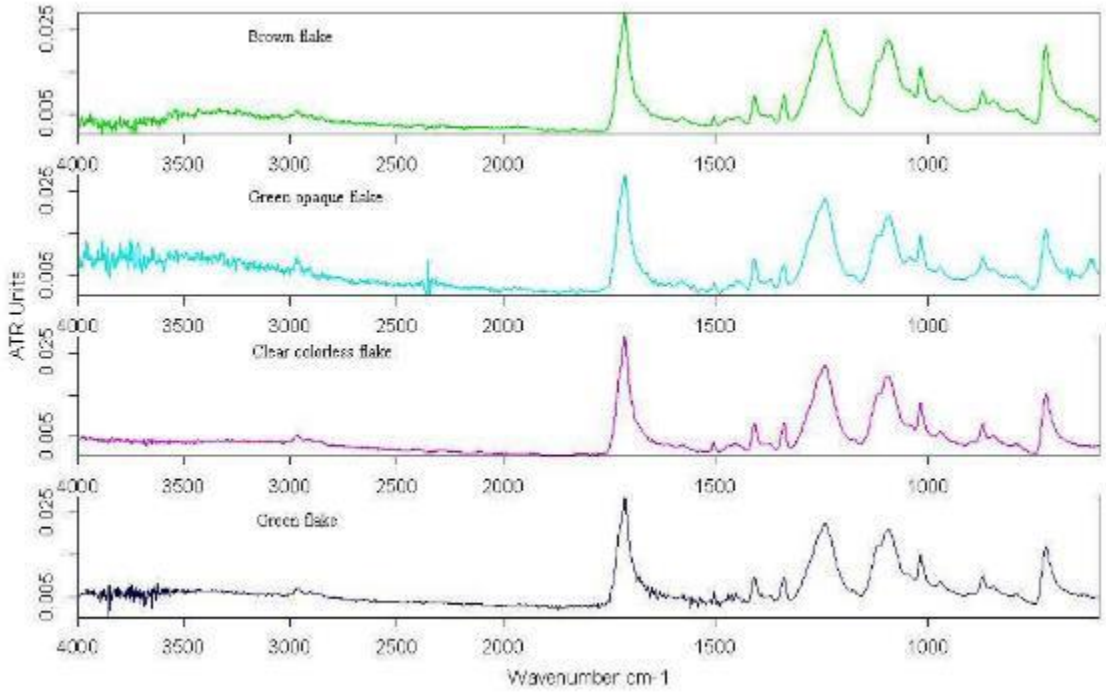

Figure 5.62. FTIR Scans of Mohawk PET Tinted and Clear Flakes

Table 5.28. FTIR Band Assignments for PET [58]

Peak (cm^{-1})	Chemical
1800-1650	Carbonyl
1470	Trans isomer
1450	Gauche isomer
1410	Aromatic ring
1370	Gauche isomer
1340	Trans isomer

The FTIR similarities between segregated PET flakes from the mixture indicated the same polymeric chemical structure of the thermoplastic material, regardless of the color (or clear nature) of the individual flake. The PET flake showed a single mass step loss during TGA analysis under nitrogen (Fig. 5.63).

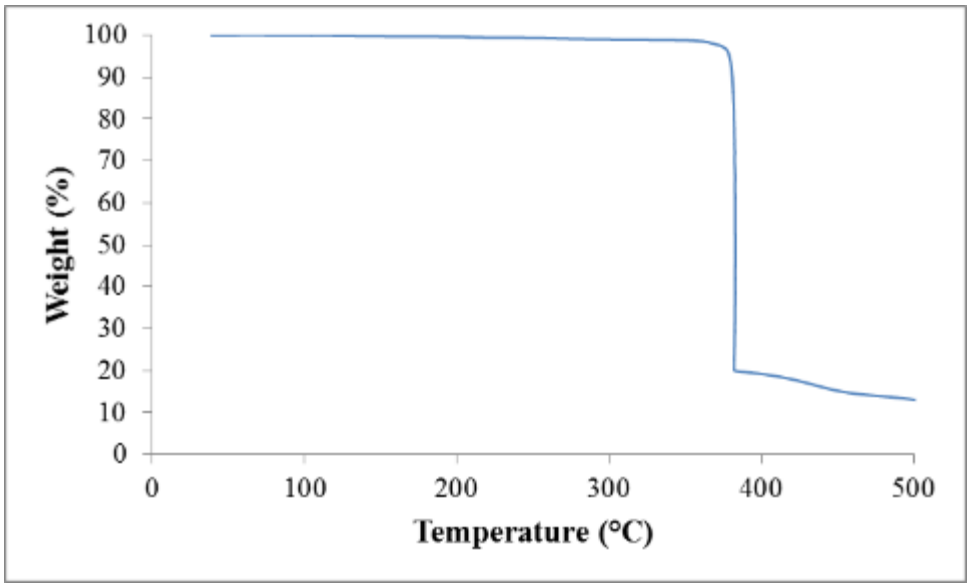

Figure 5.63. TGA Decomposition Scan of PETMH under Nitrogen

A previous study found that the decomposition of PET in an inert atmosphere occurred around 407°C and reached an ash content of 11% [59]. The mass loss in Fig. 5.63 began at 382° C and continued until ~13% ash remained. The single step in the mass loss during thermal decomposition confirmed the singular presence of only the PET polymer with little plasticizer or filler in the PET flake. As for the PETRE, the company Resilux designed the preform specifically for drink bottles that would eventually become the flake. Therefore, PETRE did not require further analysis since it was made of the same material as PETMH, a homogenous polymer matrix as opposed to heterogeneous composites like GCRI, PCCB or PCCT.

5.5.2 Physical Conditions of PET

As noted in previous turf applications, the size and shape of infill particles affected the penetration of the tufts, but the available PET forms such as the chopped flake and the preforms were too large to load into the turf. The recommended infill size for commercial GCRI was between 0.5 to 3.0 mm (see Sections 5.1.2 and 5.1.3). However, the average PET flake measured 10.79 ± 3.00 mm for its long axis with 0.42 gm/cc bulk density. The Resilux preform was a long cylinder with a 20-mm base. Thus, physical modification was utilized via grinding by the Wiley Mill (see Fig. 4.16) to change both samples under ambient conditions into acceptable particles sizes.

At initial grinding under ambient conditions, the PETMH was milled with three different metal screens to produce a wide range of particle sizes. To create different particle sizes, the flake was milled with three different screens of uniform orifices at different sizes: 2 mm, 3 mm and 4 mm as designated at the end of their sample names. In the following chart, ambient grinding with these screens created one sample with particle

distribution of 0.5 – 1.5 mm and two more samples had particles reaching up to 2.35 mm (Figure 5.64 and Table 5.29).

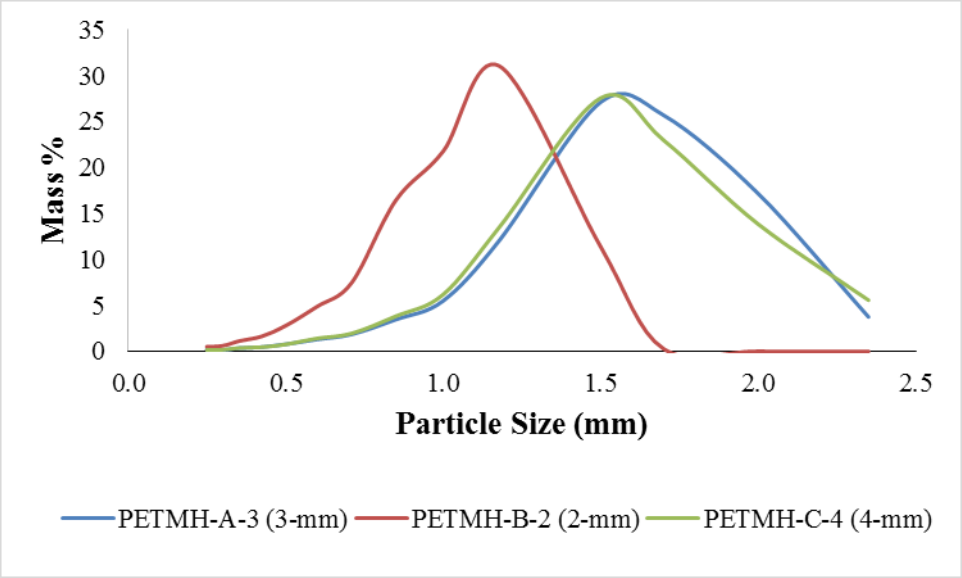

Figure 5.64. Distributions of Modified PETMH Obtained via the Wiley Mill

Table 5.29. Size of Modified PETMH Milled Fractions and GCRI-4 Standard

Lot	PETMH-A-3	PETMH-B-2	PETMH-C-4	GCRI-4
Average Particle (mm)	1.53	1.01	1.51	1.38
Standard Deviation (mm)	0.41	0.28	0.42	0.37
Bulk Density (gm/cc)	0.49	0.53	0.45	0.50
Infill Loading (lbs. / sq. ft.)	2.3	2.5	2.1	2.4

PETMH-A-3 and PETMH-C-4 were statistically equal in size distribution while PETMH-B-2 was lower probably due to the smaller screen mesh. The likely reason for the similarities between samples A and C was the measured mesh size did not closely match the designated size: the 2 mm screen openings averaged 2.0 mm diameter, the 3 mm screen mesh averaged 3.3 mm diameter, and the 4 mm mesh screen averaged 3.8 mm. In

Table 5.29, average particle size did not correlate well to mill mesh size, but bulk density showed an inverse relationship to increasing screen size with R^2 = 0.99. Under microscopic inspection of the largest particles found in a mesh 12 sieve, the particles from each grind showed random shapes and visible abrasions on the surface (Figs. 5.65-5.67).

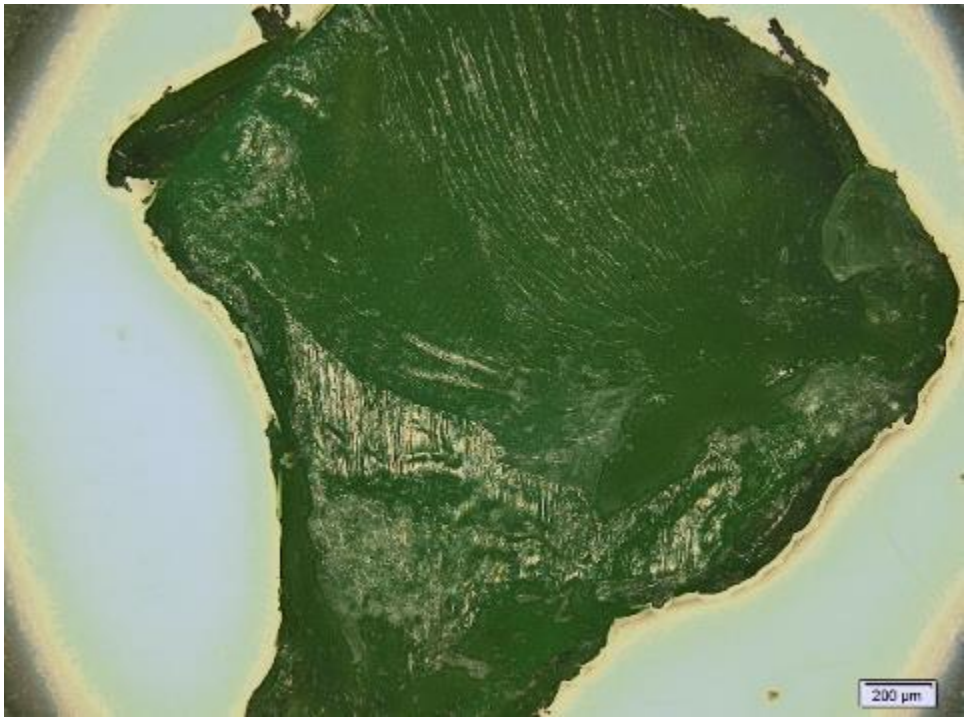

Figure 5.65. PETMH-A-3 Particle from Mesh 12

Figure 5.66. PETMH-B-2 Particle from Mesh 12

Figure 5.67. PETMH-C-4 Particle from Mesh 12

The random structure of the particles and low bulk densities listed in Table 5.29 were similar to GCRI-4, so the calculated amounts for optimum infill loading were also close to GCRI-4 in turf. If particle size and random shape were significant factors in GCRI, the PET samples could mimic the mechanical interaction between rubber infill and turf.

After initial performance testing of PET, crystallinity of the PET became another focus of attention regarding PET mechanical response to impact. Polymer crystallinity can affect physical and mechanical properties such as elongation and yield stress in conjunction to the elastic response of the amorphous PET content that also exhibits a hard, brittle state under ambient conditions due to its high glass transition (Tg) between 70° to 76° C [60]. In contrast, tire rubber exhibits a rough, leathery response to physical force due to its lower Tg below -70° C [11]. One method to gauge crystalline content was by density measurements of the volume occupied by the PET via the gas-displacement method. This type of density was influenced by the crystallinity of PET and was also related to bulk density [60]. Wide angle X-ray diffraction was another way to measure PET crystallinity (Table 5.30).

Table 5.30. Green PET Crystal Analysis By Method

Lot#	PETMH	PETMH-A-3	PETMH-B-2	PETMH-C-4
Density Method (%)	32	25	33	28
WAXD Method (%)	22	-	-	-

Between both methods, the green flake PETMH as received exhibited crystallinity from 22% to 32%. Subsequent grinding apparently did not raise the PET crystallinity since the density method produced results within experimental error of the original form.

However, WAXD could not confirm this conclusion because the particles were too small after grinding to be x-rayed. In summary, the ambient grinding process definitely affected the physical form of the PET particle but the lack of extensive thermal treatment likely left the ground samples without significant change to its internal morphology to any measurable degree.

5.5.3 Impact Measurements of PET

For impact absorption measurements, the PET-based infill underwent the same methodology applied to GCRI-4, which had a bulk density of 0.50 gm/cc and an average particle size of 1.38 ± 0.37 mm. When compared to Table 5.29, the similar particle size and bulk density of the PETMH samples yielded infill amounts between 2.1 to 2.5 lbs that would fill a 12 x 12 sq. in. section of 3D52 turf. The initial evaluation tested the infill without the turf (Fig. 5.68).

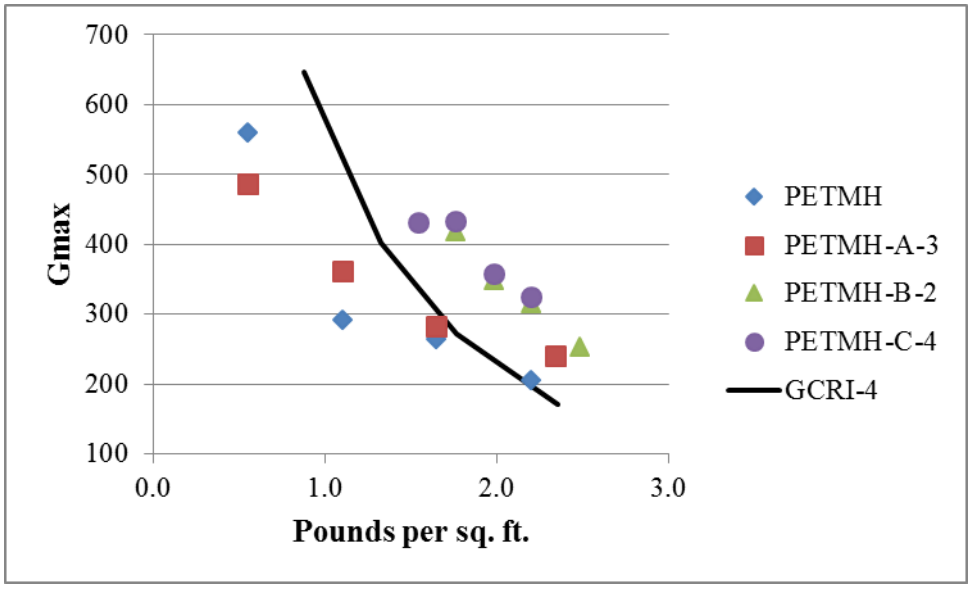

Figure 5.68. Non-turf Gmax Values of PETMH versus GCRI

The chopped flake form of the PETMH had large dimensions, yet achieved the lowest Gmax of 206 with a non-linear curve. When the PETMH went through a grinding process, the resulting crumb had more linear curves with higher impact values. The particles of PETMH-C-4 came from grinding with the 4 mm screen, and achieved the highest Gmax value at 326. Sample PETMH-A-3 went through a 3 mm screen yielding an average particle size similar to PETMH-C-4, but reached a lower Gmax of 240. Finally sample PETMH-B-2 used a 2 mm screen and achieved a non-turf Gmax of 254. So far, the factors behind these Gmax differences were not evident, but none of the PETMH samples achieved Gmax close to 171 from the rubber standard GCRI-4 without turf.

As received, the large dimensions of the chopped PET flake made integration difficult into the synthetic turf, but the grinding process created smaller particles that allowed all modified samples to be tested in the turf.

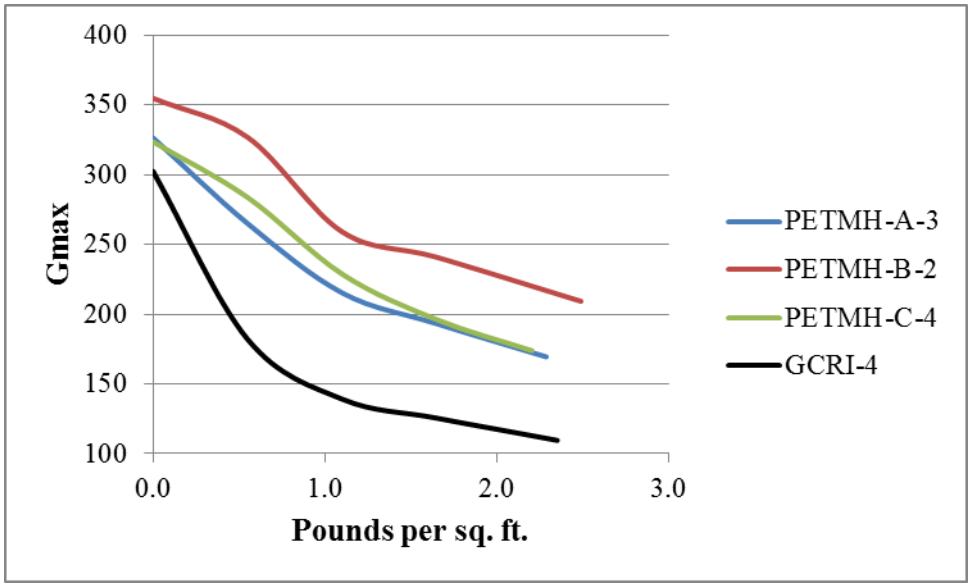

Figure 5.69. Turf-Based Gmax Values of PETMH versus GCRI

In the turf-based data, PETMH-A-3 had a 1.53-mm average particle size and reached the lowest PET Gmax of 169 although it did not reach 110 like GCRI. In addition, the PETMH-A-3 curve displayed a high correlation of R^2= 0.94 to a linear equation while GCRI data only achieved R^2=0.78. In the sample with the smallest particles, PETMH-B-2 had a particle size average of 1.01 mm and reached the highest Gmax of 209 at the highest infill load of 2.5 lbs. / sq. ft. in turf. Finally, the PETMH-C-4 particle size average was 1.51 mm and Gmax went to 174. Although the non-turf Gmax data did not correlate with particle size, the turf-based Gmax did show an inverse linear relationship between average particle size and Gmax. However, none of the samples approached low impact values close to the GCRI standard of 110.

5.5.4 Modification of PET

Despite modifications to match particle size and bulk density of GCRI, impact testing of semi-crystalline PET showed significantly lower shock absorption than rubber crumb. In polymers, percent crystallinity of the material can affect mechanical properties such as tensile, elongation and compression. Therefore, the amorphous content of PET became a possible impact variable. A source of highly-amorphous PET was found in Resilux preforms (PETRE), a material that produced an amorphous halo in WAXD without any crystallinity peaks previously seen in the green flake PETMH (Figures 5.70 and 5.71).

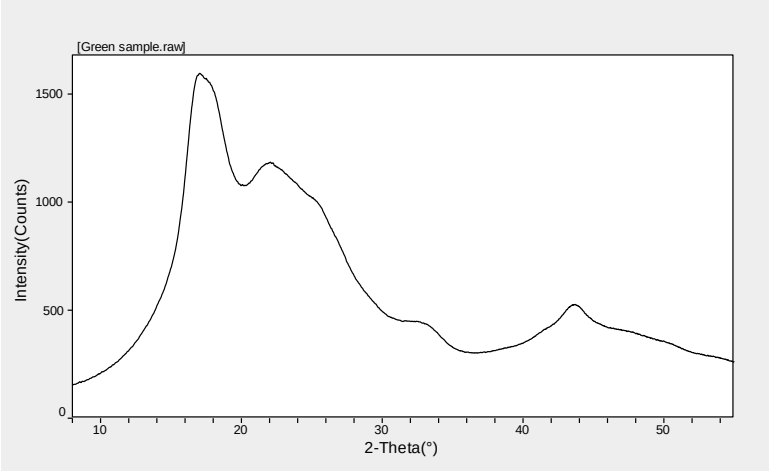

Figure 5.70. Crystalline WAXD of PETMH

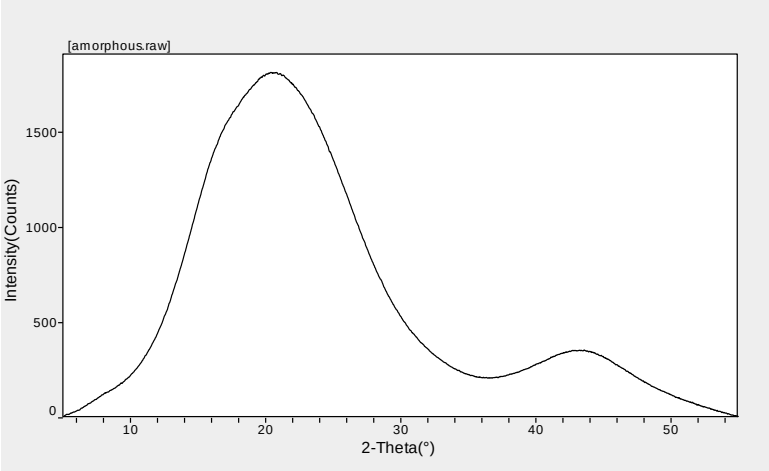

Figure 5.71. Amorphous WAXD of PETRE

After the approximate zero crystallinity of the preform was confirmed, the next step was producing test samples via the Wiley Mill and a 4 mm screen. One sample used cryogenic conditions to produce particles (PETRE-F-4) without any thermally induced crystallinity, and another sample used ambient mechanical grinding to gauge any induced crystallinity (PETRE-G-4).

Table 5.31. Results of Resilux PET Modification

Lot#	PETRE	PETRE-F-4	PETRE-G-4
Crystallinity via Density (%)	4.3	4.2	14.4
Crystallinity via WAXD (%)	0	-	-
Average Particle (mm)	-	1.36	1.41
Standard Deviation (mm)	-	0.40	0.37
Bulk Density (gm/cc)	-	0.64	0.48
Infill Loading (lbs. / sq. ft.)	-	3.0	2.3

The top row of Table 5.31 lists the relative difference in crystallinity between the preforms and the ground samples, while the second row indicates near-zero crystallinity of the preform. Although the grinding process produced similar particle size distributions with a 4 mm screen, the differences in bulk density resulted in a large disparity in the calculated infill amount for optimum turf fill. The increased crystallinity of ambient PETRE-G-4 would more likely increase than decrease bulk density; therefore, particle shape had to be more random and less dense packing than PETRE-F-4 (Figs. 5.72 and 5.73).

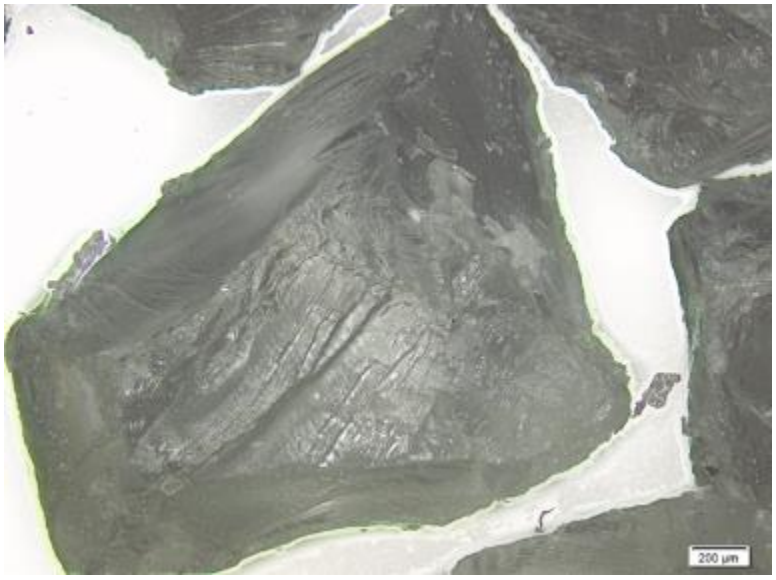

Figure 5.72. Smoother Surface from Cryogenic PETRE-F-4

Figure 5.73. Rougher Surface from Ambient Grind PETRE-G-4

With both PET samples within similar particle size ranges, impact performance would be attributed to particle shape and/or crystallinity.

With the standard 3D52 turf, the PETRE samples underwent impact testing with and without the turf to demonstrate the contribution of the tufts (Figure 5.74).

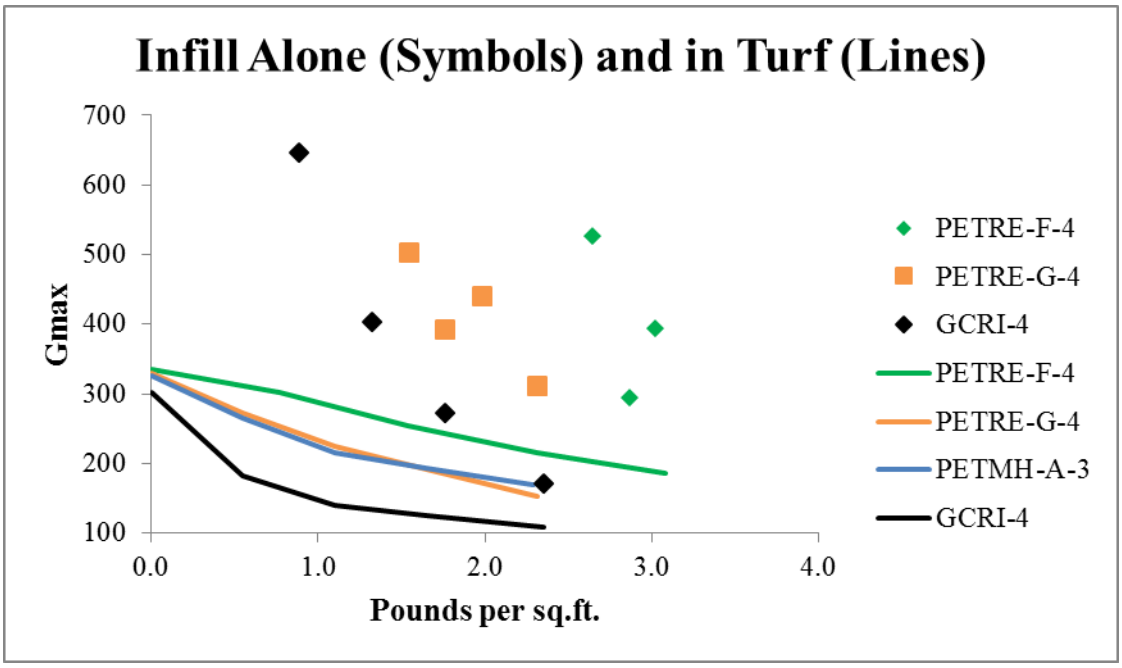

Figure 5.74. Gmax Values of Amorphous PET versus GCRI and Mohawk PET

The PET infill without turf present showed similar Gmax values despite different bulk densities. When integrated into turf, the ambient-produced PETRE-G-4 showed lower loading of the turf and then lower Gmax down to 154. Turf-based curves already had near linear trends in Figure 5.69 that indicated a unique linear interaction with the turf that was unlike the other infill. Another observation was that the lower bulk density samples, PETMH-A-3 and PETRE-G-4, had similar turf-based Gmax results despite different crystalline content (25% versus 14%, respectively). In contrast, PETRE-F-4 had near-zero crystallinity but yielded the highest turf-based Gmax of 184. Based on this impact performance, higher crystallinity in PET meant lower Gmax. However, particle

structure or surface morphology might be other significant factors to consider in future studies.

CHAPTER 6

CONCLUSIONS

The overall goal of this study incorporated three objectives related to granulated crumb rubber infill (GCRI) used in modern synthetic turf fields (STF):

1. Develop a fundamental understanding of how standard GCRI infill and STF operate synergistically to meet safety performance goals.
2. Identify and evaluate polymer waste streams that lack GCRI-related environmental and health issues to serve as potential infill replacements in STF.
3. Compare the economics between GCRI and the alternative polymeric material(s) that are shown to be technically feasible as STF infills.

The pursuit of the first objective defined a particular GCRI product line, GCRI Lot 4, which served as the standard infill for STF's by measuring impact performance of various GCRI samples as determined by a test protocol derived from industrial standards. The following conclusions resulted from testing the samples as received and then understanding two fundamental properties that affected interaction with the synthetic turf:

- Different GCRI lots displayed equivalent impact absorption Gmax values with and without turf when particle size distributions overlapped, regardless of ambient or cryogenic production. The type of GCRI processing utilized to manufacture the standard infill material was thus not a factor in determining impact properties for the infill material.

- At zero loading of infill, the impact energy absorption capacity of the complete turf originated from a combination of the tufts and the backing (the underlying supportive mat described in Reference 7), so the intercepts in Figures 5.12 and 5.13 reflected the differences of impact performance in utilized product samples of synthetic turf. Systematically reducing the tuft height gradually shifted the energy of impact absorption to the backing in Table 5.10. At the lowest tuft height, the majority, if not all, of the impact energy was absorbed by the mat and standard deviations of the impact values were at their maximum. The greater standard deviations of the turf mat thus demonstrated greater performance variation than the tufts, although it was questionable how this product variability would affect end performance of filled turf.
- The tuft pile height in the 3D52 turf without incorporated infill correlated directly with impact absorption values. Higher tuft pile height thus improved impact absorption in a linear fashion.
- Infill loading of the tuft matrix created overlapping Gmax/HIC impact values with GCRI samples of similar particle size distributions. Evidence of this interaction is in Figure 5.23 where maximum (standard) pile height created a non-linear Gmax value-based curve in the filled 3G STF, while the turf samples with lower pile height were overfilled by GCRI and produced more linear Gmax curves. In summary, GCRI alone demonstrated linear g-vs.-loading plot trends, and GRCI loading with reduction of pile height also created linear plots. However, the combination of maximum pile height and incremental GCRI loading did not create g-vs.-loading linear plots expected from non-interacting components, but

instead created non-linear curves possibly due to additional interactions in the filled turf, e.g., surface friction between crumb and tuft, or locking of tufts by the amorphous crumb that reinforced the overall matrix.

- Between the two types of impact measurements, HIC reached safe levels before Gmax while curves from both values followed similar trend lines. Non-fatal Gmax results with GCRI infill thus guaranteed non-fatal HIC, but not vice-versa.
- For GCRI samples with overlapping average particle sizes, incremental infill loading of unaltered turf created a non-linear g-vs.-loading curve that was a combination of slopes due to different interactions (Figures 5.12, 5.13 and 5.16). The first type of interaction was observed in the initial loading of GCRI in the turf that created a decreasing high slope in all impact curves, most likely due to infill particles supporting the tufts without being compressed themselves. Loading above 1.0 lbs. / sq. ft. of turf allowed GCRI to reach the turf backing and contribute to compression resistance with a lower-slope plot. At optimum GCRI loading (2.3 lbs. / sq. ft. of turf), impact absorption derived from a combination of supported tufts and compressed GCRI.
- Refinement of GCRI particle size did not improve impact absorption at optimum loading. GCRI interaction with the turf thus did not depend on particle size at optimum infill loading, at least for samples with average particle sizes in the evaluated size range of 0.86 - 1.71 mm.
- The contribution of infill was more significant than pile height to the overall impact absorption values achieved.

- The enhanced 4th generation STF absorbed impact energy more efficiently than 3rd generation STF under the same standard GCRI loadings, but no conclusions could be drawn identifying the causes of the improvement due to multi-variable differences between the two turf constructions, including blade cross-sectional shapes, face fiber densities and pile heights.

After establishing the GCRI baseline, the first alternate infill to be researched was the crumb originating from grinding the carcasses of post-consumer broadloom carpet (PCCB), i.e., the base of the tufted carpet that remained after the face fibers were shaved off:

- In 3G turf, the high percentage by weight of powdered sodium carbonate filler content of the PCCB contributed to surface hardness, and the detached fibers prevented sufficient packing in the turf. The combination of both factors led to insufficient impact energy absorption with PCCB infill that reached near-fatal Gmax and HIC levels, respectively.
- The bulk density of the refined Lot PCCB-1 was raised from 0.25 gm/cc to 0.44 gm/cc by removing via screening the majority of small particles and loose fibers, thus improving impact absorption from 208 to 177 Gmax values. Since the small particles were likely high density calcium carbonate, the increase in the bulk density of Lot PCCB-1 and consequential improved impact energy absorption was attributed to elimination of loose fibers.

The second group of alternate infill, PCCT, was the product of ambient grinding of the back support of post-consumer carpet tiles, i.e., the residual carcass of individual tiles in which the face fibers had been shaved off:

- The PCCT lots with the lowest particle size averages had the lowest bulk densities and achieved the lowest Gmax values. Unlike PCCB, loose fibers were not present in the PCCT, so other factors such as particle shape and chemical composition contributed to the observed bulk density, thus bringing the PCCT material closer to the GCRI standard in terms of high filler content and amorphous structure.
- Particle shape was especially important since the extruded pellets of Lot PCCT-4 were spherical and thus increased packing of infill between the turf blades. This influence of particle shape on efficient packing was deduced from its high bulk density relative to the other PCCT samples despite a low percentage of filler content. With little space between the spherical pellets, infill movement was limited during impact, thus reducing energy absorption and raising Gmax values.
- Narrowing Lot PCCT-5 particle size distribution did not significantly affect impact absorption, which mirrored the GCRI modification results. Likewise, particle size distribution alone did not affect impact properties of PCCT-based infill.
- Conversion to the 4^{th} generation STF improved impact performance of Lots PCCT-5 and PCCT-6 even more than with the standard GCRI, but no conclusions could be drawn on the enhanced turf-infill interactions due to multi-variable differences between the 4^{th} and 3^{rd} generation STF's, including cross-sectional

shapes of the blades, pile heights and face fiber concentrations per unit area of turf.

- The cost of PCCT reclamation and preparation per pound of product was estimated by the manufacturer, InterfaceFLOR, to be $0.75/lb. (see section 5.4.5 for the breakdown of the cost figure), which was about three times higher than standard GCRI at ~$0.22/lb. Larger, economy-of-scale production in the future should lower the per pound cost of the PCCT, but further collection, supply chain and processing research is needed to reduce the reclamation/preparation costs if the alternate infill product is to compete economically with the standard GCRI.

The third alternate infill material came from green-colored PET drink bottle reclaim that was a clean, mono-material, 100% polymer and not a multi-material composite like the PCCB/PCCT alternate infills:

- Within 3G STF, none of the semi-crystalline PET particle crumb lot forms matched GCRI Gmax value levels of impact energy absorption at the same loading despite overlapping particle size distributions and similar bulk densities. In attempting to match GCRI physical aspects, the polymer properties of PET itself became a major performance factor of the material as infill. With the glass transition temperature (Tg) of PET being 70°-76° C, the material is hard and brittle in its glassy state under ambient conditions, and thus cannot dissipate impact energy as effectively as GCRI, which is leathery and tough in its elastomeric state under ambient conditions due to the very low Tg's of tire rubber components (isoprene (Tg = -70° C) and butadiene (Tg = -100° C) were two

elastomeric polymers identified as present in the standard GCRI (see Section 5.1.1)).

- Like the other infill samples, particle size and bulk density were significant factors, e.g., the lab sample produced from PET flake, Lot PETMH-A-3, had physical values closest to GCRI and achieved the lowest energy impact values (169 Gmax) in the 3G turf. Further design of infill will thus depend on physical characteristics as much as chemical components or polymer percent crystallinity.
- For the modification step, the PET crystallinity of procured preform was kept near zero by cryogenic grinding for Lot PETRE-F-4, which lowered both bulk density and Gmax turf-based values. Conversely, ambient grinding for PETRE-G-4 raised crystallinity by 10% due to thermal annealing from friction in the grinder, lowered bulk density from 0.64 to 0.48 gm/cc, and decreased turf-based Gmax to 154. Polymer crystallinity may directly affect Gmax, but other factors such as bulk density were shown to be more significant.

An important finding of this research was, according to the multiple regression analysis, that the mass per unit area of GCRI infill loaded into the turf had more significant effects on absorption of high impact energy than the pile height of the turf itself. When focusing on the level of infill loading of STF as the key variable, only one alternate polymer waste stream material investigated, PCCT, was demonstrated to be a technically feasible replacement for GCRI. However, the estimated cost per pound of the optimum Lot PCCT-3 infill was at least three times higher than that quoted for standard GCRI. In summary, further study of large, economy-of-scale PCCT production is required to

moderately reduce related expenses to make the material an economically-competitive GCRI replacement.

CHAPTER 7

RECOMMENDATIONS

This study summarized a series of experiments that evaluated rubber-based infill while comparing the impact absorption properties of alternative sources of infill for synthetic turf. One source provided a possible replacement to crumb rubber, and the other two displayed unique issues that prevented effective shock absorption when integrated with turf. To create a viable replacement infill, further study of the rubber infill and the alternate materials should narrow the factors important to impact absorption and large-scale costs of production.

In furtherance of infill-related research, the bulk density of ground rubber would be a logical test variable since crumb density related to the amount of infill integrated into the turf. Modification of GCRI particle size had limited effect on bulk density and impact absorption. To achieve greater impact absorption, increasing bulk density could maximize the amount of infill that directly absorbs shock. Conversely, decreasing bulk density may allow greater particle movement within the space between the rubber particles and divert energy away from a falling body. To modify GCRI density, the experiment would utilize metal-free sections of rubber gleaned from discarded tires and then pulverized in ambient chopping or cryogenic conditions with the available equipment such as a Wiley Mill (Figures 4.16 and 4.17). Then adjusting the rotation rate of the mill blades and screen size would obtain a different sets of particle sizes and bulk densities to be tested for impact absorption after turf integration. Mixing the different particle sizes is another route to maximizing infill loading and particle movement in the

turf. At the conclusion, the influence of bulk density on impact absorption would be quantified and help determine the optimum bulk density that yields the lowest impact values.

Among the tested alternate infill samples, the broadloom carpet-based material consisted of the smallest particles with a low amount of binding polymer and likely no softening plasticizers. Since removal of loose fibers improved impact performance, further modification of PCCB, and specifically its particle size, would raise its cushioning ability by increasing binding polymer content. The procedure would start by collecting strips of carpet backing with the face fibers shaved off by the supplier. Cryogenic grinding of the remaining remnant carcass under laboratory controlled conditions and a sufficiently large screen would then produce significant amount of particles larger than 0.5 mm. Next, TGA analysis would measure relative amounts of volatiles, latex binder and filler that the particles retained. Finally, the Rotap sieves would be employed to sift the particles to ensure the lowest attainable content of loose fiber while narrowing the particle size distribution to 0.5-2.5 mm, and the bulk density would be monitored by a standard density cup. These factors would aid emulation of the GCRI to fill the turf to an equivalent level and act in a similar manner as the standard to allow effective impact absorption. The modified PCCB should display significantly improved impact absorption than obtained herein if the extensive properties play a significant factor.

As the most viable infill candidate, PCCT provided the most effective impact absorption and could be optimized by processing the reclaimed material under laboratory setup. Three of the PCCT samples showed effective infill behavior, but ash content varied from 5% to 36%. The ash of PCCT would be composed of carbon from

decomposed polymers, degraded calcium carbonate, and reinforcing silica according to the background literature and section 5.4.1. To start gauging PCCT component contribution to impact absorption, the overall ash content of the crumb would be adjusted by a thermally controlled process. To ensure the ash contains pre-decomposed contents, the starting material would be the post-consumer carpet tiles cut into strips after the face fibers are shaved off. The remaining strip would then be ground under a cryogenic condition to prevent thermal decomposition within the resultant crumb while maintaining consistent particle size and bulk density. To vary ash content, samples would undergo thermal treatments below 200° C to evaporate the plasticizer without decomposing the PVC binder, thereby increasing ash content that depends on selected temperature and time interval. The next step tests impact performance of the samples of varying ash content in the synthetic turf. The overall goal would be to determine the proper ash content via grinding conditions and amount of thermal decomposition that improves the infill-turf impact absorption.

APPENDIX 1

DATA SHEET FROM GENAN

Revised: Jan 2006

Data Sheet :

Datenblatt / Datablad

genan
Knowledge-based Recycling Concepts

Product name: **GENAN Rubber Granulate Fine [1] - Medium [1] - Coarse & Rubber Powder [4]**
Handelsname / Handelsnavn GENAN Gummigranulat Fein [1] - Mittel [1] - Grob & Gummipulver [4] / Fin [1] - Middel [1] - Grov & Gummipulver [4]

Producer:
Hersteller / Producent

Genan GmbH
Birkenallee 80
D - 16515 Oranienburg

Genan A/S
Jegindøvej 16
DK - 8800 Viborg

Classification: **ASTM D 5603 - 01 / Grade 1 and 5**
Klassifikation

Properties Eigenschaften Egenskaber	Test methods acc. ASTM	Specification values acc. ASTM	Typical values GENAN Granulate & Powder
Specific gravity Dichte / Massefylde	./.	./.	1,10-1,20 g/cm³ [5]
Bulk density Schüttgewicht / Rumvægt	D 5603, 8	./.	app. 500 kg/m³ [6]
Ashes Asche / Ask	D 297, 34-37	</= 8%	</= 5%
Acetone extractables Azethonextrakt / Acetonektrakt	D 297, 17-19	8-22%	app. 11-17%
Carbon black content [2] Russgehalt / Carbon indhold	D 297, 38-39	26-38%	app. 32-36%
Rubber hydrocarbon content Kautschuk-Kohlenwasserstoff	D 297,11	>/= 42%	>/= 42%
Loss on heating (2h@105°C) [3] Verlust bei Erwärmung / tab ved opvarmning	D 1509	</= 1%	</= 1%
Natural rubber [7]	D 297, 52-53	10-35%	app. 30%
Free metal content [4] Freie Metalle / fri metal	D 5603, 7.3.2	</= 0,1%	</= 0,002% w/w
Free fibre content [4] Freie Textilfasern / fri tekstil	D 5603, 7.4	</= 0,5%	</= 0,001% w/w
Free mineral content [4] Freie Minerale / frie mineraler	D 5603, 7.3.1	./.	</= 0,002% w/w

[1] Includes Mix products FINE + MEDIUM-Mix / Inkl. Mischprodukt FEIN + MITTEL-Mix / Inkl. blandet produkt FIN + MIDDEL-Mix

[2] In some tyres silica SiO_2 is used as part-replacement for carbon black
In einigen Reifentypen wird SiO_2 als Teilersatz von Russ verwendet
I nogle dæktyper anvendes SiO_2 som delvis erstatning for carbon black

[3] App. Water content / ca. Wasserinhalt / ca. vandindhold

[4] GENAN values only for rubber powder produced out of our rubber granulate in our fine grinding process
GENAN Werte gelten n ur für Gummipulver aus eigener Feinvermahlung unserer Gummigranulate
GENAN værdier gælder kun for gummipulver produceret ved finformaling af vores gummigranulater

[5] As the product is made off a large number of different tyre types, GENAN cannot give any exact values of the elastomeric composition of the material.The following can be used as a guideline:
Da das Produkt aus einer Vielzahl von Reifenfabrikaten hergestellt ist kan GENAN nur Richtwerte der Elastomeren Zusammensetzung angeben
Idet produktet er fremstillet af mange forskellige dækfabrikater kan GENAN kun angive retningsvisende data for den elstomere sammensætning

NR (Natural Rubber)	app. 30%
SBR (styrene-butadiene rubber)	app. 40%
BR (butadiene rubber)	app. 20%
IIR/XIIR (Butyl- and halogonated butyl rubber)	app. 10%

[6] Depend on material size / Abhängig von der Materialgrösse / afhængig af materialestørrelsen

Health and safety:
Not a dangerios substance when handled in accordance with good industrial hygiene and safety practice
Kein gefährliches Produkt bei Beachtung industrieller hygiene- und Sicherheitspraktikken
Ingen farlig produkt ved anvendelse af de industrielle hygiejne- og sikkerhedspraktikker.

APPENDIX 2

MULTIPLE REGRESSION OF RAW DATA
By MINITAB from Minitab, Inc.

DATA TABLE

Infill weight-lb.	Pile Height-mm	Gmax
0.0	3	595.2
0.6	3	387.2
1.1	3	262.7
1.7	3	208.4
2.3	3	173.2
0.0	3	454.8
0.6	3	408
1.1	3	299.8
1.7	3	195.7
2.3	3	174.5
0.0	3	556.4
0.6	3	419.6
1.1	3	270.9
1.7	3	230.8
2.3	3	179.7
0.0	11	492.4
0.6	11	378.4
1.1	11	256.6
1.7	11	180.9
2.3	11	130.4
0.0	12	466.1
0.6	12	382.8
1.1	12	284.3
1.7	12	208.4
2.3	12	152.9
0.0	11	434.1
0.6	11	384.2
1.1	11	279.2
1.7	11	192
2.3	11	148.8
0.0	19	412.6
0.6	19	339.2
1.1	19	209.3

1.7	19	166
2.3	19	126.8
0.0	18	489.7
0.6	18	346.7
1.1	18	242
1.7	18	177.1
2.3	18	142.3
0.0	24	471.6
0.6	24	273.7
1.1	24	216.7
1.7	24	166.4
2.3	24	134
0.0	44	337.1
0.6	44	209.2
1.1	44	150.7
1.7	44	132.4
2.3	44	119.2
0.0	41	381
0.6	41	196.6
1.1	41	151.2
1.7	41	128.1
2.3	41	110.8
0.0	44	373.6
0.9	44	184.2
1.1	44	157.2
1.7	44	133.5
2.3	44	114.7

Descriptive Statistics: gmax versus Infill weight

Variable	Infill weight-lb	N	N*	Mean	SE Mean	StDev	Minimum	Q1	Median
gmax	0.0	12	0	455.4	21.5	74.6	337.1	388.9	460.5
	0.6	11	0	338.7	23.5	77.8	196.6	273.7	378.4
	0.9	1	0	184.20	*	*	184.20	*	184.20
	1.1	12	0	231.7	15.6	54.1	150.7	170.2	249.3
	1.7	12	0	176.64	9.52	32.97	128.10	141.63	179.0
	2.3	12	0	142.28	6.90	23.90	110.80	121.1	138.15

Variable	Infill weight-lb	Q3	Maximum
gmax	0.0	491.7	595.2
	0.6	387.2	419.6
	0.9	*	184.20
	1.1	277.1	299.8
	1.7	205.23	230.80
	2.3	168.12	179.70

Descriptive Statistics: gmax versus pile height

Variable	Pile Height-mm	N	N*	Mean	SE Mean	StDev	Minimum	Q1	Median
gmax	3	15	0	321.1	36.3	140.5	173.2	195.7	270.9
	11	10	0	287.7	40.3	127.6	130.4	172.9	267.9
	12	5	0	298.9	56.9	127.2	152.9	180.7	284.3
	18	5	0	279.6	63.0	140.9	142.3	159.7	242.0
	19	5	0	250.8	54.0	120.7	126.8	146.4	209.3
	24	5	0	252.5	59.7	133.4	134.0	150.2	216.7
	41	5	0	193.5	49.0	109.6	110.8	119.4	151.2
	44	10	0	191.2	29.0	91.6	114.7	129.1	153.9

Variable	Pile Height-mm	Q3	Maximum
gmax	3	419.6	595.2
	11	396.7	492.4
	12	424.5	466.1
	18	418.2	489.7
	19	375.9	412.6
	24	372.6	471.6
	41	288.8	381.0
	44	241.2	373.6

One-way ANOVA: gmax versus Infill weight-lb

Source	DF	SS	MS	F	P
Infill weight-lb	5	788817	157763	49.48	0.000
Error	54	172164	3188		
Total	59	960981			

S = 56.46 R-Sq = 82.08% R-Sq(adj) = 80.43%

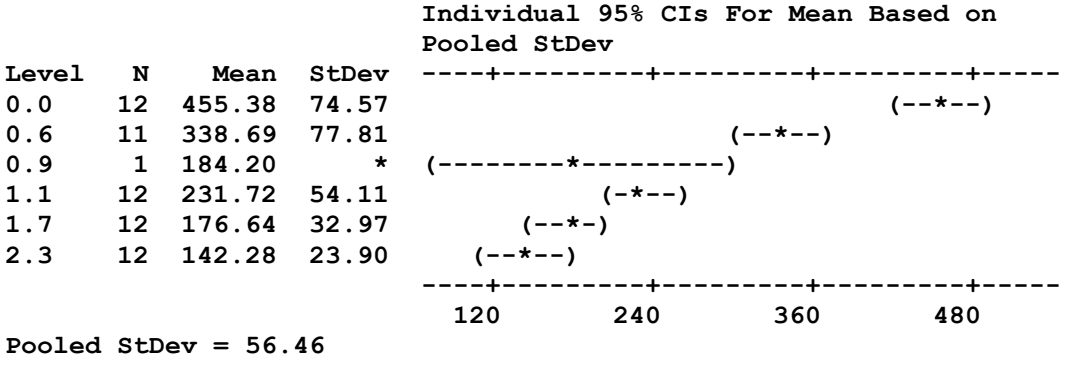

Pooled StDev = 56.46

INFERENCE: P value of 0.000 suggests that the probability of different infill weights representing the same Gmax value is zero. In other words, the Gmax values of different infill weights are significantly different at 95% confidence level.

One-way ANOVA: gmax versus Pile Height-mm

Source	DF	SS	MS	F	P
Pile Height-mm	7	140921	20132	1.28	0.280
Error	52	820060	15770		
Total	59	960981			

```
S = 125.6   R-Sq = 14.66%   R-Sq(adj) = 3.18%

                          Individual 95% CIs For Mean Based on
                          Pooled StDev
Level   N   Mean  StDev  --+---------+---------+---------+-------
 3     15  321.1  140.5                    (-----*------)
11     10  287.7  127.6                 (-------*-------)
12      5  298.9  127.2              (----------*----------)
18      5  279.6  140.9           (----------*----------)
19      5  250.8  120.7        (----------*----------)
24      5  252.5  133.4        (----------*----------)
41      5  193.5  109.6  (----------*----------)
44     10  191.2   91.6     (-------*-------)
                          --+---------+---------+---------+-------
                          100       200       300       400
Pooled StDev = 125.6
```

INFERENCE: P value of 0.28 suggests that the probability of different pile heights representing the same Gmax value is 28%. In other words, the Gmax values of the different pile heights are not significantly different at 95% confidence level.

Regression Analysis: gmax versus Infill weight-lb, Pile Height-mm

```
The regression equation is
gmax = 481 - 137 Infill weight-lb - 3.12 Pile Height-mm

Predictor             Coef  SE Coef       T      P
Constant            480.56    11.89   40.42  0.000
Infill weight-lb  -136.727    6.922  -19.75  0.000
Pile Height-mm     -3.1166   0.3690   -8.45  0.000


S = 42.8993   R-Sq = 89.1%   R-Sq(adj) = 88.7%

Analysis of Variance
Source          DF      SS      MS       F      P
Regression       2  856081  428041  232.59  0.000
Residual Error  57  104900    1840
Total           59  960981

Source            DF  Seq SS
Infill weight-lb   1  724830
Pile Height-mm     1  131251

Unusual Observations
        Infill
Obs  weight-lb    gmax     Fit  SE Fit  Residual  St Resid
  1       0.00  595.20  471.21   11.26    123.99      3.00R
 11       0.00  556.40  471.21   11.26     85.19      2.06R
 50       2.29  119.20   30.85   13.27     88.35      2.17R
 60       2.29  114.70   30.85   13.27     83.85      2.06R

R denotes an observation with a large standardized residual.
```

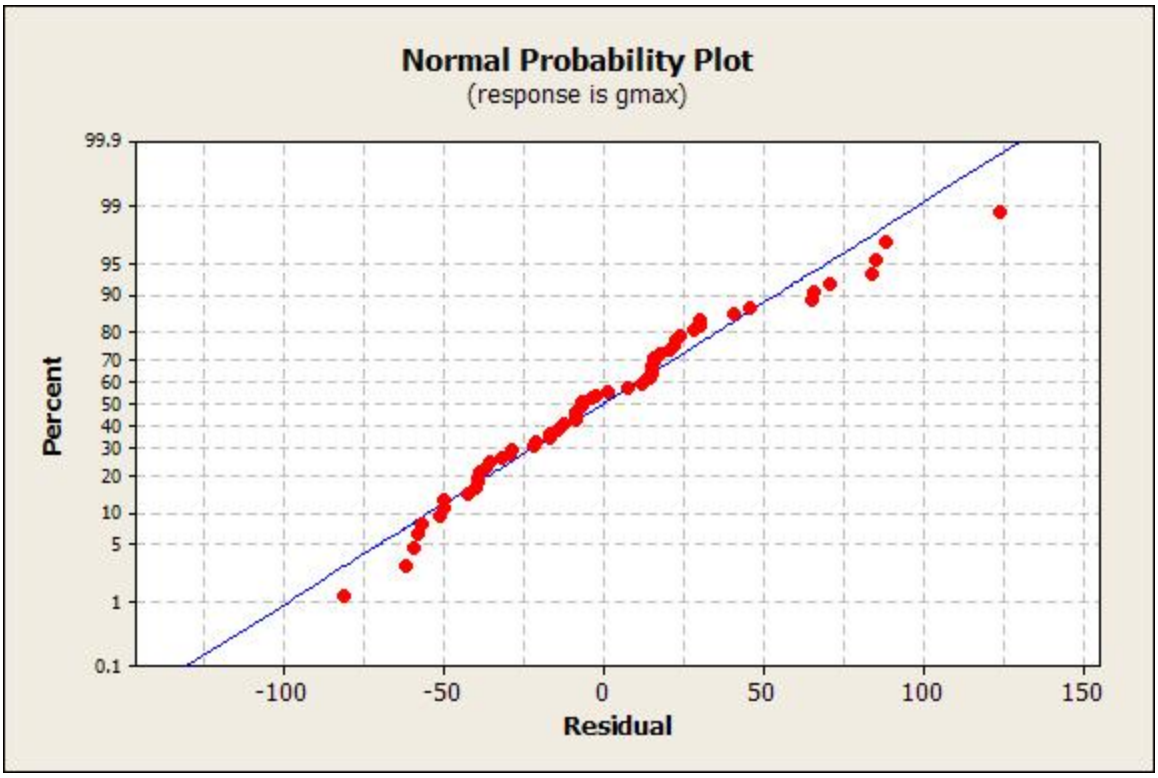
Normal Probability Plot
(response is gmax)
Percent
99.9
99
95
90
80
70
60
50
40
30
20
10
5
1
0.1
-100
-50
0
50
100
150
Residual

APPENDIX 3

MULTIPLE REGRESSION OF NORMALIZED DATA
By MINITAB from Minitab, Inc.

DATA TABLE

Infill weight-lb	Pile Height-mm	Gmax
0.0	0.1	595.2
0.2	0.1	387.2
0.5	0.1	262.7
0.7	0.1	208.4
1.0	0.1	173.2
0.0	0.1	454.8
0.2	0.1	408
0.5	0.1	299.8
0.7	0.1	195.7
1.0	0.1	174.5
0.0	0.1	556.4
0.2	0.1	419.6
0.5	0.1	270.9
0.7	0.1	230.8
1.0	0.1	179.7
0.0	0.3	492.4
0.2	0.3	378.4
0.5	0.3	256.6
0.7	0.3	180.9
1.0	0.3	130.4
0.0	0.3	466.1
0.2	0.3	382.8
0.5	0.3	284.3
0.7	0.3	208.4
1.0	0.3	152.9
0.0	0.3	434.1
0.2	0.3	384.2
0.5	0.3	279.2
0.7	0.3	192
1.0	0.3	148.8
0.0	0.4	412.6
0.2	0.4	339.2
0.5	0.4	209.3

0.7	0.4	166
1.0	0.4	126.8
0.0	0.4	489.7
0.2	0.4	346.7
0.5	0.4	242
0.7	0.4	177.1
1.0	0.4	142.3
0.0	0.5	471.6
0.2	0.5	273.7
0.5	0.5	216.7
0.7	0.5	166.4
1.0	0.5	134
0.0	1.0	337.1
0.2	1.0	209.2
0.5	1.0	150.7
0.7	1.0	132.4
1.0	1.0	119.2
0.0	0.9	381
0.2	0.9	196.6
0.5	0.9	151.2
0.7	0.9	128.1
1.0	0.9	110.8
0.0	1.0	373.6
0.4	1.0	184.2
0.5	1.0	157.2
0.7	1.0	133.5
1.0	1.0	114.7

One-way ANOVA: gmax versus Infill weight-lb

```
Source             DF      SS      MS      F      P
Infill weight-lb    5  788817  157763  49.48  0.000
Error              54  172164    3188
Total              59  960981

S = 56.46   R-Sq = 82.08%   R-Sq(adj) = 80.43%


                          Individual 95% CIs For Mean Based on
                          Pooled StDev
Level   N    Mean  StDev  ----+---------+---------+---------+-----
0.0    12  455.38  74.57                                  (--*--)
0.2    11  338.69  77.81                        (--*--)
0.4     1  184.20      *  (--------*---------)
0.5    12  231.72  54.11              (-*--)
0.7    12  176.64  32.97         (--*-)
```

```
1.0    12  142.28  23.90     (--*--)
                          ----+---------+---------+---------+-----
                            120       240       360       480

Pooled StDev = 56.46
```

One-way ANOVA: gmax versus Pile Height-mm

```
Source           DF      SS     MS     F      P
Pile Height-mm    7  140921  20132  1.28  0.280
Error            52  820060  15770
Total            59  960981

S = 125.6   R-Sq = 14.66%   R-Sq(adj) = 3.18%


                          Individual 95% CIs For Mean Based on
                          Pooled StDev
Level   N   Mean  StDev  --+---------+---------+---------+-------
0.1    15  321.1  140.5                    (-----*------)
0.3    10  287.7  127.6               (-------*-------)
0.3     5  298.9  127.2             (----------*----------)
0.4     5  279.6  140.9           (----------*----------)
0.4     5  250.8  120.7        (----------*----------)
0.5     5  252.5  133.4        (----------*-----------)
0.9     5  193.5  109.6  (----------*-----------)
1.0    10  191.2   91.6     (-------*-------)
                          --+---------+---------+---------+-------
                          100       200       300       400
Pooled StDev = 125.6
```

Regression Analysis of Normalized Data: gmax versus Infill weight-lb, Pile Height-mm

```
The regression equation is
gmax = 481 - 313 Infill weight-lb - 137 Pile Height-mm

Predictor            Coef  SE Coef       T      P
Constant           480.56    11.89   40.42  0.000
Infill weight-lb  -312.58    15.83  -19.75  0.000
Pile Height-mm    -137.13    16.24   -8.45  0.000

S = 42.8993   R-Sq = 89.1%   R-Sq(adj) = 88.7%

Analysis of Variance
Source           DF      SS      MS       F      P
Regression        2  856081  428041  232.59  0.000
Residual Error   57  104900    1840
Total            59  960981
```

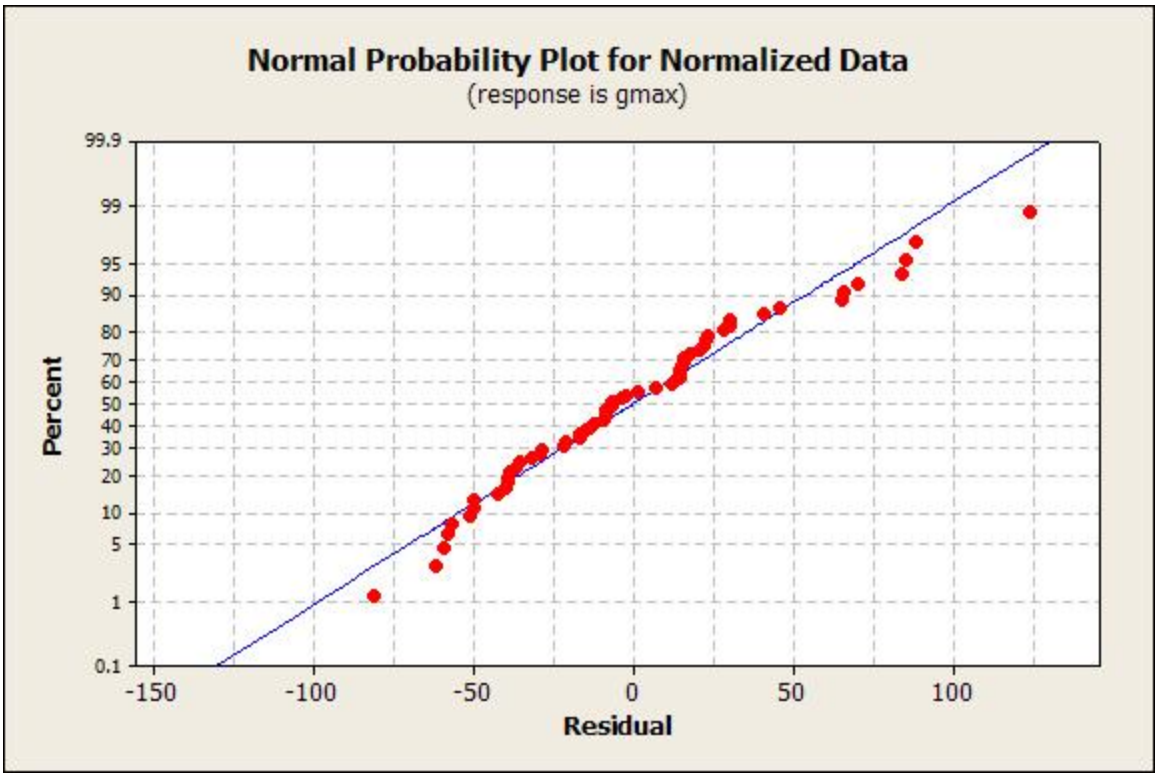
Normal Probability Plot for Normalized Data
(response is gmax)
Percent
99.9
99
95
90
80
70
60
50
40
30
20
10
5
1
0.1
-150
-100
-50
0
50
100
Residual

APPENDIX 4

MULTIPLE REGRESSION OF NON-ZERO DATA
By MINITAB from Minitab, Inc.

DATA TABLE

Infill weight-lb	Pile Height-mm	Gmax
0.6	3	387.2
1.1	3	262.7
1.7	3	208.4
2.3	3	173.2
0.6	3	408
1.1	3	299.8
1.7	3	195.7
2.3	3	174.5
0.6	3	419.6
1.1	3	270.9
1.7	3	230.8
2.3	3	179.7
0.6	11	378.4
1.1	11	256.6
1.7	11	180.9
2.3	11	130.4
0.6	12	382.8
1.1	12	284.3
1.7	12	208.4
2.3	12	152.9
0.6	11	384.2
1.1	11	279.2
1.7	11	192
2.3	11	148.8
0.6	19	339.2
1.1	19	209.3
1.7	19	166
2.3	19	126.8
0.6	18	346.7
1.1	18	242
1.7	18	177.1
2.3	18	142.3
0.6	24	273.7

1.1	24	216.7
1.7	24	166.4
2.3	24	134
0.6	44	209.2
1.1	44	150.7
1.7	44	132.4
2.3	44	119.2
0.6	41	196.6
1.1	41	151.2
1.7	41	128.1
2.3	41	110.8
0.9	44	184.2
1.1	44	157.2
1.7	44	133.5
2.3	44	114.7

One-way ANOVA: gmax versus Infill weight-lb

```
Source             DF      SS     MS      F      P
Infill weight-lb    4  252907  63227  24.50  0.000
Error              43  110989   2581
Total              47  363897

S = 50.80   R-Sq = 69.50%   R-Sq(adj) = 66.66%

                          Individual 95% CIs For Mean Based on
                          Pooled StDev
Level   N    Mean  StDev   +---------+---------+---------+---------
0.6    11  338.69  77.81                                (---*---)
0.9     1  184.20      *   (------------*------------)
1.1    12  231.72  54.11                 (---*---)
1.7    12  176.64  32.97           (---*---)
2.3    12  142.28  23.90       (---*--)
                           +---------+---------+---------+---------
                          80        160       240       320
Pooled StDev = 50.80
```

One-way ANOVA: gmax versus Pile Height-mm

```
Source           DF      SS     MS     F      P
Pile Height-mm    7  100240  14320  2.17  0.058
Error            40  263657   6591
Total            47  363897

S = 81.19   R-Sq = 27.55%   R-Sq(adj) = 14.87%

                          Individual 95% CIs For Mean Based on
                          Pooled StDev
Level   N    Mean  StDev  -+---------+---------+---------+--------
 3     12  267.54  92.21                        (------*------)
11      8  243.81  98.39                     (-------*-------)
12      4  257.10  99.62                   (-----------*----------)
```

```
18       4   227.03   89.85                (----------*----------)
19       4   210.32   92.29             (----------*----------)
24       4   197.70   61.03          (----------*----------)
41       4   146.67   37.17   (----------*----------)
44       8   150.14   32.74       (-------*--------)
                          -+---------+---------+---------+--------
                          70        140       210       280
Pooled StDev = 81.19
```

Regression Analysis of Non-Zero Data: gmax versus Infill weight-lb, Pile Height-mm

```
The regression equation is
gmax = 425 - 106 Infill weight-lb - 2.93 Pile Height-mm

Predictor             Coef  SE Coef       T      P
Constant            425.28    12.65   33.61  0.000
Infill weight-lb  -106.185    7.284  -14.58  0.000
Pile Height-mm     -2.9345   0.3090   -9.50  0.000

S = 32.1256   R-Sq = 87.2%   R-Sq(adj) = 86.7%

Analysis of Variance
Source          DF      SS      MS       F      P
Regression       2  317454  158727  153.80  0.000
Residual Error  45   46442    1032
Total           47  363897
```

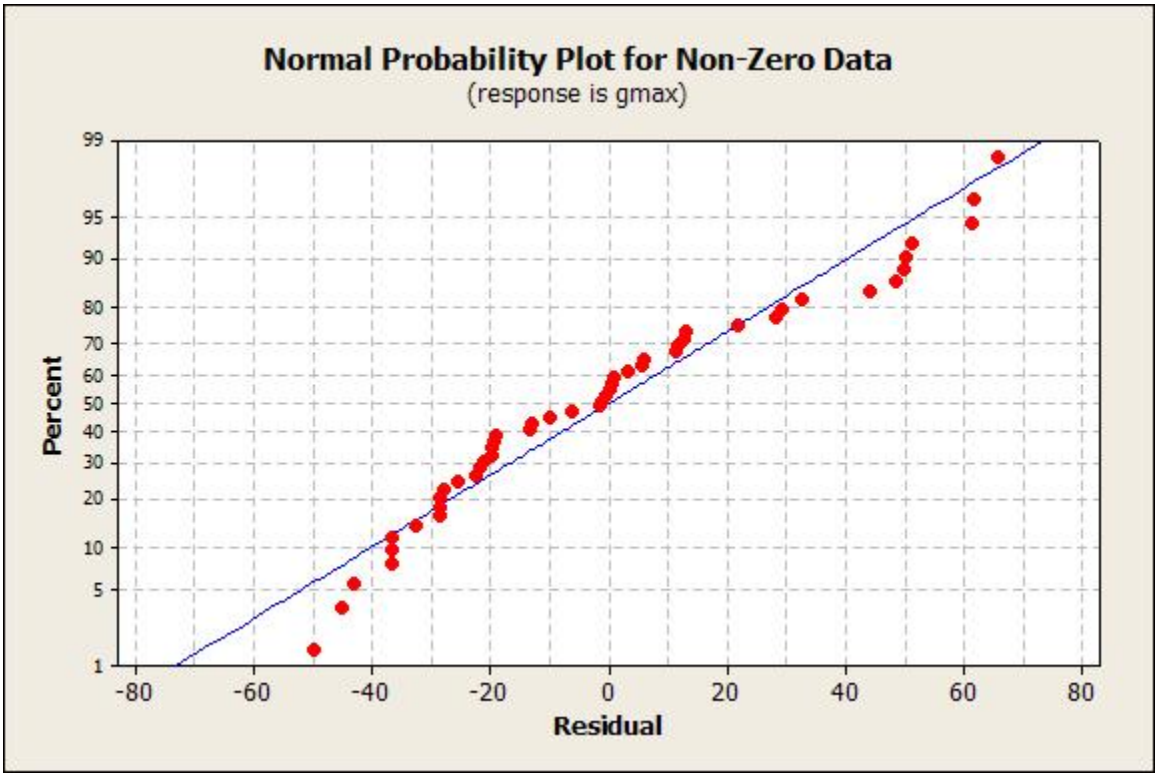

REFERENCES

[1] Claudio, L., *Synthetic Turf: Health Debate Takes Root*. Environmental Health Perspectives, March 2008. 116(3): p. A116-A122.

[2] Morehouse, C.A., *Artificial Turf. Turfgrass - Agronomy Monograph No. 32*. 1992. D.V. Waddington, et al., Eds., American Society of Agronomy: Madison, WI: p. 89-127.

[3] Ekstrand, J., T. Timpka, and M. Häggland, *Risk of Injury in Elite Football Played on Artificial Turf Versus Natural Grass: a Prospective Two-cohort Study*. British Journal of Sports Medicine, 2006. 40: p. 975-980.

[4] Lockyer, J., *Third Generation Artificial Football Surfaces: Maintenance Understandings Revealed*. Pitchcare Magazine, June/July 2006. 7: p. 64-67.

[5] NFL Players Association. *Artificial or Natural? Players Respond*. NFL Players Playing Surfaces Survey, May 16 2008. Accessed on 10/31/2010. http://www.nflplayers.com/Articles/Public-News/Artificial-or-Natural-Players-Respond/

[6] Baleki, R., J. Courter, P. Ruiz, B. Sanders, T. Steele, and I. Vulic, *Fielding the Challenges of Artificial Turf Stabilization*. Paper presented at the FlexConPack 2008 International Polyolefins Conference: Houston, TX.

[7] Prévost, J., *Synthetic Turf* in USP 6,723,412 B2. 2008.

[8] Knox, J., *Synthetic Sports Turf Having Improved Playability and Wearability* in USP 7,189,445 B2. 2007.

[9] Henderson, R.L., D.V. Waddington, and C.A. Morehouse, *Laboratory Measurements of Impact Absorption on Turfgrass and Soil Surfaces*. Natural and Artificial Playing Fields: Characteristics and Safety Features, ASTM STP 1073, 1990. R.C. Schmidt, E.F. Hoerner, E.M. Milner, and C.A. Morehouse, Eds., American Society for Testing and Materials: Philadelphia: p. 127-135.

[10] Shorten, M.R., B. Hudson, and J.A. Himmelsbach, *Shoe-Surface Traction of Conventional and In-Filled Synthetic Turf Football Surfaces*. Proceedings of XIX International Congress of Biomechanics, 2003. P. Milburton, Ed., University of Otago: Dudedin, New Zealand.

[11] Bras, B., T. Guldberg, A. Calione, and P. George, *Economic Advantages of Using Ultra Fine Scrap Tire Rubber (UFSTR) in Virgin and Recycled Rubber and Plastic Compounds - A Comprehensive Life Cycle Assessment*. Fall 172nd

Technical Meeting of the Rubber Division of American Chemical Society, Inc., October 16-18 2007. Paper no. 79.

[12] Rubber Manufacturers Association, *Scrap Tire Markets in the United States 9th Biennial Report*, May 2009. Accessed on 11/2/2011. http://www.rma.org/publications/scrap_tires/index.cfm?PublicationID=11502

[13] EPA, *Municipal Solid Waste Generation, Recycling, and Disposal in the United States: Facts and Figures for 2008*, November 2009. EPA-530-F-009-021.

[14] EPA, *State Scrap Tire Programs*, August 1999. EPA-530-B-99-002.

[15] Brandrup, J., Ed., Recycling and Recovery of Plastics. 1996, New York: Hanser.

[16] Marvin, M. and D.A. MacKillop, *Rubber Recycling*. Rubber Chemistry and Technology, Jul/Aug 2002. 75(3): p. 429-474.

[17] Denly, E., K. Rutkowski, and K.M. Vetrano, *A Review of the Potential Health and Safety Risks from Synthetic Turf Fields Containing Crumb Rubber Refill*. May 2008, New York City Department of Health and Mental Hygene: New York. Prepared by TRC, Windsor, Connecticut. Accessed on 11/3/2010. http://www.nyc.gov/html/doh/downloads/pdf/eode/turf_report_05-08.pdf

[18] McGraw, E., *Turf Toe*. Coach and Athletic Director, February 2008. 77(7): p. 34-37.

[19] New Jersey Consumer and Environmental Health Services, *Artificial Turf and Human Health Concerns*. Pitchcare Magazine, April 2008. Accessed on 11/3/2010. http://www.pitchcare.com/magazine/artificial-turf-and-human-health-concerns.html

[20] *Sod It: The Latest Plastic Pitches are a Goal-scorer's Delight*. The Economist, November 20 2009. Accessed on 11/8/2010. http://www.economist.com/node/14943565?story_id=14943565

[21] Popke, M., *Shock Value: The Process of Determining the Forgiveness Factor of Athletic Fields - Both Natural and Synthetic - is Packed with Variables*. Athletic Business, August 2002. Accessed on 6/18/2015. http://www.athleticbusiness.com/shock-value.html

[22] McKenna, M., *MRSA: The Drug-resistant 'Superbug' that Won't Die* [Author Interview]. March 23 2010. National Public Radio. Accessed on 11/8/2010. http://www.npr.org/templates/story/story.php?storyId=124999740&sc=fb&cc=fp

[23] Kirkland, E.B. and B.B. Adams, *Methicillin-resistant Staphylococcus Aureus and Athletes*. Journal of the American Academy of Dermatology, 2008. 59: p. 494-502.

[24] The Carpet and Rug Institute, Inc., CRI - The Carpet Primer. 2003, CRI: Dalton, GA. ISBN 0-89275-084-7.

[25] Shaw EcoWorx, Last accessed on 6/23/2013. http://www.owencarpet.com/shaw_ecoworx.htm

[26] CARE™, CARE Annual Report. 2013. Last accessed on 6/18/2015. https://carpetrecovery.org/wp-content/uploads/2014/04/CARE-2013-Annual-Report.pdf

[27] Subbiah, V., J. Muzzy, and M. Realff, *Life Cycle Inventory of Recycling Post-Consumer Carpets*. Spring National Meeting conference proceedings, April 6-10 2008. American Institute of Chemical Engineers: New Orleans, Louisiana.

[28] Williams, J., Director of Research, Mohawk Ind., Personal Communications, 2008.

[29] Organite Advertisement. Last accessed on 6/25/2013. http://www.targapro.com/products/sports-fields-and-running-tracks/Technical-Product-Specifications/tech-specs/organite

[30] TargaPro Advertisement. Last accessed on 6/25/2013. http://www.syntheticturfmd.com/

[31] Charaf, K.C. and R.W. Avery, *Antimicrobial Compositions Containing Quaternary Ammonium Compounds* in USP 6,528,472 B2. 2003.

[32] Wibowo, D., and C.K. Lee, *Nonleaching Antimicrobial Cotton Fibers for Hyaluronic Acid Adsorption*. Biochemical Engineering Journal, 2010. 53: p. 44–51.

[33] Tomsic, B., D. Klemencic, B. Simoncic, and B. Orel, *Influence of Antimicrobial Finishes on the Biodeterioration of Cotton and Cotton/Polyester Fabrics: Leaching Versus Bio-Barrier Formation.* Polymer Degradation and Stability, 2011. 96: p. 1286-1296.

[34] Shorten, M.R. and J.A. Himmelsbach, *Sports Surfaces and the Risk of Traumatic Brain Injury*. Sports Surfaces, 2003: p. 49-69.

[35] Smith, S., *Ex-NFL Players Feel Concussions' Long-Last Damage*. CNN.com, February 5 2010. Last accessed on 6/18/2015. http://www.cnn.com/2010/HEALTH/02/05/concussions.visger.football/index.htm

l?eref=rss_topstories&utm_source=feedburner&utm_medium=feed&utm_campaign=Feed%3A+rss%2Fcnn_topstories+%28RSS%3A+Top+Stories%29

[36] Tanner, L., *ER Visits For Concussions Soar among Kid Athletes*. NBCNEWS.com, August 30 2010. Associated Press. Last accessed on 11/15/2010. http://www.msnbc.msn.com/id/38916554/ns/healthkids_and_parenting/?ocid=twitter#

[37] Associated Press. *All Clear? Head Injuries Get More Attention*, January 28 2010. Last accessed on 11/14/2010. http://www.msnbc.msn.com/id/35122652

[38] Schwarz, A., *N.F.L. Asserts Greater Risks of Head Injury*. The New York Times, July 26 2010. Last accessed on 6/6/2013. http://www.nytimes.com/2010/07/27/sports/football/27concussion.html

[39] Fleming, P., *Artificial Turf Systems for Sport Surfaces: Current Knowledge and Research Needs*. Proceedings of the Institution of Mechanical Engineers, Part P: Journal of Sports Engineering and Technology, 2011. 225: p. 43-64.

[40] Balandin, D.V. et al., *Optimal Impact Isolation for Injury Prevention Evaluated by the Head Injury Criterion*. Shock and Vibrations, 2007. 14: p. 355-370.

[41] Brosnan, J.T., Effects of Varying Surface Conditions on Baseball Field Playing Quality (dissertation), 2007. Pennsylvania State University.

[42] McNitt, A.S., P.J. Landschoot, and D.M. Petrukak, *Evaluation of the Playing Surface Hardness of an Infilled Synthetic Turf System*. Acta Horticulturae, 2004. 661: p. 559-563.

[43] Nussbaum, A., *NFL Players Have Greater Risk of Death from Alzheimer's*. Bloomberg News, September 5 2012. Last accessed on 6/18/2015. http://www.businessweek.com/news/2012-09-05/nfl-players-have-greater-risk-of-death-from-alzheimer-s

[44] Shorten, M.R., Sports Surface Impact Test System Instruction Manual, 2003. Biomechanica: Portland.

[45] Chalmers, J.M. and R.J. Meier, Comprehensive Analytical Chemistry, Volume 53 - Molecular Characterization and Analysis of Polymers, 2008. Elsevier Publishing Company: New York.

[46] Fernàndez-Berridi, M.J., N. Gonzàlez, A. Mugica, and C. *Bernicot, Pyrolysis-FTIR and TGA Techniques as Tools in the Characterization of Blends of Natural Rubber and SBR*. Thermochimica Acta, 2006. 444: p. 65-70.

[47] Gunasekaran, S., R. K. Natarajan, and A. Kala, *FTIR Spectra and Mechanical Strength Analysis of Some Selected Rubber Derivatives*. Spectrochimica Acta Part A, 2007. 68: p. 323-330.

[48] Colom, X., F. Carrillo, and J. Cañavate, *Composites Reinforced with Reused Tyres: Surface Oxidant Treatment to Improve the Interfacial Compatibility*. Composites Part A, 2007. 38: p. 44-50.

[49] Gisbert, A.N., J.E.C. Amorós, J.L. Martínez, and A.M. Garcia, *Study of Thermal Degradation Kinetics of Elastomeric Powder (Ground Tire Rubber)*. Polymer-Plastics Technology and Engineering, 2008. 47(1): p. 36-39.

[50] Brase, C.H and C.P. Brase, Understanding Statistics, 5th ed. 1995, D.C. Head and Company: Lexington, MA.

[51] Microsoft Help. Last accessed 10/21/2013. http://office.microsoft.com/en-us/excel-help/linest-function-HA102752956.aspx#BMexample4

[52] Huang, C.K. and P.F. Kerr, *Infrared Study of the Carbonate Minerals*. The American Mineralogist, 1960. 45: p. 311-324.

[53] Tria, J. J., K. K. Balasubramanian, and M. K. Goodin, *Analysis of Carpet Recycle Streams Using Differential Scanning Calorimetry, Thermogravimetric Analysis and Gas Chromatography (1037).* ANTEC - Conference Proceedings, 2002. 3: p. 3969-3973.

[54] Pretch, E., P. Bűhlmann, and M. Badertscher, Structure Determination of Organic Compounds, 4th ed. 2009, Springer: Berlin.

[55] Realff, M.J., J.C. Ammons, and D. Newton, *Strategic Design of Reverse Production Systems*. Computers and Chemical Engineering, 2000. 24: p. 991-996.

[56] Hobbes, J., Director of Research, Interface Research and Development, Personal Communications, 2015.

[57] Kostreba, G. General Manager, Liberty Tire Recycling, LLC, Personal Communications, 2011.

[58] Gruver, V., D. Showers, M. Kao, and L. Klebanov, *The Determination of PET Crystallinity by Different Analytical Techniques*. Society of Plastics Engineers, 2000. Last accessed on 7/9/2014. http://www.4spe.org/Resources/resource.aspx?ItemNumber=13559

[59] Gupta, Y.N., A. Chakraborty, G.D. Pandey, and D.K. Setua, *Thermal and Thermooxidative Degradation of Engineering Thermoplastics and Life Estimation*. Journal of Applied Polymer Science, 2004. 92: p. 1737–1748.

[60] Denardin, E.L.G., S. Tokumoto, and D. Samios, *Stress–Strain Behaviour of Poly (Ethylene Terephthalate) (PET) during Large Plastic Deformation by Plane Strain Compression: The Relation Between Stress–Strain Curve and Thermal History, Temperature and Strain Rate*. Rheol Acta, 2005. 45: p. 142–150.

[61] *InterfaceFLOR and PVC*. Last accessed on 7/16/2015. https://www.pharosproject.net/uploads/files/sources/1365/pvc-stabilizers.pdf

[62] Official Journal of the European Union, C90/4, April 2013, 2006, Part 5. Last accessed on 7/17/2015. http://eur-lex.europa.eu/legal-content/EN/TXT/?uri=CELEX:52006XC0413(01)